KERNFORSCHUNGSZENTRUM

KARLSRUHE

November 1973 KFK 1768

Zyklotron Laboratorium

Systematic Experiments on Neutron Deficient Nuclei in the Region $50 \leqslant (N,Z) \leqslant 82$

I. Radioactive Decay

J. van Klinken
(Natuurkundig Laboratorium der Rijksuniversiteit Groningen)

D. Habs, H. Klewe-Nebenius, K. Wisshak
(II. Physikalisches Institut der Universität Heidelberg)

G. Nowicki, J. Buschmann, S. Göring,
R. Löhken, H. Rebel, G. Schatz
(Kernforschungszentrum Karlsruhe)

GESELLSCHAFT
FÜR
KERNFORSCHUNG M.B.H.

KARLSRUHE

GESELLSCHAFT FÜR KERNFORSCHUNG M. B. H.
KARLSRUHE

KERNFORSCHUNGSZENTRUM KARLSRUHE

KFK 1768

Zyklotron-Laboratorium

Systematic Experiments on Neutron Deficient Nuclei in the Region $50 \leq (N,Z) \leq 82$

(I. Radioactive Decay)

J. van Klinken[+], D. Habs[++], H. Klewe-Nebenius[++], K. Wisshak[++], G. Nowicki, J. Buschmann, S. Göring, R. Löhken, H. Rebel and G. Schatz

Gesellschaft für Kernforschung m.b.H.,Karlsruhe,Germany

[+]Permanent address: Natuurkundig Laboratorium der Rijksuniversiteit Groningen, The Netherlands

[++]II. Physikalisches Institut der Universität Heidelberg, Germany

Abstract

Basic data on half-lives, partial decay schemes and isomerism have been obtained for several adjacent nuclei in the neutron deficient region with $58 < Z \leq 64$.

Single spectra of γ-rays and conversion electrons, as well as γγ- coincidences have been measured for the (α,xn + yp + zα)-reaction products of enriched targets of ^{144}Sm, ^{142}Nd, ^{141}Pr, ^{140}Ce, ^{138}Ce, ^{136}Ce and ^{139}La. For several new radioisotopes (partial) decay schemes have been constructed using a set of general rules for nuclidic-,level-, and spin assignments. Detailed discussions are presented for: ^{144}Gd(4.4 min), $^{143m2}Sm$ (30 ms), ^{143}Gd(1.9 min), ^{142m}Pm(2.38 ms), ^{142g}Eu(≤30 s), ^{142m}Eu(1.2 m), ^{142}Gd(1.5 min), ^{141g}Sm(11 min), ^{141g}Eu(28 s), ^{141m}Eu(~7 s), ^{140g}Pm(9.2 s), ^{140}Sm(14.7 min), ^{140}Eu(20 s), ^{139g}Pm(4 min), ^{139m}Pm(0.5 s), ^{139g}Sm(2.6 min), ^{138}Pm(3.5 min), ^{137g}Nd(38 min), ^{137}Pm(2.4 min) and ^{135}Nd(12 min).

Zusammenfassung:

Im Nuklidbereich mit $58 < Z \leq 64$ wurden neue neutronenarme Isotope identifiziert und ihre Zerfallsschemata untersucht. Hierzu wurden γ-Einzelspektren, Konversionselektronenspektren, γγ-Koinzidenzen und Lebensdauern gemessen, nachdem die Kerne bei der Bestrahlung von angereicherten Targets aus ^{144}Sm, ^{142}Nd, ^{141}Pr, ^{140}Ce, ^{138}Ce, ^{136}Ce und ^{139}La über (α,xn+yp+zα)-Reaktionen produziert worden waren. Die Zerfallsschemata folgender Nuklide werden ausführlich diskutiert: ^{144}Gd(4.4 min), $^{143m2}Sm$(30 ms), ^{143}Gd(1.9 min), ^{142m}Pm(2.38 ms), ^{142g}Eu(≤ 30 s), ^{142m}Eu(1.2 m), ^{142}Gd(1.5 min), ^{141g}Sm(11 min), ^{141g}Eu(28 s), ^{141m}Eu(~7 s) ^{140g}Pm (9.2 s), ^{140}Sm(14.7 min), ^{140}Eu(20 s), ^{139g}Pm(4 min), ^{139m}Pm (o.5 s), ^{139g}Sm(2.6 min), ^{138}Pm(3.5 min), ^{137g}Nd(38 min), ^{137}Pm (2.4 min) und ^{135}Nd (12 min).

I. Introduction

Between the axes of magic nuclei with N = 82 and Z = 50 and far from the valley of stability lies a region of nuclei with stable deformation[1]. To explore this area it is desirable to obtain basic data of these new isotopes and to investigate their level structure in a systematic way. During the last years a part of the lower-Z region has been approached and reached with heavy ion reactions[2,3], and with α-particles[4], while the present investigation aims at somewhat higher Z-values. We performed α- and deuteron-activations of targets from a row of stable isotones: ^{144}Sm, ^{142}Nd, ^{141}Pr, ^{140}Ce, ^{139}La and in addition of ^{138}Ce and ^{136}Ce. The targets were irradiated at the Karlsruhe Isochronous Cyclotron with α-particles of up to 104 MeV and deuterons of up to 52 MeV.

The production goes mainly via reactions of the type (α,xn+yp+zα) with $x \leq 8$, and y and z equal to 0,1 or 2. A pure reaction (α, xn) with y = z = 0 reaches farthest from the valley of stability, but finds its limit in the onset of charged particle evaporation. The processes with y or $z \neq 0$ have an increasing probability with increasing neutron deficiency. This is because after production of the intermediate compound nucleus the evaporation of each neutron has to compete with the emission of a proton or an alpha particle. The ratio of proton to neutron emission can be estimated from calculated binding energies (see ref.[5]). In fig. 1 the line $\sigma_n = \sigma_p$ for equal probability for the (xn)- and the ((x-1)n+p)-reactions is shown. As a consequence, ^{142}Gd, ^{140}Eu, ^{141}Eu, and ^{137}Pm are produced as weak activities dominated by other reaction products, but still sufficiently present for identification.

Our experimental results are divided into two parts: the radioactive decay and data from in-beam studies. With the latter we mean experiments on prompt transitions and isomers with half-lives less than 20 μs. The present part I of the publication is concerned with the radioactive decay, while in part II the data from in-beam studies and a summarizing description of the collective properties of the present region of nuclei will be given.

22.1o.1973

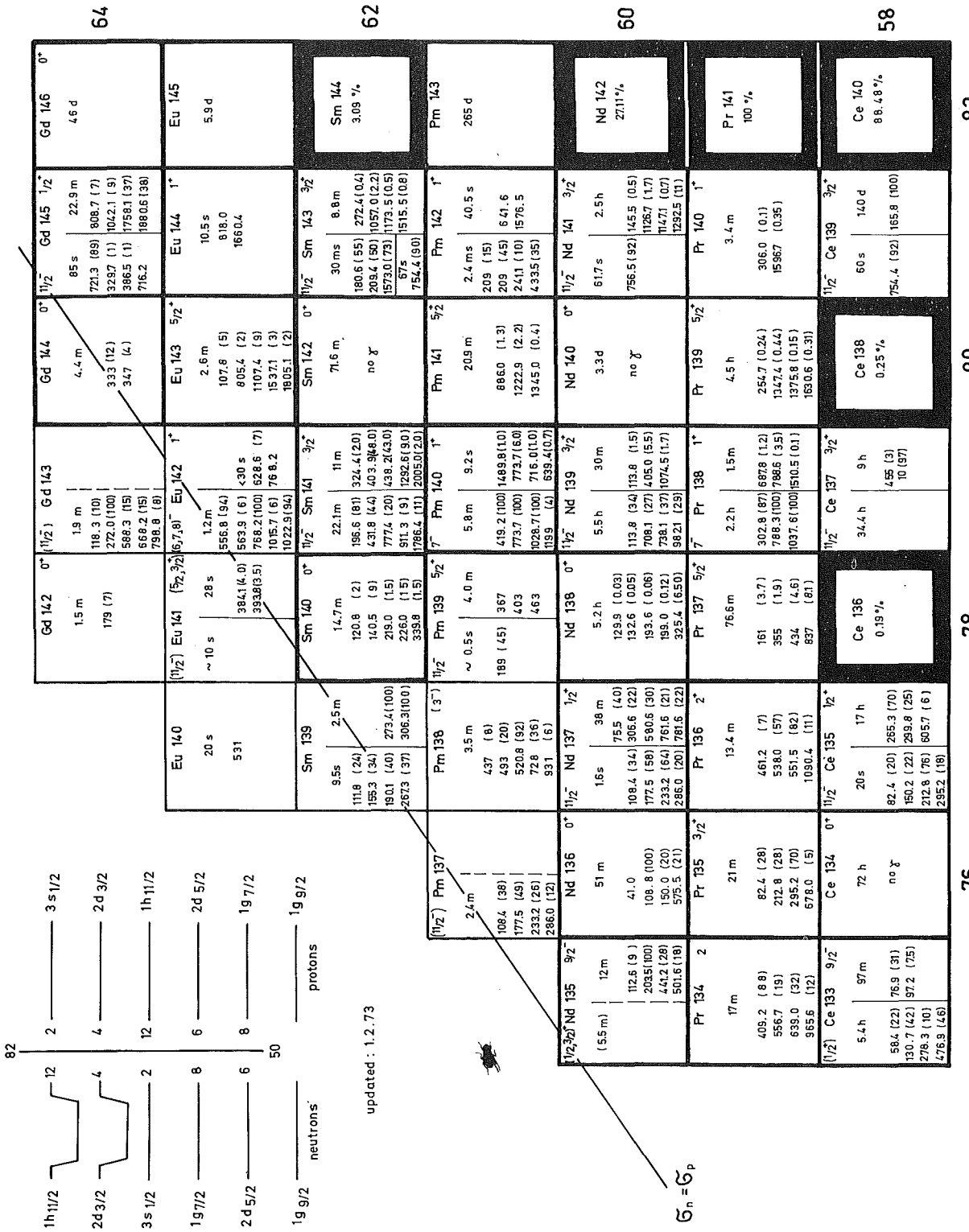

Fig. 1: Part of the chart of nuclides. Prominent γ-rays assigned to each radioactive decay are quoted together with their relative intensities. The special case of ^{136}Pm demonstrates that surprising things may happen in this mass region which are also of relevance for biologists.

Though in specific cases the experimental results are partly incomplete, the presented status of the experimental knowledge gives a survey on many trends in this mass region and shows which isotopes will be selected for more detailed studies.

A survey of the radioactive decay data is given in fig. 1. The inset of the figure shows the relevant shell model levels, and explains the groundstate spins and the occurrence of $11/2^-$-isomers in most of the odd mass nuclei. The identification of the nuclei surrounded by weak lines(^{142,143}Gd, ^{140,141,142g}Eu, $^{139m+g}$Sm and ^{137,138,139m}Pm) are based on this work. For nuclei closer to stability the nuclidic assignments can be found in literature. All reported nuclidic assignments find confirmation in our data.

We constructed partial decay schemes or added further information to: ^{144}Gd, ^{142m}Eu, $^{140,141m+g,143}$Sm, ^{139g,140m,142}Pm and ^{135,137}Nd.

All assignments are based on rules formulated in section III. The individual nuclei are discussed in detail in section IV, and a compilation of relevant data is given in the appendix (table 2).

II. Experiments

1. Methods

A variety of experimental methods, which by nature depend on the half-lives involved are classified as follows: Activities with half-lives of less than 30 s were measured with the detector being installed near the beam line and the target remaining in the irradiation position. These experiments without target transport can still be divided in two types: (i) Observation of radioactive decay in the sec-range, where after a proper time for target activation the decrease of the spectra was followed using different counting periods, (ii) Measurements with gated ion source of the cyclotron aimed at γ-rays related to the decay of short-lived isomers with half-lives between 20 μs and 1 s.

Longer lived activities($T_{1/2}$ > 30 s) are studied better in a low background area to which the irradiated target is brought by means

of pneumatic transport systems. There they were investigated in the same way as the shorter-lived activities of type (i). The longer lived activities correspond to the isomeric decay as well as to the ß-decay.

For radioisotopes with half-lives longer than 2 minutes, mass separations were possible. However, it should be remarked that the cost of highly-enriched target materials (e.g. ^{138}Ce, ^{136}Ce) needs consideration for single experiments.

The experiments and measurements performed in a general and systematic approach are the following:

a. Cross bombardements of various targets with α-particles and deuterons at various bombarding energies.

b. Multispectrum scaling of γ rays observed with a Ge(Li) detector and of conversion electrons with a Si(Li) detector in a special arrangement.

c. Gamma-gamma coincidences observed with two Ge(Li) detectors.

These measurements resulted in a large number (more than 10^3) of Ge(Li) and Si(Li) spectra, which are combined to a spectrum catalogue. In this catalogue one can follow the behaviour of a certain transition and see whether it appears or disappears when going from one set of parameters (target, α or d, E_{beam}, counting time) to another.

2. Facilities and Equipment

For the present cross bombardments, we used the external α-beam of the Karlsruhe Isochronous Cyclotron up to its maximum energy of 104 MeV. Though less frequently, a deuteron beam of 52 MeV has also been used. By means of Be absorbers in the beam-line the energy of the α-and d-beam has been varied, usually in steps of 5 or 10 MeV from 104 to 45 MeV for α particles and from 52 to 30 MeV for deuterons, respectively.

The oxides of the following stable isotopes were used as targets: ^{144}Sm (enriched to 95%), ^{142}Nd(98%), ^{141}Pr(100%), ^{140}Ce(88%), ^{139}La (99,9%), ^{138}Ce(20%), and ^{136}Ce(22%).

The targets are pressed disks of 0.5 mm thickness or powder layers of between 5 and 20 mg/cm^2. The disks are self-supporting; the powder layers are kept in-between aluminium foils of 7 µm or hostaphan foils of 10 µm thickness. At lower bombarding energies the thinner powder targets have been used, because of the increasing energy loss in the target layer. Powder targets have been used also for activations with the internal beam of the cyclotron. For measurements of conversion electrons we used targets of less than 1 mg/cm^2 evaporated on 0.1 mm Be. Mass separated isotopes were implanted into 20 µm aluminium foils.

Internal activation of targets requires transport times of the order of 3 min. For activations with the external beam a pneumatic system has been used,with typical transport times of 30 s. During the course of this work another system has been developed which transports a target within 10 s over 100 m towards the off-beam detection equipment (ref.6). In addition it was possible to transport the target by a slider within the vacuum of the beam guiding system from the irradiation position to a place at a distance of about 60 cm. Using this facility, target transport took about 1 s.

For measuring γ-ray spectra and γγ- coincidences, two Ge(Li) detectors were at our disposal, each with an effective volume of ~30 cm^3 and an energy resolution (FWHM) of 2.3 keV at 1.3 MeV. For some spectra we used a larger detector (60 cm^3) inside a NaI(Tl) anticoincidence ring for Compton suppression. For this arrangement the ratio of photo peak height to Compton peak height amounts up to 80:1 (due to the special geometry), while the ratio of photo peak to Compton plateau is about 150:1.

A number of activated samples have been studied with γγ-coincidence measurements.The pulses were digitized in two 4096 channel ADC's (Laben), interfaced to the CDC 3100 computer of the Cyclotron Laboratory, and the pairs of events were stored on magnetic tape. The time resolution 2 τ of the coincidence apparatus was 10-30 ns, the lower energy limit for registration of coincident γ-rays was about 40 keV.

For conversion electron measurements a so called "mini-orange" spectrometer has been developed. It consists of a Si(Li) detector of 2 or 5 mm depth, 200 mm^2 area, an energy resolution of ~ 3 keV (at 1 MeV) and a special magnetic filter for suppression of background from the target. A complete description of this instrument has been given in ref.7), while an improved version, which was used for most of the experiments of this paper is described in ref.8).

In order to obtain estimates for half-lives in the μs-range, the ion source of the cyclotron was pulsed. With a proper delay, the gates of two ADC's were opened for counting during the beam pulses and with a delay of up to 0.5 ms after the beam-on time. The minimum duration of the ion-source pulses was about 50 μs. The distance between two subsequent pulses had to be at least 120 μs in order to obtain correct ignition. By means of these measurements we were able to estimate half-lives $T_{1/2} > 20$ μs.

The electronic equipment contained standard NIM modules (Ortec, Canberra, Chronetics) and - in addition to the Laben ADC's interfaced to the CDC 3100 computer - a Geoscience analyser. This analyser was equipped with dual 4K ADC's and a magnetic tape unit with recording time of about 7 s.

3. Analysis

Part of the individual pulse height spectra have been searched by a peakfinding program. The energies and intensities of the peaks were determined by computer codes (e.g. ref.9). Energy calibration was readily obtained by a number of well-known transitions occuring in many of the present spectra. Efficiency calibration of the Ge(Li) detectors was known from measurements with a set of calibration sources from IAEA, that of the mini-orange spectrometer is taken from ref.8). Thus, the energy values of gamma and internal conversion peaks are mostly known to within 0.5 keV (for energies $\lesssim 1$ MeV), and the relative intensity values often to within less than 10 %.

Sometimes it appears that two or more γ-rays have the same intensity with respect to each other, for all available sets of the

parameters (target, projectile, beam energy and counting period). Those γ-rays with constant intensity ratios are then accepted as belonging to one and the same radioisotope. In practice, this concept of "radioisotope" is unambiguous as long as the corresponding peaks remain clearly visible in the spectra obtained with different values of Z_{Target} and E_α. Of course, the most distinct assignment of several γ-rays to the same activity comes from observation of γγ-coincidences.

Information on half-lives was obtained from multi-spectrum scaling in a small number (between 2 an 10) of subsequent counting periods. The influence of systematic errors (e.g. as due to dead-time corrections, varying geometry etc.) can be reduced by measuring the decrease of a radioisotope relative to the decay of a simultaneously produced activity of known half-life. Such activities are for instance those of table 1 in the appendix. Often the half-life and the activation curve of an activity is deduced only from the observation of its most prominent γ-ray transition.

It may be noted that a few half-lives lie close to each other: ^{143}Gd, ^{142}Gd, ^{139g}Sm, ^{138}Pm, ^{137}Pm cluster around two minutes and ^{140}Eu, ^{139m}Sm and $^{141m2}Eu$ around 20 s. However, the production of these activities with similar half-lives is largely different for various settings of the parameters Z_T and E_α.

III. Basic rules for assignments

The identification of unknown transitions can be divided into three degrees with increasing physical significance:

1) the nuclidic assignment
2) the placement of the transitions into a partial level scheme and
3) the assignment or at least restriction of spin values and parities of the deduced levels.

All of the nuclidic assignments and most of the others are supported by experimental and systematic as well as theoretical arguments. In the following they are surveyed in the form of mostly well-known rules and methods. These rules are far from complete and contain only the methods employed in our experiments especially. For easy reference the rules will be numbered, sometimes with the

addition "weak" (W). The latter rules must be weighed as tendencies. It is still possible, e.g. in cases of poor statistical accuracy, that a strong rule, which seems to have no exceptions, offers weak evidence for a certain conclusion.

1. Nuclidic assignments

Rule 1: Mass separations determine A

With a double-focussing magnetic mass separator it was possible to obtain a row of samples from adjacent isobars in an activated sample. The separation times were such that counting could start about 3 min after the end of the activation. With this time elapse it appears still feasible to study strongly produced isotopes like ^{143}Gd and ^{138}Pm, though they have half-lives of a few minutes only.

Rule 2 : Radioactive decay for the present region of nuclei is related to one A-chain. A complex decay curve, with growth, or with more than one decay constant, indicates a parent-relationship in this A-chain.

This rule ist trivial since the present radioisotopes lie far from any region with measurable α,p, or n emission; their half-lives are due to β^+-decay or isomeric decay.

Rule 3 : Excitation functions indicate A uniquely if Z is known from other sources of evidence. If for α-activations it is known that Z is equal to either $Z_{Target}+2$ or $Z_{Target}+1$, then the determination of A may be uncertain to within one unit.

An excitation function for a certain radioisotope is the plot of its relative yield against the energy E_α. The excitation functions given in the appendix (figs. A1-A4) show that a curve starts after a threshold energy. This energy is related to the Q value obtained from a mass table[10]. The reactions (α,xn+yp+zα) go through the formation of a compound nucleus and show no marked discontinuities for small changes in the values of Z_T, Z, A, E_α (and E_d). The excitation curves for reactions with y = z = 0 show peaking with a full width at half-maximum of 10 to 20 MeV. The maximum is shifted by

some 10 MeV for each additional neutron evaporated by the compound nucleus. In practice this shift is easy to observe with a few data points at different beam energies, if one is able to observe the excitation functions of a row of successive isotopes.

The weakened part of the rule applies to cases with z = 0 but y = 0,1 . Here the theoretically predicted shift between an $(\alpha,(x-1)n+p)$-curve and the respective (α,xn)-curve depends on x. When a few nucleons are evaporated only (e.g. $x \leq 4$) the $(\alpha,(x-1)n+p)$-curve peaks between the (α,xn)-curves. For large numbers of evaporated neutrons one expects the $(\alpha,(x-1)n+p)$- curve to coincide approximately with the (α,xn)-curve.

α-induced reactions leading to a final nucleus with $Z = Z_T$ are recognized uniquely if the excitation functions are measured over a wide energy range, because they show two distinct maxima due to the reactions $(\alpha,xn+\alpha)$ and $(\alpha,(x+2)n+2p)$. If one observes the maximum of the $(\alpha,xn+\alpha)$-reaction only, this excitation function can be mistaken for a reaction where (x+1) or (x+2) nucleons are evaporated.

Rule 4: A unique assignment of Z can be deduced from the spectra of conversion electrons.

With this rule we take advantage of the increase of the K-binding energy by about 1.6 keV, when Z increases by one unit. By observation of γ-rays and conversion electrons this Z-dependent binding energy can be observed when Ge(Li) and Si(Li) detectors are used. The energy resolution of these detectors allows energy determination within much less uncertainty than 1.6 keV. Also sufficient for a determination of Z is the energy difference between K and L conversion lines. However, the L line is often weaker and not clearly visible.

Rule 5 : Cross bombardment indicate Z and A

We use the term "cross bombardment " for the activation of various targets with α particles or deuterons at a sequence of different bombarding energies. It is a more general procedure than that of considering excitation functions for a single target alone (rule 3). Activation of isotonic targets gives an upper limit of Z, since

with α-activation: $Z \leq Z_T + 2$ and with d-activation: $Z \leq Z_T + 1$. This makes it of interest to look for the lowest value of Z_T, to be called Z_T^1, with which an activity searched is still produced. It eliminates for an assignment any Z larger than $Z_T^1 + 2$ for α- and larger than $Z_T^1 + 1$ for d-activation. In fact it suggests that $Z = Z_T^1 + 2$ or $Z = Z_T^1 + 1$, respectively. However, there may be exceptions to this suggested rule. They are due to the Yrast-mechanism discussed later on (rule 10). This mechanism enhances the production of high-spin-states. Thus, for a nucleus with two long lived states (e.g. an isomer and the groundstate), the low-spin state may not be produced in detectable amounts. As an example: 11-min ^{141g}Sm is produced by ^{144}Sm (α,6n+p) $^{141}Eu^{\beta^+}$, ^{141g}Sm, but not in detectable amounts by $^{142}Nd(\alpha,5n)$ ^{141g}Sm. Thus, for the production of the low spin isomer of ^{141}Sm the suggested rule $Z = Z_T^1 + 2$ is not valid.

In practice, the d-activations have been of limited use because the reaction (d,xn) does not reach much farther than x = 5 at the maximum energy available for the d-beam (52 MeV).

2. Level assignments

Rule 6 : Coincidence and energy sum relations determine the sequence of energy levels.

An observed sum relation (Ritz' principle) is a strong argument for constructing a γ-ray cascade with a cross-over transition, as long as only a few transitions are assigned to a decay. However, depending on the accuracy of the measured γ-ray energies, the probability for accidental sum relations increases with the number of observed γ-rays. It is advisable to deduce level assignments from additional coincidence measurements. However for γγ-coincidences caution is still needed, since an unobserved low-energy γ-ray transition may be present between two coincident transitions. At present the ordering of cascading transitions with no cross-over transition can sometimes be derived from striking differences in γ-ray intensities (e.g. when a ß-ray branch feeds the first excited state).

Rule 7(W): The strongest transitions within a decay scheme which are not in coincidence with transitions of comparable intensities indicate an excited level above the ground-state or an isomeric level at the energy of the γ-ray.

Although this rule is applied frequently, one has to take into account the possibility that the intensity of a strong transition between highly excited states may split up into many weaker transitions. However, such a case may often be excluded by additional sources of evidence (e.g. systematic trends).

3. Spin and parity assignments

There are many observable nuclear properties which depend on the spin and parity (I^{π}) of the states involved. We mention log ft-values of ß-ray branches, conversion coefficients,(isomeric) half-lives and the production mechanism. Besides this there exist coupling rules in the framework of the basic shell-model.

Rule 8 : Log ft-values can be estimated for ß-ray branches with deduced partial half-lives if the ß-ray endpoint energy is derived from experiment or from calculated mass tables[10].

The half-lives of the present radioisotopes always have been measured. Although specific ß-ray measurements have not yet been performed, it still remains possible to estimate the relative intensities of pronounced ß-ray branches. The ß-ray feeding of different levels is deduced from the intensity balance of the populating and depopulating radiation of these levels. To obtain the ß-ray branching into the different excited states one has to determine the feeding of the groundstate. This can be deduced from: (i) the intensity of the annihilation radiation or (ii) from in-beam observation of γ-rays with known relative intensities in the parent nucleus (prompt) as well as in the daughter nucleus (delayed). Since we are interested only in a rough determination of log ft-values, it is sufficient to take the disintegration energies from calculated mass tables, e.g. from Garvey et. al.[10]. For all measured values of disintegration energies the Garvey tables are accurate to about 0.2 MeV.

Farther from the valley of stability the uncertainty is of course increasing, but for the present nuclei it seems safe to assume that the overall uncertainty will not be much more than 0.5 MeV. With the deduced partial half-lives and disintegration energies the log ft-values can be obtained from histograms as given in ref.[11], with consideration of the uncertainties in both E^{o}_{β} and $T_{1/2}$. The electron capture can be taken into account by using theoretical β^{+}/EC ratios after Zweifel[12].

Rule 9 : a) If $4.0 < \log ft < 5.8$, the transition is allowed.
b) For nuclei in this mass region $0^{+} \rightarrow 0^{+}$ transitions will proceed only with large hindrance factors.($\log ft > 7$)
c) If $6.0 < \log ft < 10.6$, the transition is allowed or first forbidden. For $\log ft > 7$ first forbidden transitions become more likely.
d) If $\log f_1 t < 7.6$, the transition is not unique first forbidden.

These rules[13] restrict the possibilities for a difference in spin and parity between levels connected by ß-decay. In the present mass region log ft-values between 4.0 and 5.8 occur mainly for allowed transitions between single particle states. Allowed ß-decay to excited levels often seems to be strongly hindered because of their collective nature, resulting in log ft-values between 6 and 7. Allowed $0^{+} \rightarrow 0^{+}$ ß-transitions are caused solely by the Fermi matrix element, which requires that the transitions have $\Delta T=0$. In medium-weight and heavy nuclei the isobaric spin T is a good quantum number. In these nuclei the Fermi strength is concentrated in an energy-forbidden transition to an isobaric analogue state; therefore, $0^{+} \rightarrow 0^{+}$ ß-transitions to low-lying states are highly hindered (ref.14).
The rule 9c) includes the fact that it is not possible to distinguish between allowed and first forbidden transitions merely by means of log ft-values. Regarding transitions between single particle states a log ft-value larger than 6.5 is likely to indicate a forbidden transition. The log $f_1 t$-values of rule 9d) can be calculated from usual log ft-values according to a formula derived by Davidson[15].

Rule 10 : Measured conversion coefficients α_K, K/L and L/M ratios restrict the number of possible multipolarity assignments.

Our measurements of conversion electrons restrict the multipolarity of a transition often to one or two possibilities. The higher multipolarities (e.g.E3, M4) could be determined uniquely in most cases when they were observed. However, transitions with not too different conversion coefficients (e.g. M1, E2) often cannot be distinguished. Small admixtures can never be excluded due to the relatively large errors in the intensities and in the transmission curves of the electron spectrometer.

Rule 11: Enhancement factors relative to the Weißkopf-estimate restrict the possible multipolarities.

This rule is based on experimentally found limits cited in ref.13) from which one can exclude special multipolarities in the following manner:

If the γ-half-life is:	The transition is not:
$< 0.1 \cdot T_W(M1)$	M1
$< 1.0 \cdot T_W(M2)$	M2
$< 0.1 \cdot T_W(M3)$	M3
$< 0.033 \cdot T_W(M4)$	M4
$< 100 \cdot T_W(E1)$	E1
$< 0.001 \cdot T_W(E2)$	E2
$< 0.01 \cdot T_W(E3)$	E3

Here, T_W means the Weißkopf-estimate of the half-life. When determining the γ-half-life of a level one has to estimate the other contributions to the total half-life by internal conversion, ß-decay and electron capture from various graphs in handbooks[11]. For half- lives shorter than 1 s the latter two can be neglected. Cascading γ-rays, which are judged to be in prompt coincidence without significant losses of coincidences, give $T_{1/2} \lesssim 10$ ns for the intermediate state.

Rule 12: The observation of prompt coincidences with $2\tau \approx 20$ ns excludes the following assignments of multipolarities for the lower members of the γ-ray cascade:

If E_γ is:		The multipolarity is not:
(< 50)	keV	E2
< 600	keV	M2
< 900	keV	E3
< 3000	keV	M3
< 7000	keV	M4

For E2 transitions in the present mass region no enhancement factors as large as 10^3 have ever been observed. Using a factor of 100 as an upper limit, one can exclude an E2 assignment for the lower of two coincident γ-rays of less than 50 keV. As an example, the 49 keV transition in ^{143}Sm cannot be a pure E2-transition, because it connects the two coincident transitions of 209 keV and 181 keV.

Rule 13(W): Branching ratios and non-observed cross-over transitions limit the spin difference between the upper and lower level of an observed cascade.

The absence of branching of γ-rays depopulating higher excited states can always be stated only within the statistical limits.When the decay scheme of a nucleus is well established it is useful to compare the values or limits for branching ratios with those known from neighboring nuclei. Often this may offer systematic trends, which support the constructed level scheme.

Rule 14 : The α-and d-activations produce preferentially states with high spin.

After the formation of a highly excited compound nucleus several neutrons and sometimes a few charged particles are evaporated. Below the threshold for particle emission the residual energy is de-excited via γ-rays. This behaviour can be described with the aid of the so-called "Yrast"-curve[16] (s. fig. 2). This curve represents the levels of lowest excitation energy with a specific angular momentum. Reactions with α-particles of 104 MeV lead to an initial compound nucleus with an angular momentum of ~25 ħ,which corresponds to the hatched area of fig. 2. The following neutron evaporation gives a

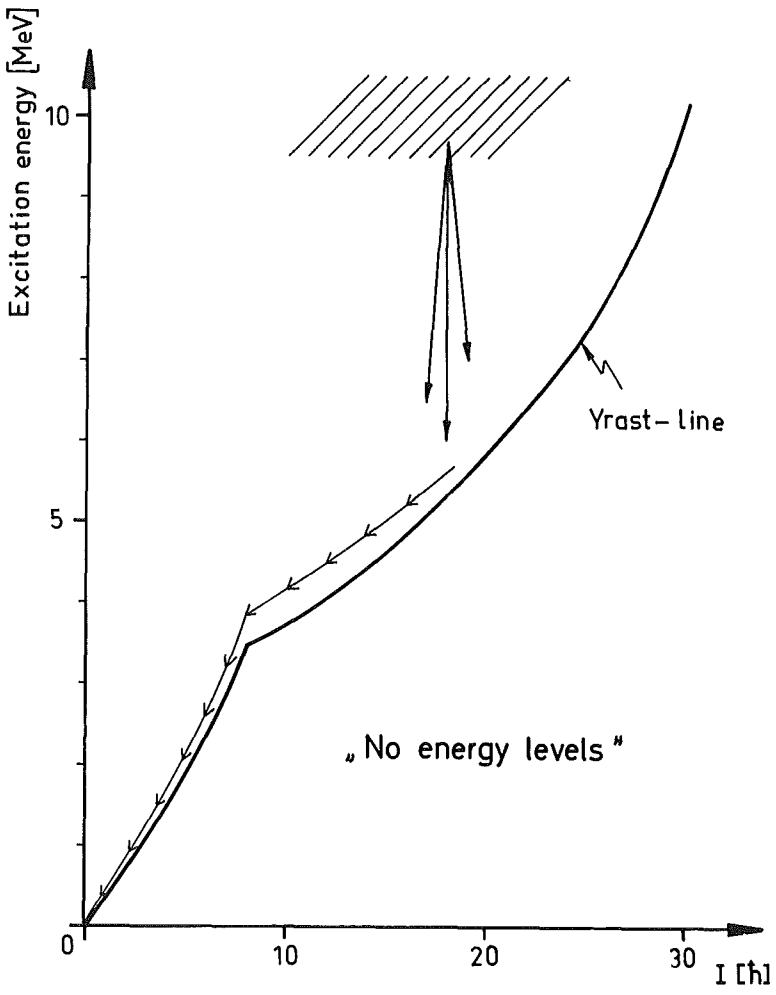

Fig. 2: Schematic "Yrast" - diagram

considerable reduction of energy, but almost no change in angular momentum. The lowering of angular momentum comes stepwise from a following de-excitation by a band of cascading γ-rays, until the nucleus arrives at a longer-lived isomeric state or at its ground-state. If there are more longer-lived states besides the ground-state, then the state with highest spin will be favoured. Isomeric ratios for most of the present nuclei are given in the appendix (table 3).

Rule 15 : Often the low spin ß-decay of a nucleus A_Z can be studied by producing the parent nucleus A_{Z+1} which feeds the low spin isomer of A_Z via ß-decay.

This rule applies to nuclei which have a high spin isomer, which decays by ß-decay and blocks the feeding of the low spin isomer by the compound nuclear reaction. If, however, the parent nucleus has a low spin groundstate, which is strongly fed by the"Yrast"-cascade, the ß-decay populates low spin states in the daughter and makes a

study of the low spin ß-decay possible.

Rule 16 : Isomerism occurs in all odd-mass nuclei of fig. 1.
a) The odd-neutron nuclei tend to have $11/2^-(9/2^-)$-isomers with half-lives longer than 1 s.
b) The odd-proton nuclei, not too far from the closed shells, tend to have $11/2^-$ - isomers with half-lives between 10^{-6} and 10^{-9}s.

The isomerism can be explained by the shell model states as indicated in the inset of fig. 1; the active protons are in the 1g7/2, 2d5/2 or 1h11/2 shells and the neutrons or neutron holes in the (1g7/2), 3s1/2, 2d3/2 and 1h11/2 shells. In many cases the isomerism is caused by the 11/2 orbitals but it manifests itself differently for the odd-neutron and odd-proton nuclei.

The odd-neutron nuclei often have low-lying states with I^π equal to $1/2^+, 3/2^+$ or $5/2^+$. For N=81 the isomeric transitions are of the type M4 ($11/2^- \rightarrow 3/2^+$) with half-lives around 1 min. For N=79 the state with $11/2^-$ is lowered and is depopulated by ß-decay mainly, with $T_{1/2} >> 1$ min. Note that in ^{143}Gd only the high spin isomer has been observed, while its low spin state is hard to produce by our present possibilities of activation (rule 14). For N=77 the $11/2^-$ - levels are found at relatively high energies again, giving rise to E3($11/2^- \rightarrow 5/2^+$)-transitions with half-lives of several seconds. Farther from the shell closure at N=82 a $9/2^-$ -level occurs below the $11/2^-$ - level, resulting in an isomeric state or even the groundstate.The systematic behaviour of these $9/2^-$ states is shown in fig. 5c.

The odd-proton nuclei are characterized by the subsequent filling of the 1g7/2 and 2d5/2 shells. Thus, the $11/2^-$ - particle state lies often above the $7/2^+$ - level, resulting in an M2 transition of medium energy: e.g. in ^{139}Pm at 708 keV ($T_{1/2}$ = 40 ns), in ^{143}Eu at 112 keV ($T_{1/2} > 30$ ns). In all cases the $11/2^- \rightarrow 7/2^+$ isomeric transition is observed in cascade with the $7/2^+ \rightarrow 5/2^+$ transition. With increasing distance from N=82 the $11/2^-$ level is moving towards and below the $7/2^+$ level. This results in an E3

transition to the $5/2^+$ state e.g. for ^{139m}Pm, with a respective longer half-life. In ^{137}Pm a very low-lying $11/2^-$ level is expected from level systematics which can even be the groundstate.

Rule 17 (W) : The even-even nuclei tend to have no isomeric states with $T_{1/2} > 1$ s.

In even-even nuclei states of high spin and negative parity are often observed at somewhat higher energies (about 2500 keV). These states are mostly due to two quasiparticle configurations consisting of a h 11/2 - nucleon coupled to another one in a positive parity orbit (e.g. d5/2). Sometimes the energy gap between such a level and one of the quasirotational groundstate band becomes narrow. Then the half-life of the negative parity state can be in the µs- or ms-range. In ^{140}Nd a 7^- state at 2216 keV decays with $T_{1/2}$ = 0.6 ms to the 4^+ level at 1797 keV. In ^{140}Sm we obtained evidence for a longer-lived state above the 4^+ level at 1246 keV with a half-life between 10 and 50 µs (see sect. IV, 5). In ^{136}Ba the 7^- state at 2040 keV and the 4^+ state at 1870 keV lie closely together resulting in a half-life of 320 ms. Though the rule may not be considered a strong one, it seems to have no exceptions in the present mass region.

Rule 18: Double isomerism with half-lives longer than 1 s will not occur in odd-mass and even-even nuclei.

Isomerism with half-lives longer than 1s is due to the fact that the isomeric state has a spin which differs from that of all lower states by three or more units. The absence of double isomerism for odd-neutron,odd-proton and even-even nuclei shows that-except for the lowest excitation energies with small level density-there are in general no increases by more than two units of spin between successive "Yrast"-levels. Throughout the complete chart of nuclei such double isomerism has been observed only for a few odd-odd nuclei like ^{124}Sb or ^{192}Ir.

Rule 19: The groundstate spin of odd-odd nuclei with A < 150 can be predicted from the angular momenta of the last proton and neutron.

This rule, which has been derived in detail by Peker et.al.[17] can

be subdivided into the following cases with respect to the configuration of the last odd nucleons:

a) If the configuration is of the type particle-particle or hole-hole, and if: $j_1 = \ell_1 \pm 1/2$, $j_2 = \ell_2 \mp 1/2$, then $I = |j_1 - j_2|$

but if: $j_1 = \ell_1 \pm 1/2$, $j_2 = \ell_2 \pm 1/2$, then $I = |j_1 \pm j_2|$

b) If the configuration is of the type particle-hole then:

$I = j_1 + j_2 + 1$

c) For configurations with a half-filled proton or neutron shell one has: $\Pi = (-1)^{I+1}$ in the special case with $j_1 = 1/2$ or $j_2 = 1/2$.

In all cases j_1 and j_2 represent the total angular momenta and ℓ_1 and ℓ_2 the orbital angular momenta of the last neutron and proton, respectively. Π is the parity of the wave function of the configuration.

By means of these rules all of the groundstate spins of odd-odd nuclei in fig. 1 can be explained except for ^{136}Pr. The 2^+ groundstate of this nucleus may be explained from the Gallagher - Moszkowski rules[18] for strongly deformed nuclei which are expected to be relevant for this and the neighboring odd-odd nuclei further away from the closed shells. In general, one cannot expect the Peker rules to give unique predictions for all nuclei far from closed shells, since the levels in these nuclei lie close together. Then predictions for their ordering and therefore for the assignment of the groundstate become difficult.

4. Level systematics

The systematic behaviour of corresponding energy levels throughout a whole region of nuclei can give important predictions for the position of the level under consideration in yet unknown nuclei. An essential precondition for inter- or extrapolations is the smoothness of such systematic trends.

Rule 20 : The energy of the first 2^+ level in even-even nuclei can be predicted from systematic trends of adjacent known nuclei to within an accuracy of 30 keV.

The systematic trend of the 2^+ transition is given in fig. 3.

This transition is identified now in almost all of the even-even nuclei of this mass region and shows an exceptionally smooth pattern. The $2^+ \rightarrow 0^+$ transitions are outstanding in prompt in-beam spectra as well as in the γ-ray spectra from radioactive decay.

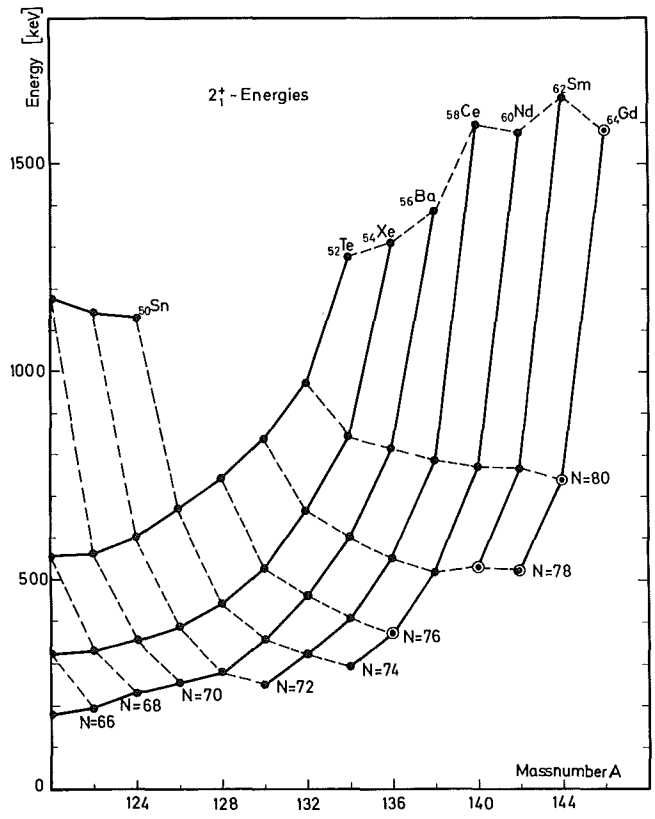

Fig. 3: Systematics of the first 2^+ level in even-even nuclei. The dots surrounded by circles refer to assignments of the present work.

Rule 21(W) : For even-even nuclei the energy of $4^+, 6^+, 8^+, 2_2^+$ and 3^+ levels above the first 2^+ state can be predicted from systematic trends to within 50 to 100 keV.

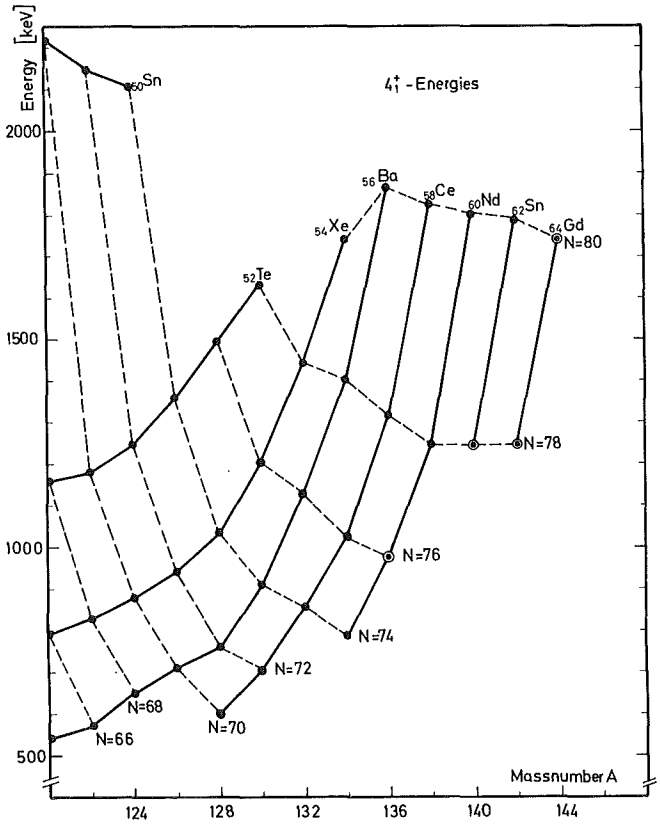

4 a:

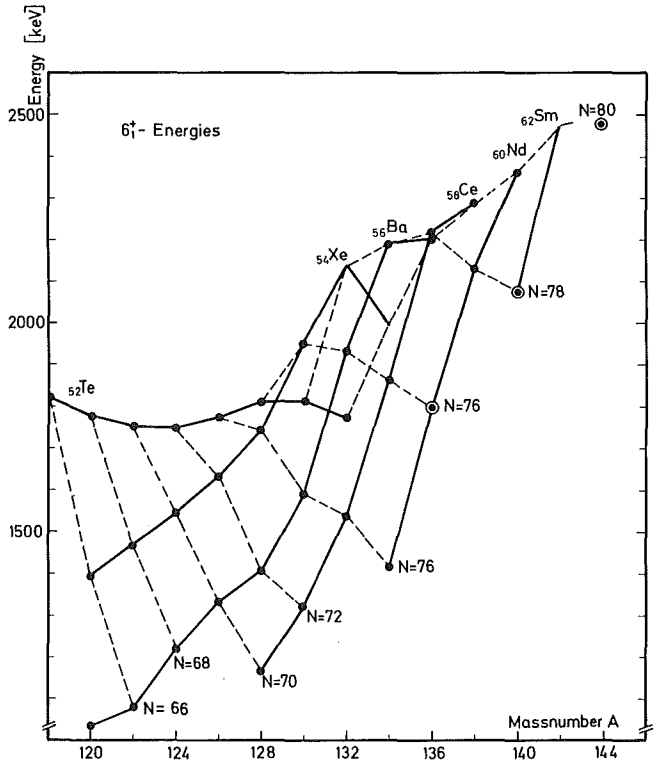

4 b:

Fig. 4a -f: Systematics of levels in the even-even nuclei. The dots surrounded by circles refer to assignments of the present work.

4 c:

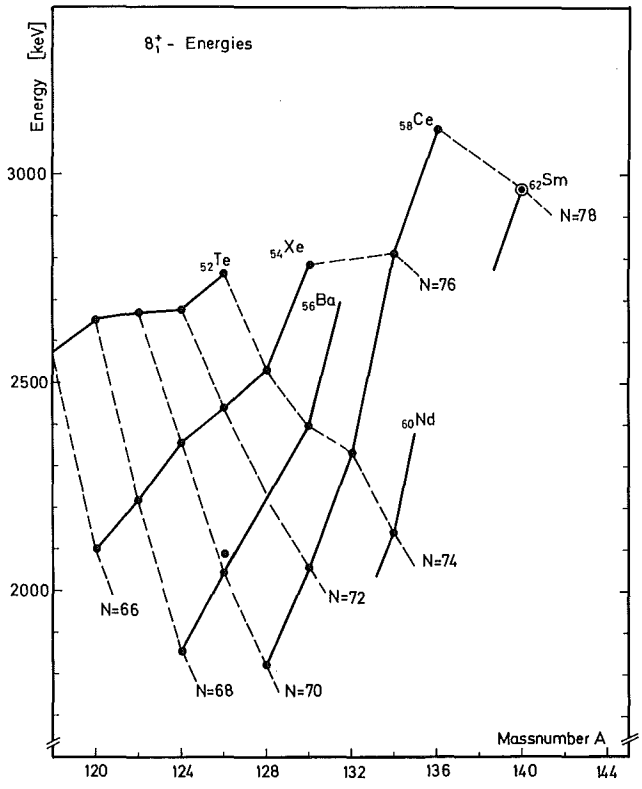
8$_1^+$ - Energies
Energy [keV]
3000
2500
2000
$_{58}$Ce
$_{62}$Sm
N=78
$_{54}$Xe
N=76
$_{52}$Te
$_{56}$Ba
$_{60}$Nd
N=74
N=72
N=66
N=68
N=70
Massnumber A
120
124
128
132
136
140
144

4 d:

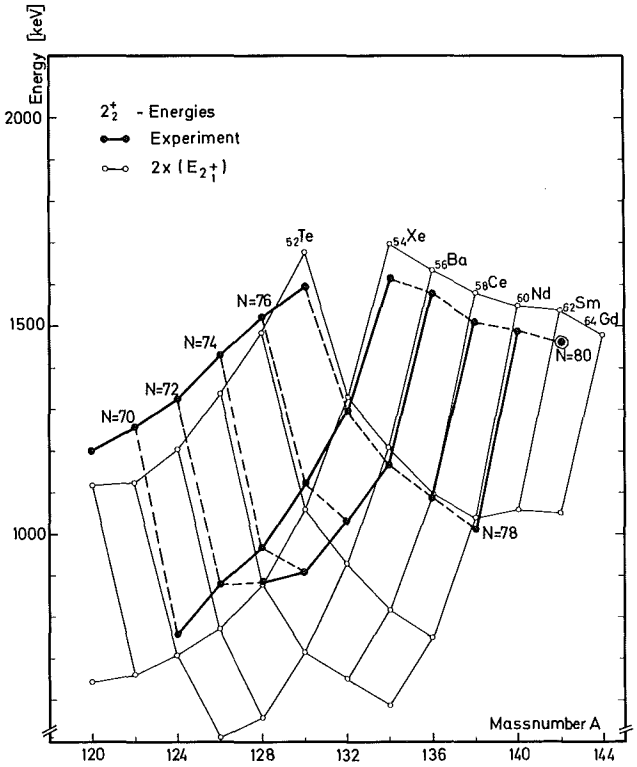
Energy [keV]
2000
1500
1000
2$_2^+$ - Energies
Experiment
2x (E$_{2_1^+}$)
$_{52}$Te
$_{54}$Xe
$_{56}$Ba
$_{58}$Ce
$_{60}$Nd
$_{62}$Sm
$_{64}$Gd
N=80
N=76
N=74
N=72
N=70
N=78
Massnumber A
120
124
128
132
136
140
144

4 e:

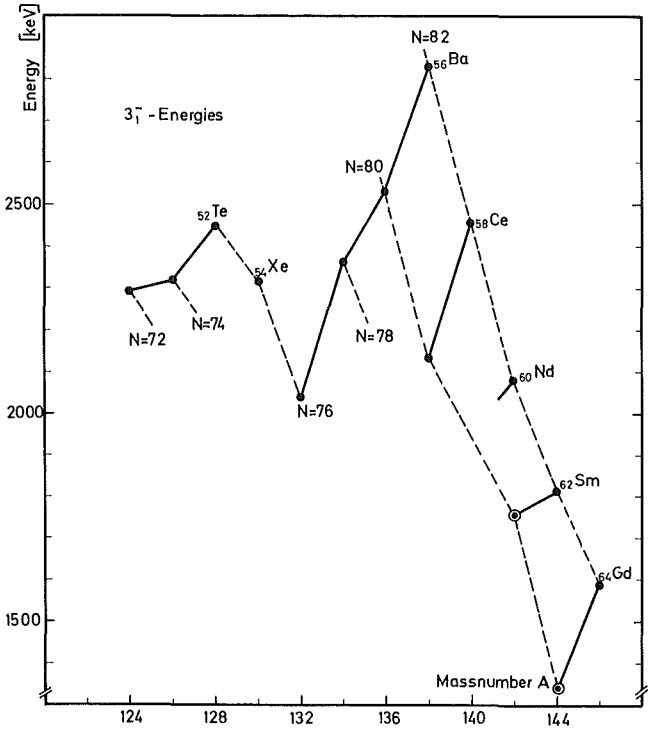
Energy [keV]
3_1^- -Energies
N=82
56Ba
N=80
52Te
58Ce
54Xe
N=74
N=72
N=78
60Nd
N=76
62Sm
64Gd
Massnumber A
2500
2000
1500
124
128
132
136
140
144

4 f:

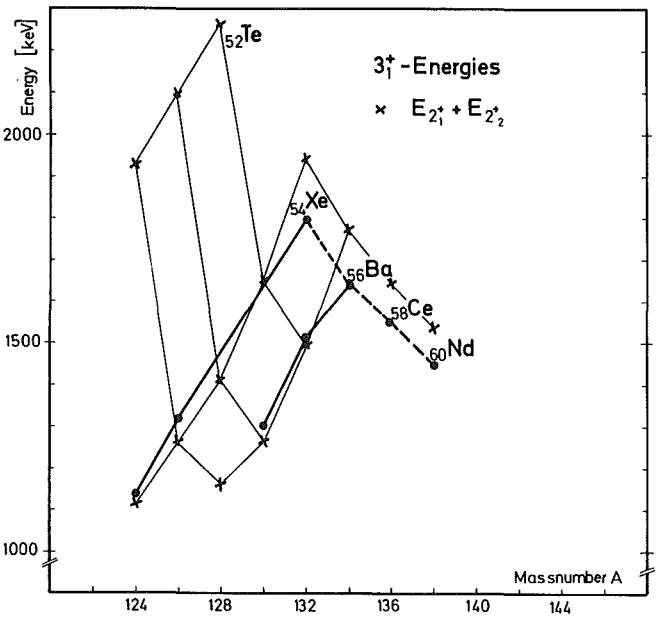
Energy [keV]
52Te
3_1^+ -Energies
× $E_{2_1^+} + E_{2_2^+}$
54Xe
56Ba
58Ce
60Nd
Massnumber A
2000
1500
1000
124
128
132
136
140
144

The systematic trends of further energy levels of even-even nuclei, which have been studied in our experiments, are shown in figs. 4a-f. In cases where deviations from a smooth behaviour occur, one finds these deviations to be systematical. Often they can be explained in terms of nuclear models (e.g. the 6^+ levels of the Te-isotopes see fig. 4b and ref. 19). When the predictions of levels are not so accurate one needs, in general, further support for identification (e.g. the monotonous decrease of intensity between members of the groundstate band or coincidence measurements).

Rule 22 (W) : In odd-neutron nuclei the energy difference between $1/2^+ - 3/2^+$, $5/2^+ - 3/2^+$, $9/2^- - 3/2^+$ and $11/2^- - 3/2^+$ states can be predicted from the trends in neighboring nuclei to within 50 to 100 keV; in odd-proton nuclei the $3/2^+ - 5/2^+$, $7/2^+ - 5/2^+$ and $11/2^- - 5/2^+$ differences have the same error limits, the $1/2^+ - 5/2^+$ and $9/2^+ - 5/2^+$ distances can be predicted in most cases only within large errors.

The odd nuclei have many levels with equal spin and parity. They are due to collective as well as single particle excitations. Only for the lowest of these levels systematic trends could be established for a sufficient number of cases (s. figs. 5a-d and 6a-f). In general, the equivalence for two levels of equal spin in adjacent nuclei cannot be proved. Therefore, only the first excited levels (e.g. $1/2^+$, $3/2^+$ in odd-neutron nuclei, $5/2^+$, $7/2^+$ in odd-proton nuclei) and the $11/2^-$ -level could be distinguished uniquely resulting in a clear and smooth systematics. However, the unsteady behaviour of the first $1/2^+$ state (s. fig. 6d) in odd-proton nuclei indicates that in this case probably the equivalent level was not taken everytime .

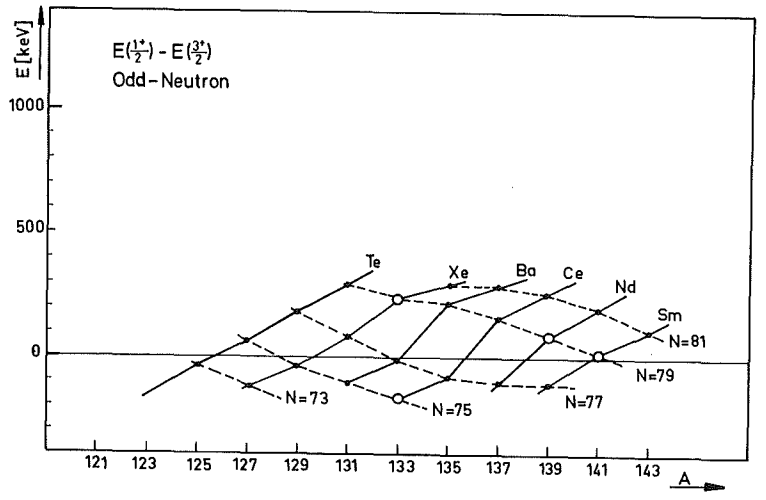

5 a:

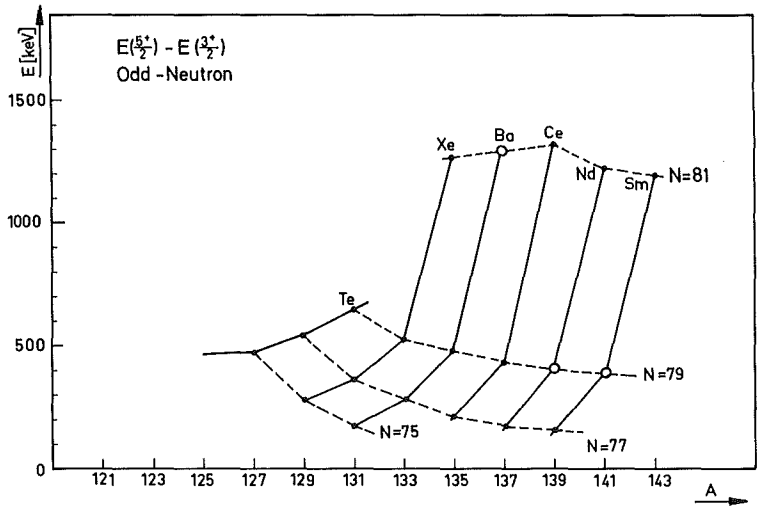

5 b:

Figures 5a - d : Systematics of energy differences between the lowest levels in odd-neutron nuclei. Open circles correspond to predictions from systematics.

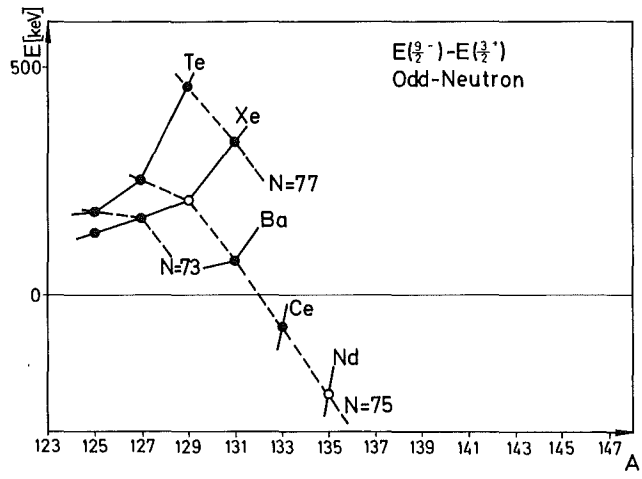
E[keV]
500
0
E(9/2⁻)-E(3/2⁺)
Odd-Neutron
Te
Xe
N=77
Ba
N=73
Ce
Nd
N=75
123 125 127 129 131 133 135 137 139 141 143 145 147
A

5 c:

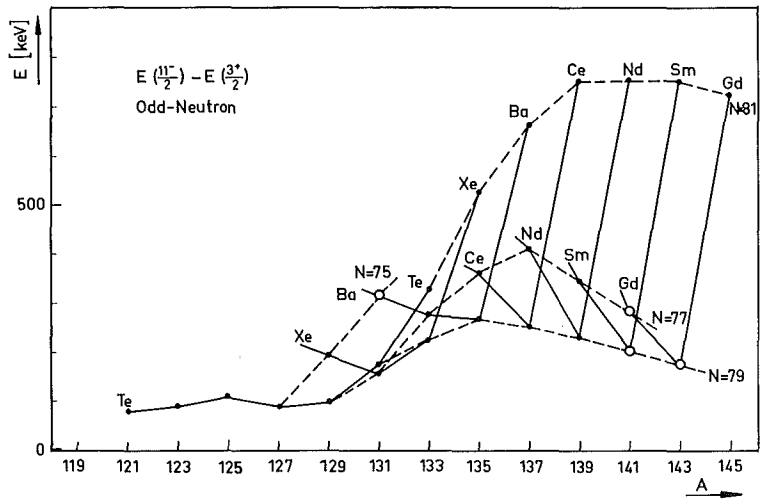
E [keV]
500
0
E (11/2⁻) - E (3/2⁺)
Odd-Neutron
Ce
Nd
Sm
Gd
N=81
Ba
Xe
Nd
Ce
Sm
N=75
Te
Ba
Gd
Xe
N=77
N=79
Te
119 121 123 125 127 129 131 133 135 137 139 141 143 145
A

5 d:

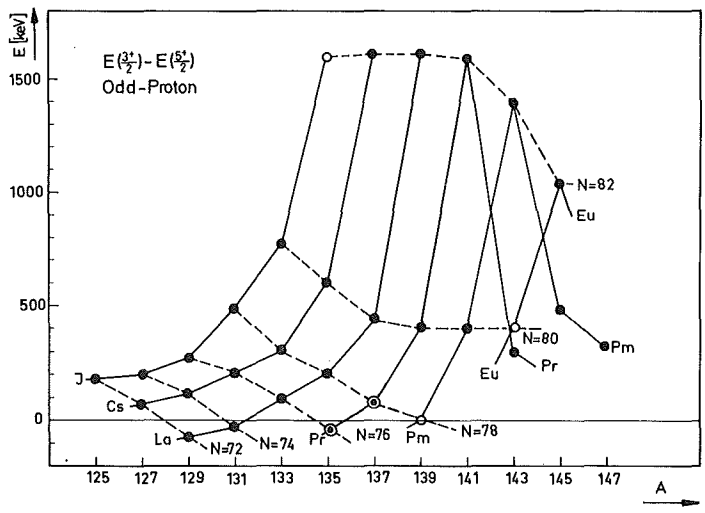

6 a:

Fig. 6 a - e: Systematics of the energy differences between the lowest levels in odd-proton nuclei. Open circles correspond to predictions from systematics. Dots surrounded by circles refer to assignments of the present work.

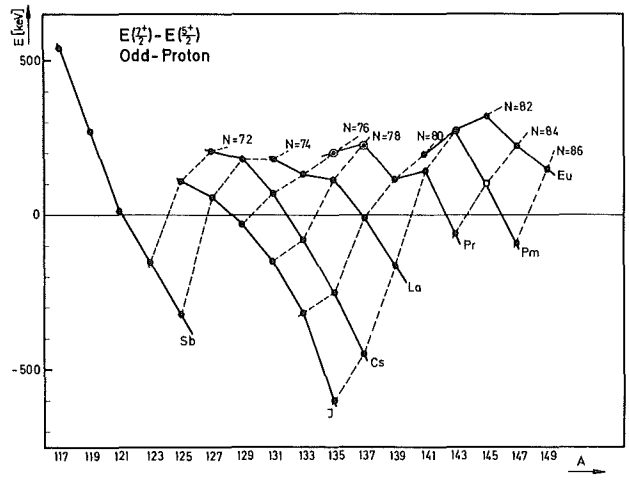

6 b:

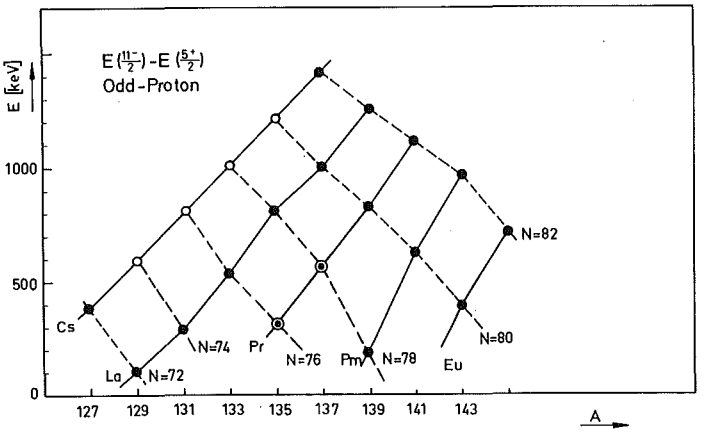
E [keV]
$E(\frac{11^-}{2}) - E(\frac{5^+}{2})$
Odd-Proton
1000
500
0
Cs
La
N=72
N=74
Pr
N=76
Pm
N=78
Eu
N=80
N=82
127 129 131 133 135 137 139 141 143
A

6 c:

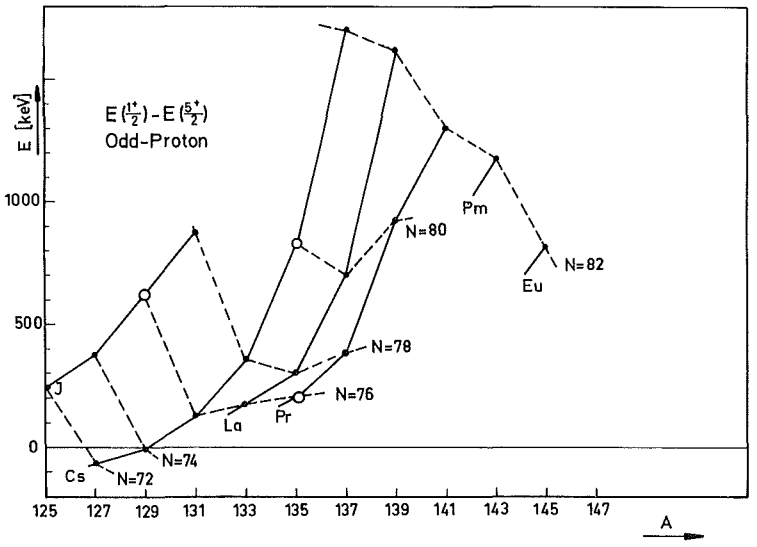
E [keV]
$E(\frac{1^+}{2}) - E(\frac{5^+}{2})$
Odd-Proton
1000
500
0
J
Cs
N=72
N=74
La
Pr
N=76
N=78
N=80
Pm
Eu
N=82
125 127 129 131 133 135 137 139 141 143 145 147
A

6 d:

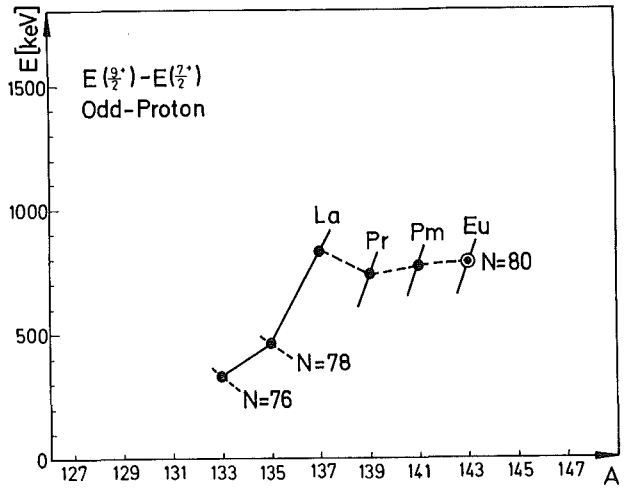
E [keV]
$E(\frac{9^+}{2}) - E(\frac{7^+}{2})$
Odd-Proton
1500
1000
500
0
N=76
N=78
La
Pr
Pm
Eu
N=80
127 129 131 133 135 137 139 141 143 145 147
A

6 e:

IV. Discussion of Individual Nuclides

In this section all new nuclides as well as known nuclides with essentially supplemented data will be discussed in detail. The nuclides are arranged in mass chains with decreasing A. The combination of rows of equal A facilitates a simultaneous discussion of more than two members of a decay chain (see e.g. A = 142). Within each A chain the discussion proceeds with increasing Z.

For the individual nuclides we describe: (i) the nuclidic assignments,(ii) the decay scheme and (iii) spin and parity assignments based on the rules formulated in the previous chapter. The rules will be cited only in cases of special relevance.

The proposed decay schemes contain the information from our experiments as well as data from other references. All energies are given in keV without error specifications. The exact values and errors are compiled in the appendix. The relative intensities refer to γ-ray intensities (without conversion) and are normalized to the transition marked by "norm". Transitions which could not be observed (e.g. because of their low energy) but which could be deduced from coincidence measurements and sum relations are marked by "c". Their (γ+e)-intensities are deduced from intensity balances. γ-rays assigned to a special decay, which could not be placed in the decay scheme, are quoted on top of the respective level scheme with relative intensities in parentheses.

Due to similar conversion coefficients we often were not able to distinguish between e.g. M1, E2 or mixtures of both. Those transitions are marked by M1 + E2, while M1(+E2) indicates a clear M1 component excluding a pure E2 multipolarity.

On the right-hand side of all decay schemes the disintegration energies are given as calculated from the mass tables of Garvey et.al.[10]. The log ft-values were determined from an intensity balance according to rule 8 (sect. III).

In some cases, especially for shorter-lived radioisotopes, half-lives could be obtained with large errors only. This fact is indicated in the figure using a "∿" sign for an accuracy of about 50 %.

Observed coincidences are marked by the usual dots. If relevant, matrices of coincident transitions are given in the text.

Throughout this paper information from in-beam measurements is quoted only if needed for an assignment or proof. For instance, this is the case for radioisotopes decaying predominantly to the groundstate of the daughter nucleus. Then the often weak ß-ray branches to other levels can be deduced from in-beam observation of an almost 100 % γ-ray transition which populates the parent state. Those transitions from in-beam measurements are given in the figures by arrows without a level of origin.

To the right of the experimental decay schemes, the predictions form level systematics are shown. They are not to be taken as a general proof for experimental assignments, but in all cases there is good agreement. Extrapolated level energies are given with error limits in brackets. The reference states of the systematics ($3/2^+$-state for odd-neutron nuclei and $5/2^+$-state for odd-proton nuclei) are given with brackets but without errors, in cases where they are not the groundstate. Consequently, the groundstate is then given with the associated error limit. The estimated errors are related to the uncertainties expected for the individual level systematics. They depend on the smoothness and number of data points of the systematics and rely on having used equivalent levels of the individual nuclei.

1) The decay chain A = 144

The decay chains with even mass number often proceed by dominant ß-decays between the groundstates ($0^+ \rightarrow 1^+ \rightarrow 0^+$). Consequently, the γ-ray transitions following the ß-decay are few and weak, as it is typical for the present case with A = 144.

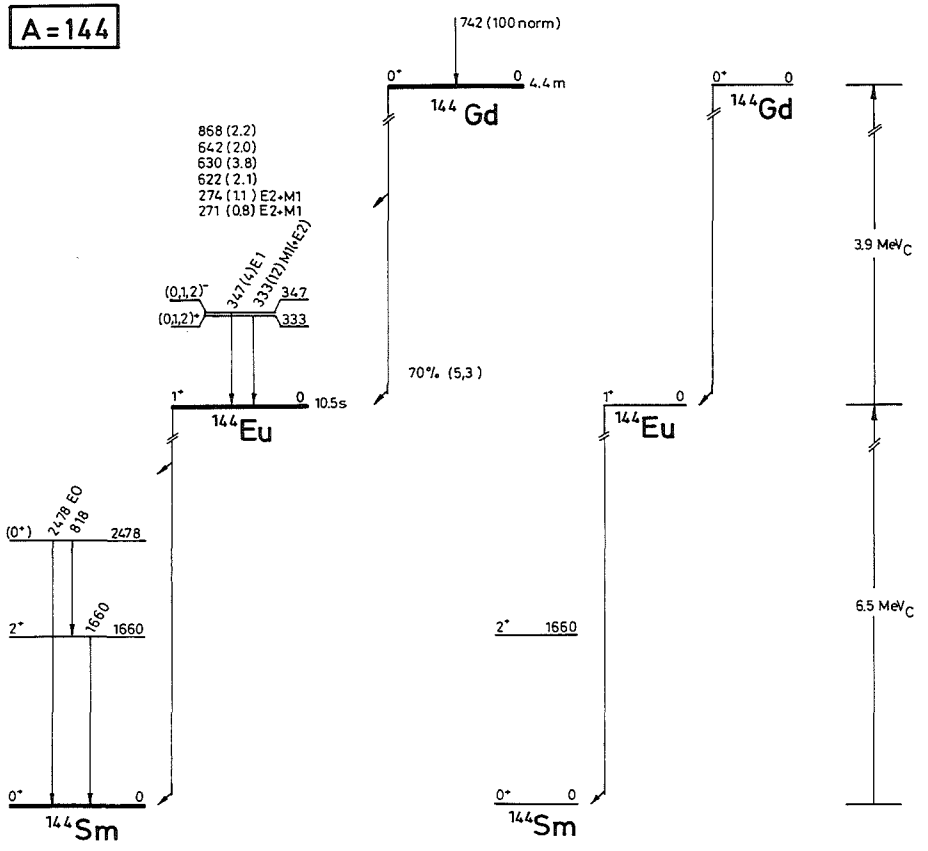

Fig. 7 : The decay chain A = 144. The ß-decay of ^{144}Eu to ^{144}Sm is described in ref. 21).

^{144}Gd

Arlt et al.[20] determined the half-life of ^{144}Gd from the decrease of the ß-spectrum to be 4.9 ± 0.4 min. The subsequent decay of ^{144}Eu to ^{144}Sm has been studied by Geiger et al.[21], who proposed the decay scheme shown in fig. 7. In order to obtain further information on this mass chain we performed mass separations after producing ^{144}Gd via the reaction ^{144}Sm(α,4n)^{144}Gd. The measured γ-ray and conversion electron spectra are shown in fig. 8. While we could determine the Z-value of the transitions with 271, 274, 333 and 347 keV from a comparison of the γ-ray and conversion electron spectra (rule 4) to be 63 (Eu), an assignment of the transitions with 622, 630, 642 and 868 keV to Europium resulted from comparison with the Ge(Li)-spectra given in ref.21). From the decay rate of the transition at 333 keV we determined the half-life of ^{144}Gd to be (4.4 ± 0.3) min. The 333 keV transition occurs in approximately 12 % of the ^{144}Gd decays measured relative to the prompt $2^+ \rightarrow 0^+$ transition of ^{144}Gd. Since the other transitions are rather weak, ^{144}Gd decays predominantly with an allowed ß-decay into the 1^+ groundstate of ^{144}Eu. The 333 and 347 keV γ-rays were strong transitions during in-beam studies of ^{144}Eu. We performed a γγ-coincidence measurement when irradiating ^{144}Sm with 70 MeV α-particles. The coincidence spectra contained γ-transitions of ^{144}Eu from the prompt production as well as from the ß-decay of ^{144}Gd. Because the 333 keV and 347 keV transitions were not observed in coindidence, we adopted levels at 333 and 347 keV (s. fig. 7). From the measured conversion coefficients the I^π-values of the levels could be confined to the values given in fig. 7, since the groundstate of ^{144}Eu has the spin 1^+. While the placement of the levels at 333 and 347 keV agrees with the results of a recent publication by Funke et al [59], their assignment of an I^π-value of 3^+ to the level at 347 keV contradicts our experimental data.

2) The decay chain A = 143

The members of this mass chain (s. fig. 9) could be produced strongly when irradiating ^{144}Sm with α-particles of about 80 MeV

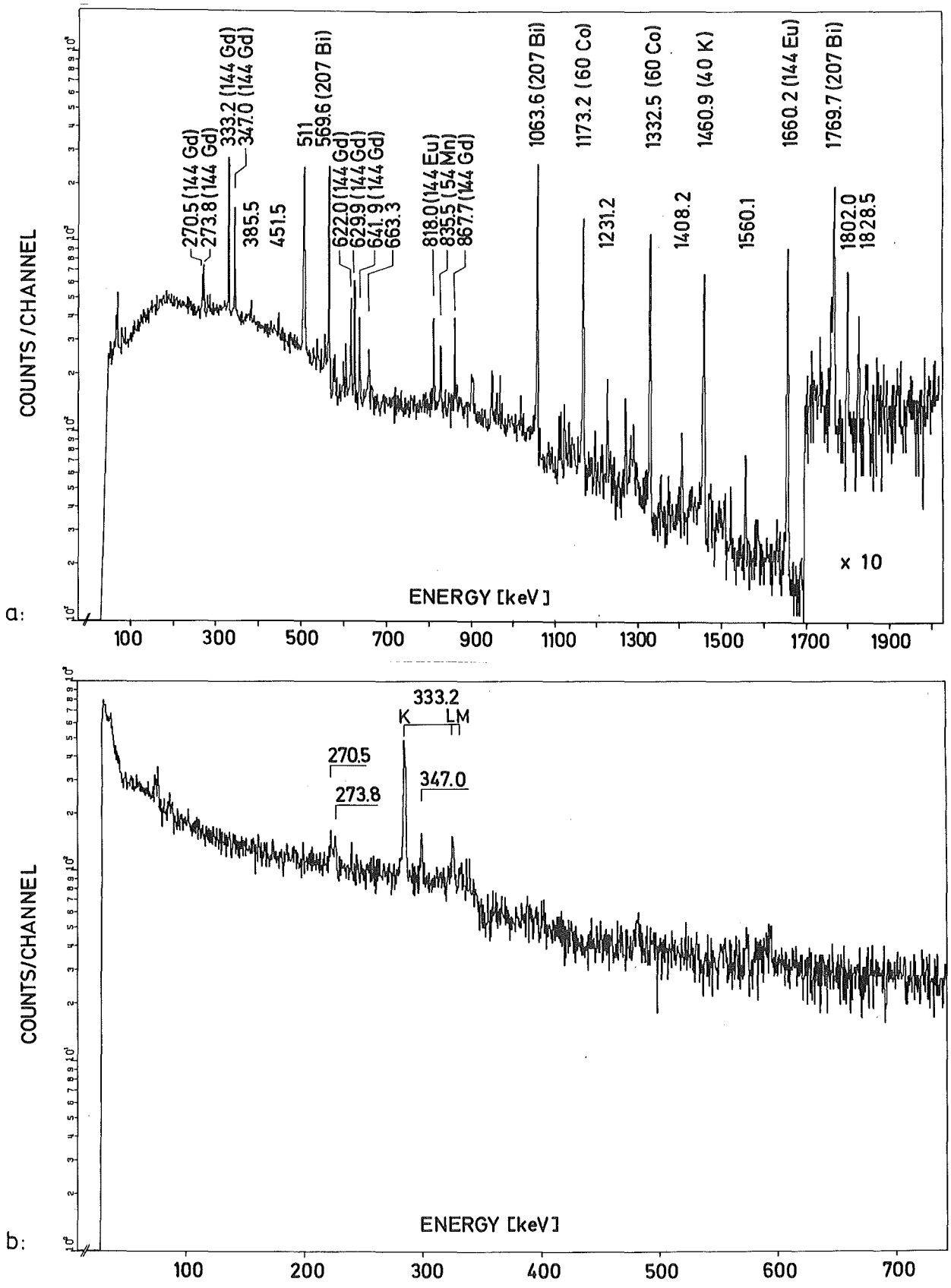

Fig. 8: γ-ray (a) and conversion electron (b) spectrum of the mass chain A =144 obtained from mass separated sources after the irradiation of ^{144}Sm with 65 MeV α-particles. γ-lines with given transition energies but without a nuclidic assignment belong either to the decay of ^{144}Gd or ^{144}Eu

or deuterons of about 35 MeV. Due to the Yrast-rule (rule 14) it seems probable that we only produced a high spin isomer in ^{143}Gd. This assumption is supported by the constructed decay scheme. The decays of ^{143}Eu and ^{143}Sm have been reported in refs. 22,23,24). Additional information could be obtained on the short-lived (30 ms) high-spin isomer of ^{143}Sm.

^{143m2}Sm

Neubert et al.[24] reported a 30 ms-isomer in ^{143}Sm and constructed a decay scheme based on intensity considerations mainly. We confirmed their arrangement of the levels by coincidence measurements shown in fig. 10. The observed coincidence relations are compiled also in the following matrix.

	181	209	1573	1705
181	-	+	+	-
209	+	(-)	+	+
1573	+	+	-	-
1705	-	(+)	-	(-)

Table 1: Coincidence relations between transitions of ^{143m2}Sm

In the coincidence spectrum of the 1573 keV transition the γ-ray intensity of the 181 keV transition is about twice as large as the γ-ray intensity of the 209 keV transition. Hence, both transitions have approximately equal intensity when internal conversion is taken into account. This shows that the half-lives of the levels at 2583 and 2508 keV are such that no losses of coincidences are observed. Therefore, the half-life is less than 10 nsec. From rule 12 we may then conclude that the transition at 75 keV has a maximum admixture of 0.1 % M2. In ref.24) a total conversion coefficient α_{tot}(75 keV) = 2.6 ± 1.2 is reported, which is compatible only with an M1 + E2 transition, when the restriction of the M2 admixture is

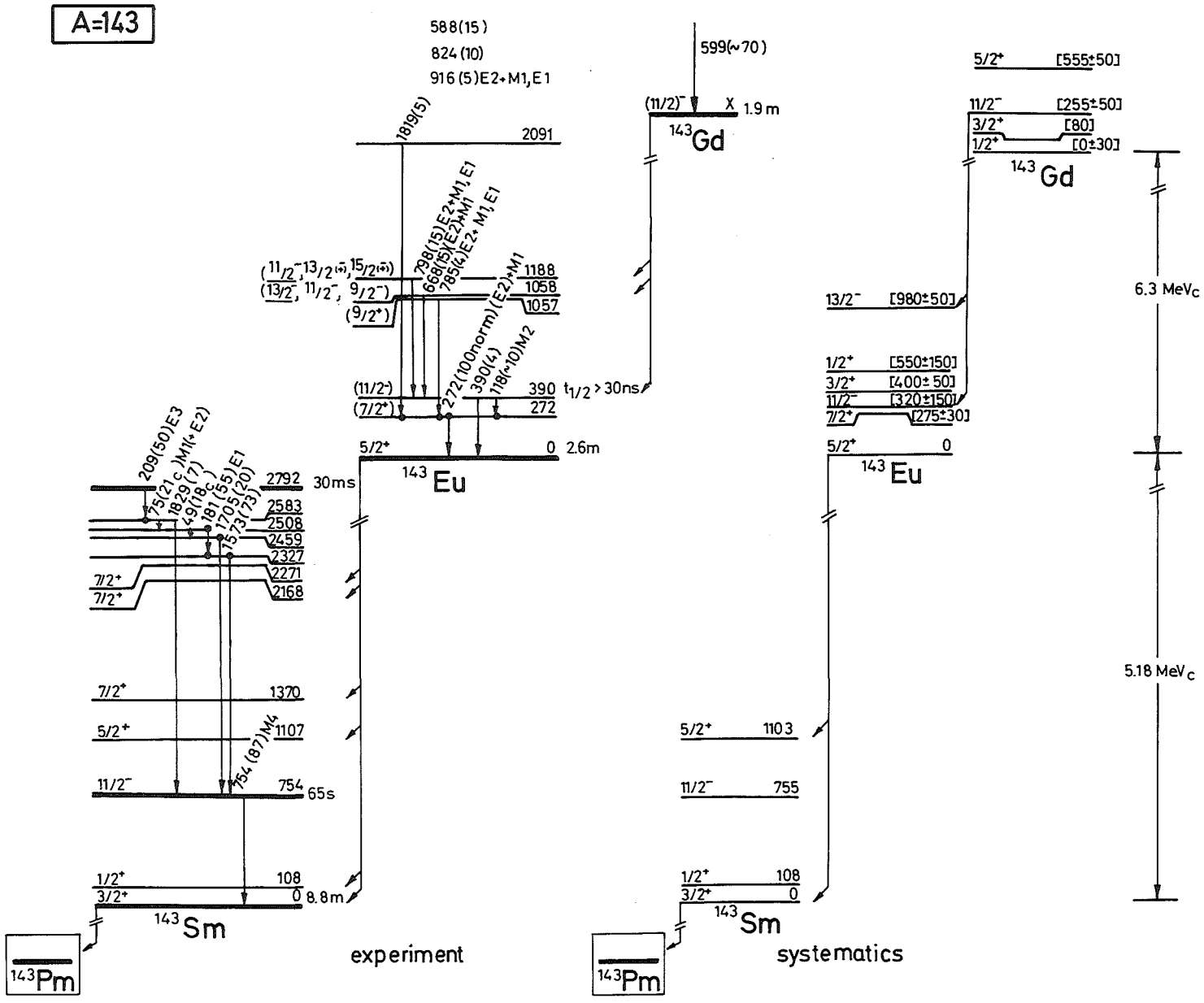

Fig. 9: The decay chain A = 143

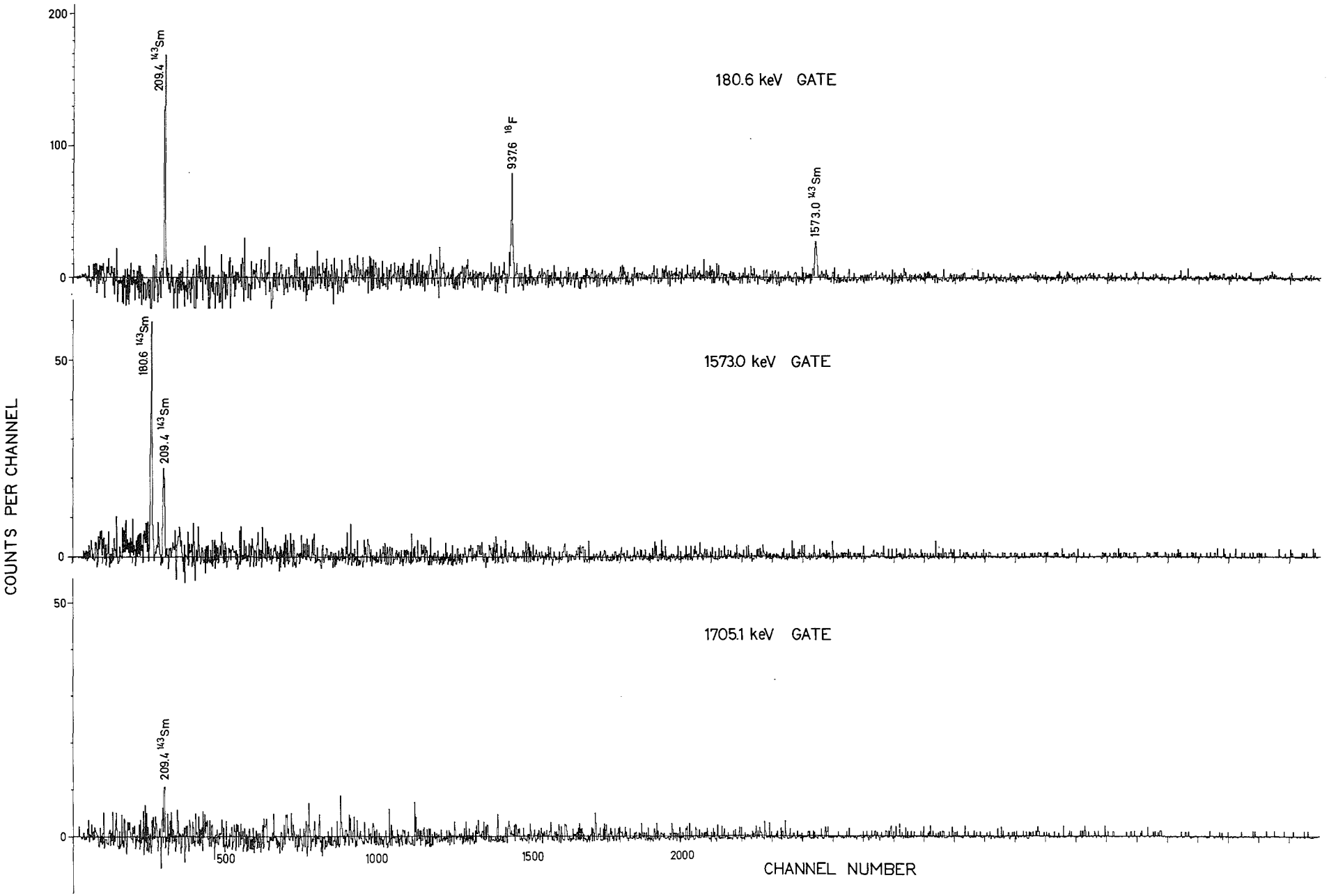

Fig. 1o: The coincidence - spectra of the 181, 1573 and 17o5 keV transitions obtained after irradiation of ^{144}Sm with 6o MeV α-particles.

taken into account. The 75 keV transition probably is a rather pure M1, because it would have a very large enhancement factor of about 180 for pure E2.

A similar argument applies to the 49 keV transition, where we can rule out both a M2 admixture larger than 0.05 % as well as a pure E2 transition. Therefore, the spin difference between the levels at 2508 and 2459 keV should be less then two units. These results have recently been extended by Arnold et al.[60], who were able to determine a multipolarity of E3 for the 1829 keV transition. This leads to a spin assignment of the level at 2583 keV of $17/2^+$ and an I^π-value of $23/2^-$ for the 30 ms isomer.

^{143}Eu

The ß-decay of ^{143}Eu has been studied by Firestone[22]. For the discussion of the ß-decay of ^{143}Gd his determination of the groundstate I^π-value of ^{143}Eu ($5/2^+$) is of importance.

^{143}Gd

Keller and Münzel[26] referred to ^{143}Gd and concluded that the half-life would probably be shorter than one or two minutes. ^{143}Gd is produced with optimum intensity in the reaction ^{144}Sm(α,5n)^{143}Gd at about E_α = 80 MeV. Fig. 11 shows two spectra measured 1min and 5 min after the end of activation. They indicate the decrease of many transitions following the ß-decay of ^{143}Gd. For this decay we obtained a half-life of 1.9 ± 0.3 min. The decay scheme of ^{143}Gd ist shown in fig. 9.

The level at 272 keV

In the ß-decay of ^{143}Gd as well as in the in-beam studies of ^{143}Eu the transition of 272 keV is the strongest one. The full γ-ray intensity of a transition of 118 keV is observed to be in coincidence with the transition of 272 keV. The spectra

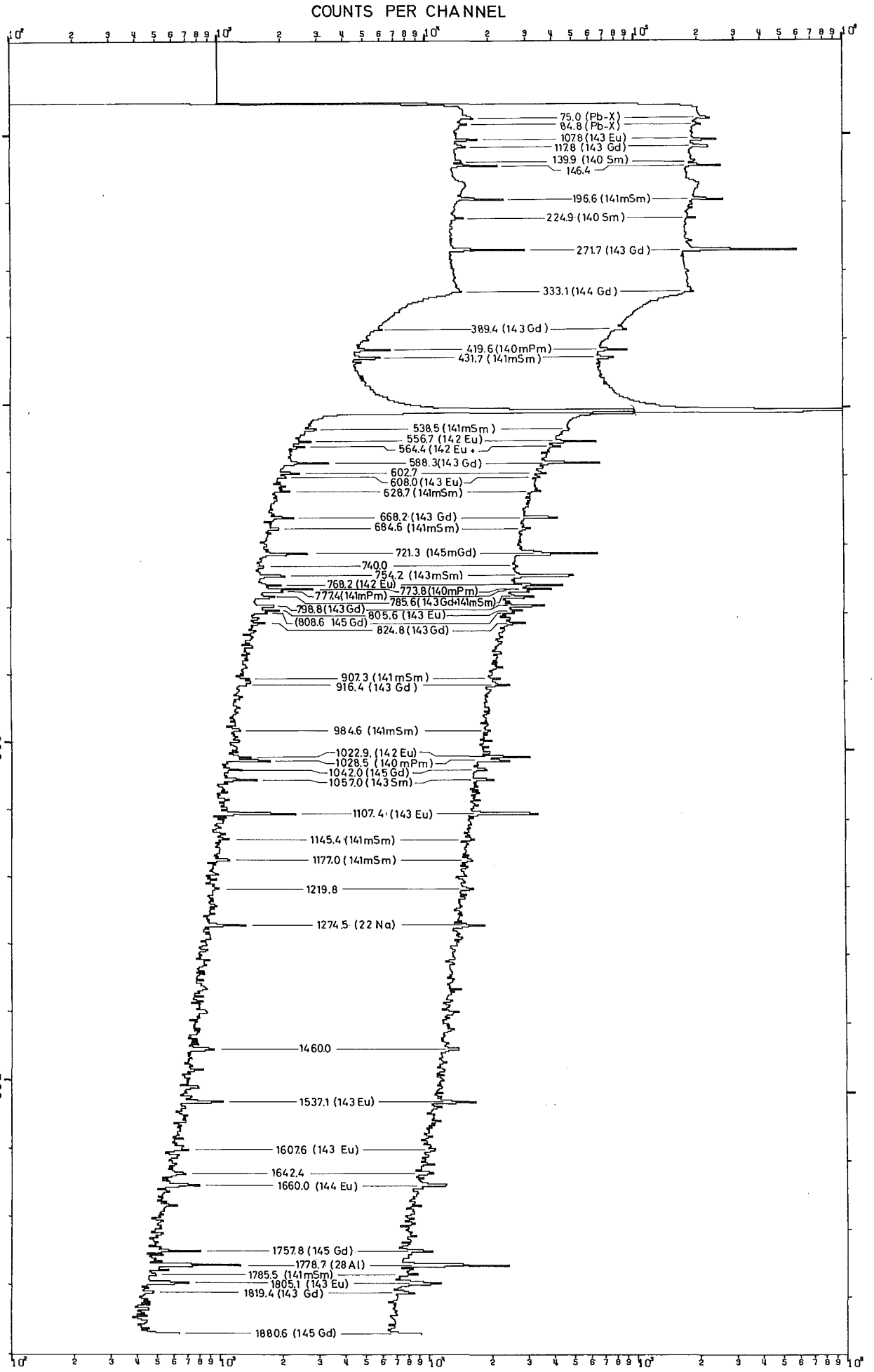

Fig. 11: γ-ray spectra obtained 1 min (upper part) and 5 min (lower part) after the irradiation of ^{144}Sm with 80 MeV α-particles.

of conversion electrons showed that this transition of 118 keV has the multipolarity M2. Hence it should depopulate a state with a half-life longer than our coincidence resolving time. Thus, the transition of 118 keV has to be placed above the one of 272 keV and not vice versa. The 272 keV transition corresponds to the decay of the first excited state in ^{143}Eu(rule 7). The level must have the spin $(7/2, 5/2, 3/2)^+$ because the spectra of conversion electrons showed that the transition of 272 keV is mainly of M1 character.

The level at 390 keV

Starting with the $5/2^+$ groundstate of ^{143}Eu, the multipolarities M1 and M2 of the transitions of 272 and 118 keV restrict the I^π-values of the level at 390 keV to $(1/2, \ldots, 11/2)^-$. The total intensity of the 118 keV transition is about 90 % of the intensity of the 272 keV transition, when conversion is taken into account. Therefore, the crossover transition of 390 keV with an intensity of about 4 % is a rather weak transition. We can exclude the spin values of $(3/2, 5/2, 7/2^-)$ for the 390 keV level, because an E1 transition of 390 keV should be much stronger than the M2 transition of 118 keV. The spin $9/2^-$ is improbable, since a M2 transition of 390 keV should be stronger than the M2 transition of 118 keV. The spin value of $1/2^-$ can be ruled out because the decay of the level is observed strongly during in-beam measurements (Yrast rule 14). The only remaining possibility of a spin of $11/2^-$ is expected from level systematics. It determines the spin of the level at 272 keV to be $7/2^+$. The branching ratio of the M2 transition with 118 keV and E3 transition of 390 keV is reasonable, when compared to neighboring nuclides like ^{141}Pm.

In ^{143}Gd one observes a strong cascade of prompt transitions in in-beam measurements. One can estimate that the lowest member of this cascade at 599 keV occurs in (70 $\pm$ 30) % of the 272 keV transition belonging to the following ß-decay of ^{143}Gd. Consequently, all strong ß-ray branches populate directly or indirectly the $11/2^-$-level at 390 keV.

The levels at 1058 and 1188 keV

Since the 798 and 688 keV transitions are not found in coincidence with any γ-transitions ($I_\gamma > 3$), we assume levels at 1058 and 1188 keV. The spectra of conversion electrons restrict the spins of the level*) at 1058 keV to $(13/2, 11/2, 9/2)^-$ and the spin of the level at 1188 keV to $(15/2^-, 13/2^\pm, 11/2^\pm, 9/2^\pm, 7/2^-)$. A spin of $7/2^-$ or $9/2^\pm$ is not probable for these two levels because otherwise strong transitions into the 272 keV level should be observed. Both the 798 and the 668 keV transitions are observed strongly during in-beam measurements. Therefore the levels ought to have high spins. The levels probably can be interpreted to be members of the one-phonon-multiplet.

The level at 1057 keV

A transition of 785 keV is observed in coincidence with the 272 keV transition. This leads to a level at 1057 keV, close to the one at 1058 keV. Yet, these levels cannot be identical, because the intensity ratios of the 785 and 668 keV transitions are different by a factor of at least 3 in the spectra of the 1.9 min decay and in the spectra of the in-beam measurements. Based on level systematics one can predict a spin $9/2^+$ for the level at 1057 keV.

The 1.9 min isomer in ^{143}Gd

The 798 and 668 keV transitions are observed in fast coincidence with the annihilation radiation, but with no other γ-rays. Therefore, we assume that the levels at 1058 and 1188 keV are populated predominantly by direct ß-decay. The feeding of the levels indicates an allowed or non-unique first forbidden ß-decay. Since they have a spin between 15/2 and 11/2, the spin of the isomer in ^{143}Gd can be restricted to 17/2 .... 9/2. From level systematics the only

---

*) An E2 multipolarity of the transition of 668 keV could be ruled out, since we observe an $A_2 = -0.53 \pm 0.15$ in in-beam angular distribution measurements.

expected low-lying high-spin level in ^{143}Gd is an $11/2^-$-level. The energy of the level predicted from systematics explains why this $11/2^-$level decays predominantly by ß-decay and not by an isomeric γ-ray transition. (10^4:1)

3. The decay chain A=142

The present data show an unexpected high number of different activities with half-lives between 10 and 100 s which have to be assigned to the decay chain ^{142}Gd → ^{142}Eu → ^{142}Sm. The nuclidic assignments and the decay schemes of these activities are strongly interconnected and make a simultaneous discussion advantageous.

A 1.2 min high-spin isomer of ^{142}Eu has been published already in ref.27). This decay populates the strong γ-ray cascade of the quasirotational groundstate band in ^{142}Sm. The members of this band are also observed as strong transitions in in-beam measurements, when ^{142}Sm is produced via the reaction ^{142}Nd(α,4n)^{142}Sm. These transitions were used as a basis for further inditifications and for reference in this decay chain. The low-spin groundstate of ^{142}Eu could be produced by the reaction ^{144}Sm(α,6n)^{142}Gd$\xrightarrow{\beta+}$ ^{142}Eu (rule 15).

More independent from this decay chain, we obtained additional information on the decay of a 2.36 ms isomer in ^{142}Pm which was already reported by Goncharov et al.[28].

^{142m}Pm

Goncharov et al.[28] assigned two γ-transitions of 200 ± 5 and 430± 5 keV to an isomeric decay of ^{142}Pm with a half-life of 2.36 ± 0.10 ms. In ref.29) the authors reported α_k = 0.2 for the transition at 200 keV and α_k = 0.03 for the transition at 430 keV.

Based on the excitation functions we were able to assign three transitions of 208,5 ± 0.5, 241.1 ± 0.5 and 433.5 ± 0.5 keV to ^{142}Pm. Since they are not observed when ^{140}Ce is bombarded with α-particles, values of Z ≤ 60 (Nd) are excluded. Using a pulsed ion source we found that all three transitions decay with a half-life

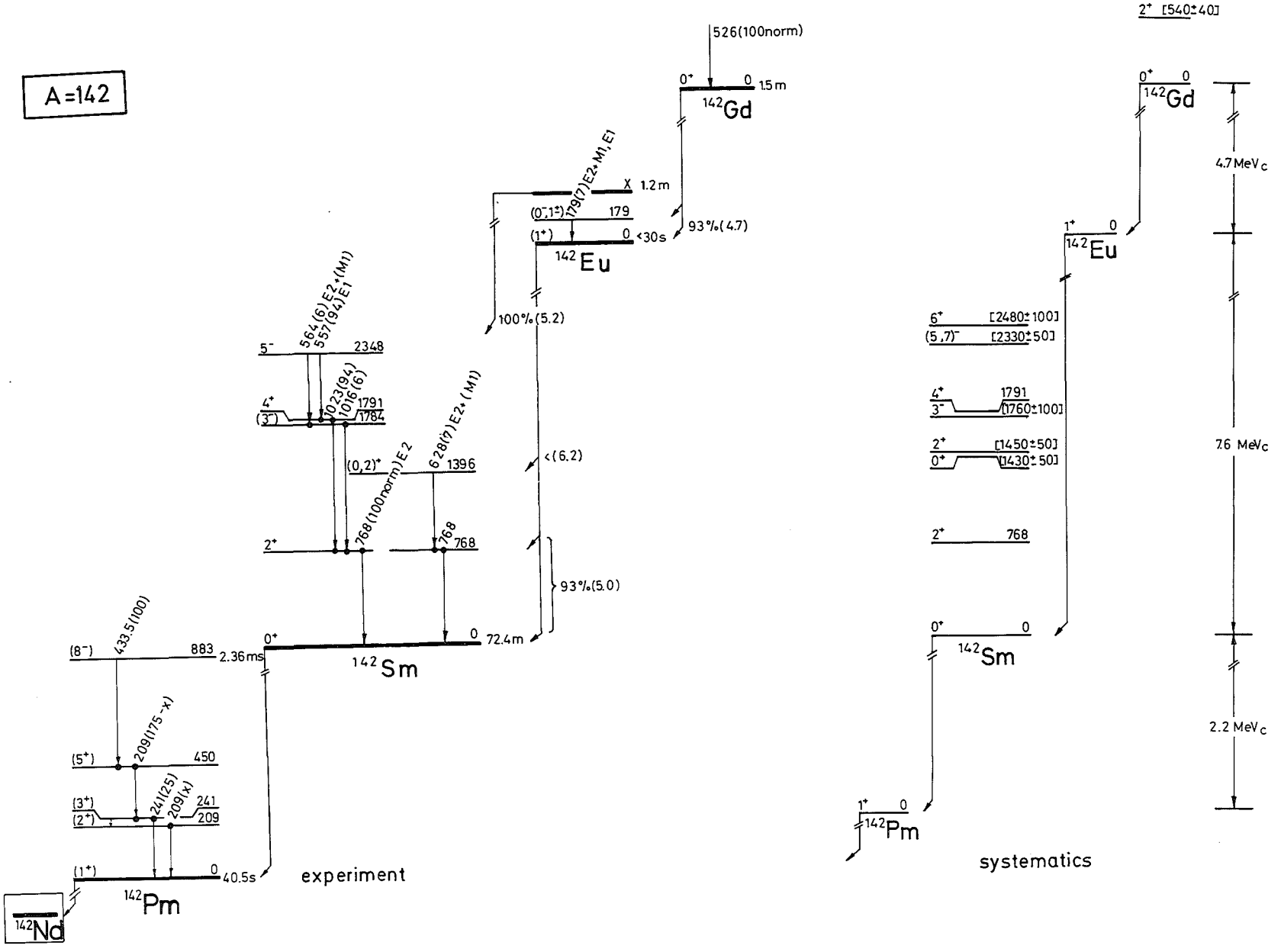

Fig. 12: The decay chain A = 142. The decay scheme of ^{142m}Pm was taken from ref.59.

$T_{1/2}$ > 100 µs. From off-beam measurements we estimated an upper limit for the half-life: $T_{1/2}$ < 0.5 s. Therefore, this decay is assumed to be the same isomeric decay as reported in ref.28).

The coincidence spectra for the three transitions are shown in fig. 13, and the coincidence relations are compiled in the following matrix:

	209	241	434
209	+	+	+
241	+	-	?
434	+	?	-

Apparently, the 209 keV transition is in coincidence with another transition at the same energy. From our γ-ray single spectra we can conclude that the two transitions at 209 keV differ in energy by less than 0.3 keV. The intensity of the 209 keV line in the coincidence spectra and the single spectra reveals that both 209 keV transitions are of comparable strength. When comparing the theoretical α_k-values for a 209 keV transition (M1:0.17, M2: 0.90, E1: 0.03, E2: 0.12, E3: 0.5) with the experimental value of 0.2 from ref.[29], one finds that both 209 keV transitions should have a multipolarity of E1, E2 or M1. The measured α_k-value of 0.03 of ref.[29] for the 434 keV transition is compatible with an E3-transition or a transition with lower multipolarity (M2(+E1) or M1(+E2)).

Recently, the arrangement of the transitions of ^{142}Pm given in fig. 12 was proposed by Funke et al.[59]. It is consistent with our coincidence data, the absolute γ-intensities and the reported conversion coefficients. The given placement of the 241 keV transition is supported furthermore by the fact that the intensity ratio I(241 keV)/I (434 keV) is about a factor of 1.8 larger during in-beam measurements than in the delayed spectra.

The decay ^{142}Gd → ^{142}Eu → ^{142}Sm

As reported in ref.27) in-beam as well as off-beam measurements revealed the 2^+ and 4^+ levels of the quasirotational groundstate band of ^{142}Sm at 768 and 1791 keV. Conversion data showed that the strong 768 keV transition is of E2 character and belongs to a

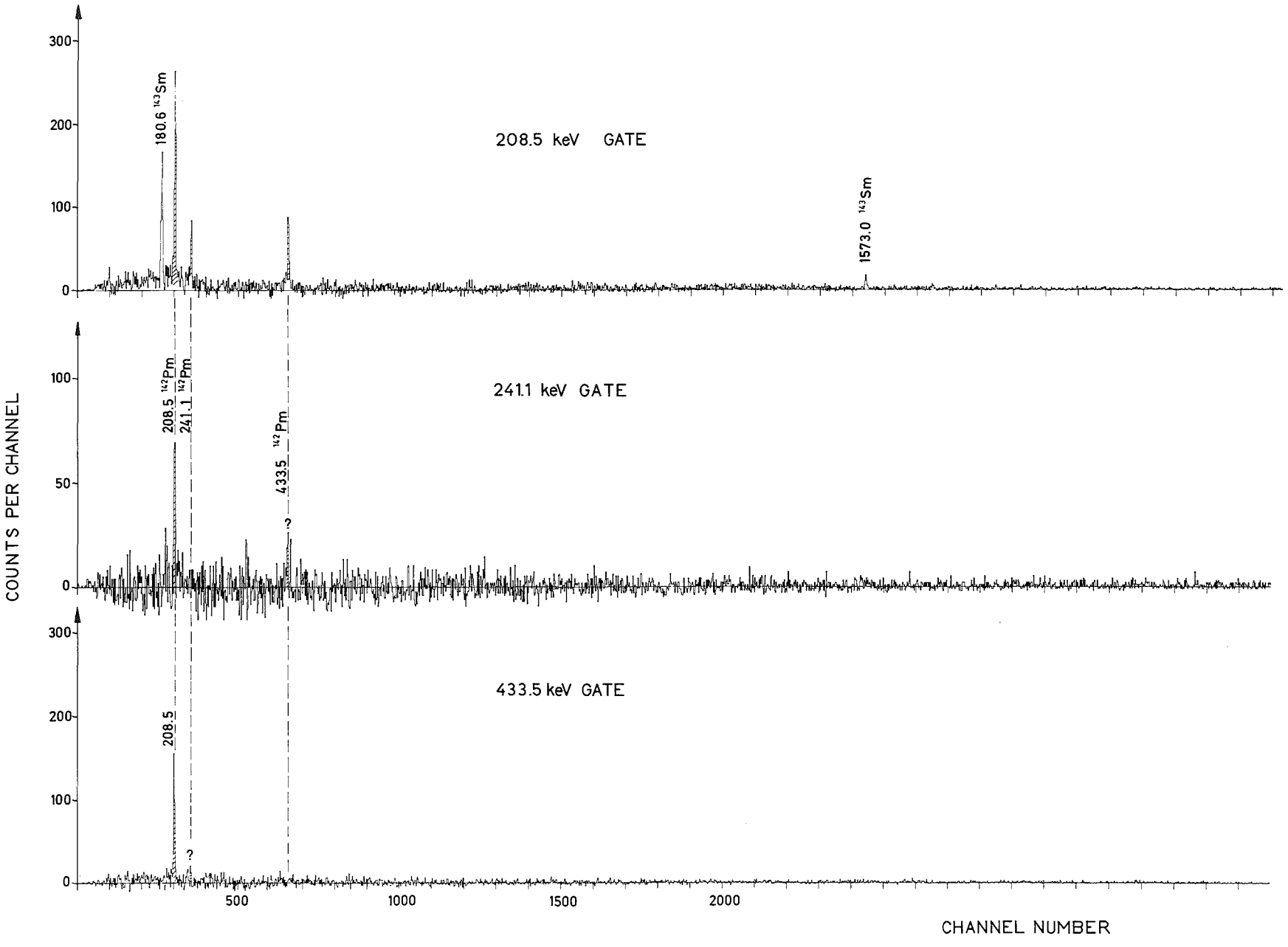

Fig. 13: In-beam coincidence spectra of the 209, 241 and 434 keV transitions obtained from an irradiation of ^{142}Nd with 60 MeV α-particles. Besides the transitions of ^{142}Pm also lines of ^{143}Sm are observed, because the 208.5 keV transition also occurs in the ^{143m2}Sm decay (s.fig.8).

nucleus with Z = 62. The 768 keV transition is among others in coincidence with the strong transitions of 1023 and 557 keV (see fig. 14) The arrangement of this triple cascade 557 keV → 1023 keV → 768 keV (see fig. 12) is supported by $^{144}Sm(p,t)^{142}Sm$ measurements of Edwards et al.[30]. This triple cascade is a characteristic feature of all off-beam spectra obtained from activations of ^{144}Sm with α-particles of suitable energy.

The groundstate decay of ^{142}Eu

From the excitation function we assigned a transition of 628 keV to the mass number 142. In fig. 15 this excitation function is shown relative to that of the 557 keV transition in ^{142}Sm. It was obtained by comparing the relative intensities of these two transitions two minutes after the end of the irradiation of ^{144}Sm with α-particles. In the γ-ray and conversion electron spectra the energy difference $E_\gamma - E_k$ of the 628 keV transition showed that this transition belongs to Sm. This assignment is confirmed by observed in-beam coincidences between the 768 keV transition of ^{142}Sm and the 628 keV transition (s. fig. 14). When irradiating ^{144}Sm with deuterons the transition at 628 keV was not observed 1 min after the irradiation, in contrast to the strong 557 keV transition. It follows that the 628 keV transition cannot be fed by the 1.2 min decay of the high-spin isomer of ^{142}Eu, though it has a similar half-life and α-activation curve (s. figs. 15,16) when produced from ^{144}Sm with α-particles. A second 1.5 min isomer in ^{142}Eu which is populated with α-particles should be observed also in d-activations. Therefore, the observed half-life of 1.5 ± 0.3 min corresponds to the decay of ^{142}Gd which will be deduced also from the 179 keV transition in the following. In fig. 16 the decay curves of both these transitions are compared to the decay of the 557 keV transition of the 1.2 min isomer of ^{142}Eu. From the in-beam intensity of the prompt $2^+ \rightarrow 0^+$ transition in ^{142}Gd we could estimate a feeding of 7 ± 3 % of a level in ^{142}Eu, depopulated by the 179 keV transition. Since no other strong transitions were observed, ^{142}Gd must decay mainly via allowed ß-decay to a 1^+ state of ^{142}Eu (rule 9a+b). This state should mainly populate the 0^+ groundstate of ^{142}Sm, since the 628 keV

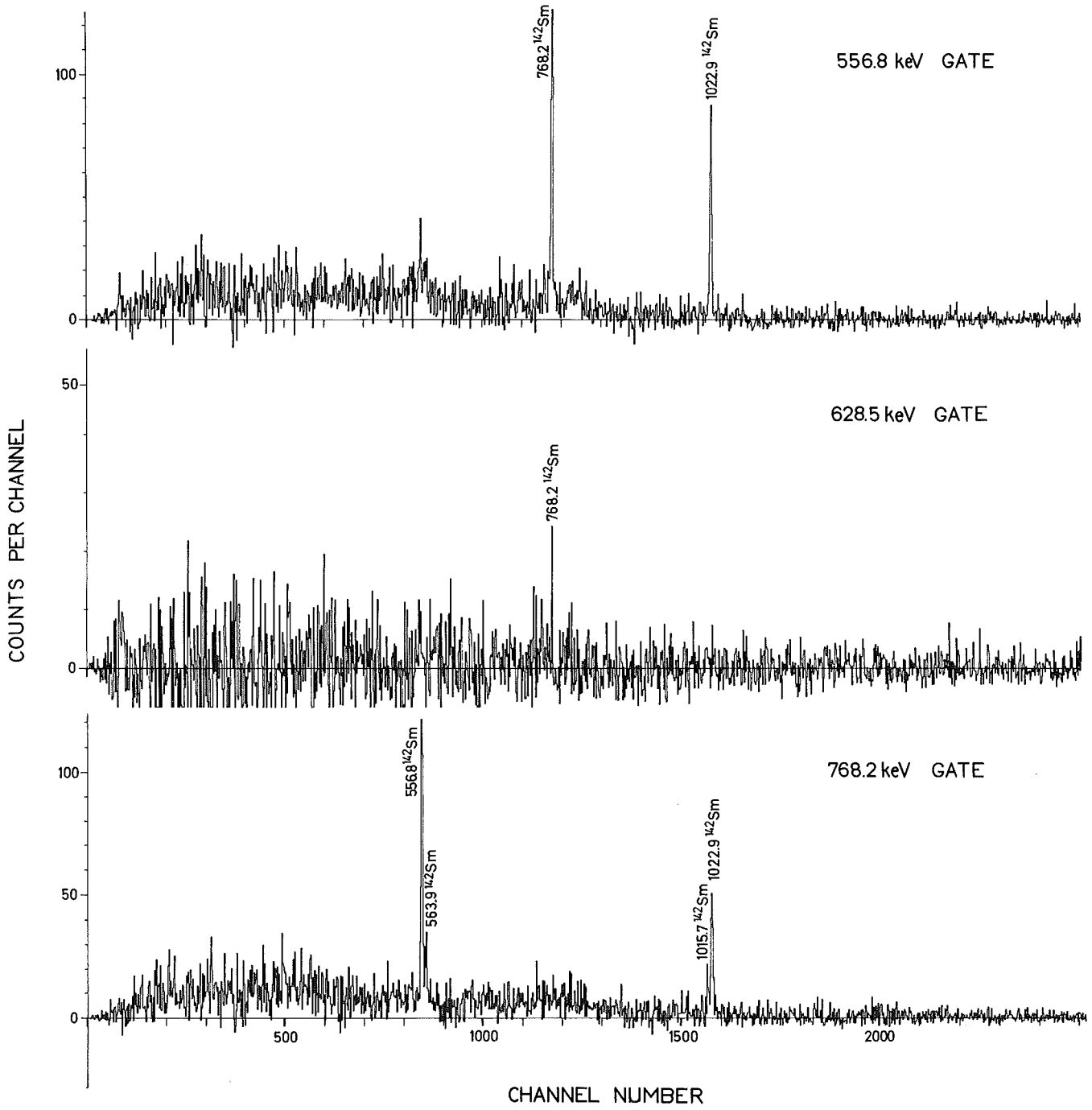

Fig. 14: In-beam coincidence - spectra of the 557, 628 and 768 keV transitions obtained from an irradiation of ^{142}Nd with 60 MeV α-particles.

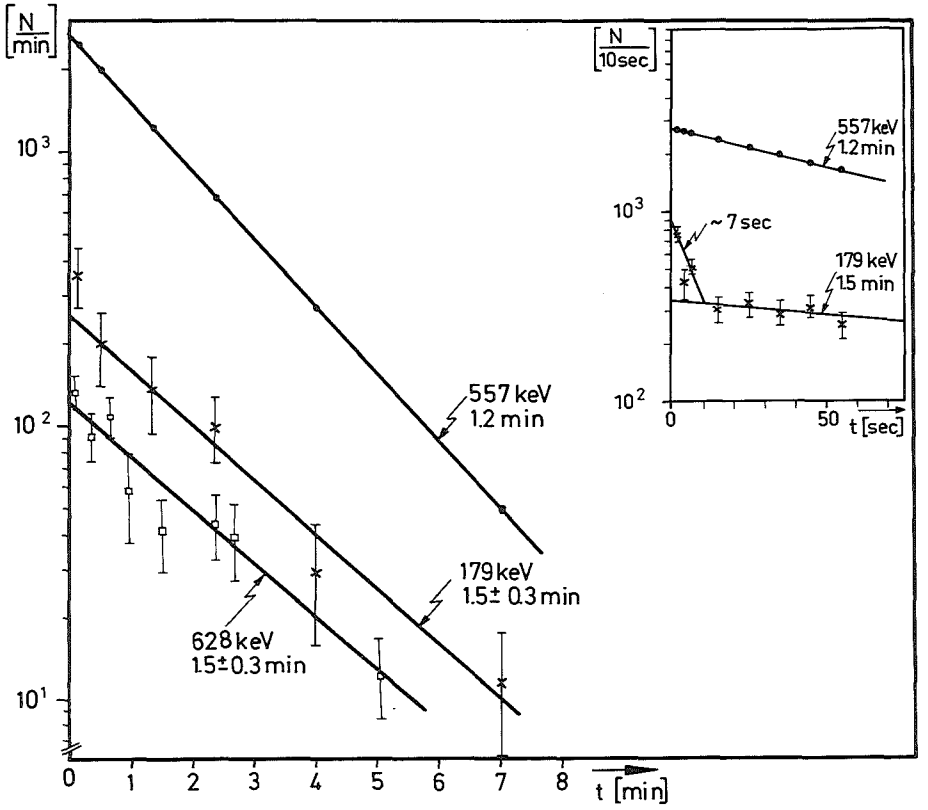

Fig. 16: Decay curves for the 628 and 179 keV transitions in different time intervals, compared to the 557 keV transition of ^{142}Eu.

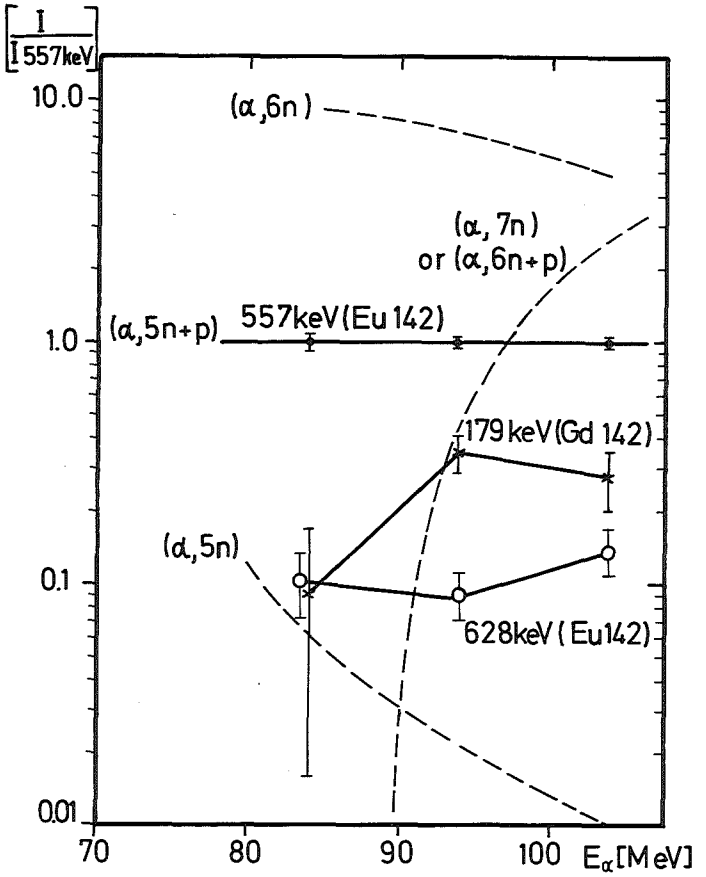

Fig. 15: Exitation functions of the 628 and 179 keV transitions from an irradiation of ^{144}Sm with α-particles. The transitions are normalized to the 557 keV transition of ^{142m}Sm. Theoretical curves for several reactions are given as dashed lines.

transition occurs in about 7 ± 3 % of all decays of this level and no other transitions of comparable strength were observed. In ^{142}Eu one expects from the coupling rules (rule 20) a low lying 1^+ level with the configuration $\left[\pi(d_{5/2}) \times \nu(d_{3/2})\right]_{1^+}$.

The decay curve of the 628 keV transition (s. fig. 16) shows no definite growth related to the decay of the 1^+ state of ^{142}Eu. From an estimate of the production ratio for ^{142}Gd and ^{142}Eu we obtained a rough upper limit for the half-life of this 1^+ state of ^{142}Eu: $T_{1/2} \lesssim 30$ s. In fig. 12 we assumed this 1^+ level to be the groundstate of ^{142}Eu, since in the neighboring odd-odd nucleus ^{138}Pr the high-spin isomer $\left[(7.8)^-\right]$ lies also above the 1^+ groundstate (at 340 keV, s.ref.[31]). A final experimental proof of the position and the half-life of the 1^+ state in ^{142}Eu can be obtained from future ß-ray measurements.

The 628 keV transition depopulates a level at 1396 keV which itself is populated by ß-decay of the 1^+ state of ^{142}Eu with log ft≤6.2. Taking the multipolarity of the 628 keV transition (M1 + E2) into account, spin and parity of the 1396 keV level are restricted to $(0, 1, 2)^+$. Of these, the assignment 2^+ is supported by systematics and by the in-beam observation of the 628 keV transition, which points to a higher spin value. On the other hand, the missing of a cross-over transition of 1396 keV ($I_\gamma(628)/ I_\gamma(1396) > 10$) and the comparison with the decay of the neighboring nucleus ^{138}Pr favour $I^\pi = 0^+$. Since the level systematics also predict a 0_2^+ -level in this energy range, a decision between the possibilities 2_2^+ and 0_2^+ cannot be given.

The decay of ^{142}Gd

In fig. 15 the excitation function of the 179 keV γ-ray is given relative to the 557 keV transition of ^{142}Sm. A comparison with the cross-sections for neighboring nuclides assigns the transition to $A \leq 142$. Since the transitions of 384 and 394 keV from the decay of ^{141}Eu are not observed in an irradiation of ^{144}Sm with 93 MeV α-particles - in contrast to the 179 keV transition - the 179 keV transition belongs to the mass chain A = 142. Fig. 16

shows the decay curve of the 179 keV transition after irradiating ^{144}Sm with 104 MeV α-particles. The long-lived component has a half-life of 1,5 ± 0.3 min. Since two different half-lives of 4 and 28 s have been assigned to the decay of ^{141}Eu (see p. 51) this again shows that this 1.5 min activity belongs to the A =142 chain (rule 18). Furthermore, this activity corresponds to the decay of ^{142}Gd, because it is not observed when ^{144}Sm is irradiated with deuterons. Relative to the $2^+ \rightarrow 0^+$ transition of ^{142}Gd, the 179 keV transition is observed in (7±3)% of the decays. Like other even-even nuclei in this mass region, ^{142}Gd decays primarily into the 1^+ isomer of ^{142}Eu.

The 7s-component of the 179 keV transition

As can be seen from fig. 15, there exists a short-lived component of the 179 keV transition with $T_{1/2} \sim 7$s. Since both components have approximately the same activation curves, the short-lived component belongs to ^{142}Gd, ^{142}Eu, ^{142}Sm or with less probability to ^{141}Eu. Because in in-beam experiments with a pulsed ion source no sec-components in the $2^+ \rightarrow 0^+$ transitions of the even-even nuclei ^{142}Gd and ^{142} Sm were observed, an assignment to these nuclides can be excluded. While the half-life of ∿7s agrees approximately with the 4s component assigned to ^{141}Eu (see p.51), the agreement of the transition energy with the long-lived 179 keV γ-ray (1.5 min) to within 0.5 keV points to a further isomer in ^{142}Eu with a half-life of ∿7s.

4. The decay chain A=141

In this mass chain (s. fig. 17) we first present the information on the decay of the groundstate of ^{141}Sm obtained from the literature[34,35] and from the present measurements. Following the reaction ^{142}Nd(α,5n)^{141}Sm, one observes mainly the decay of the high-spin isomer ^{141m}Sm (Yrast rule 14). The groundstate of ^{141}Sm was produced by ^{144}Sm(α,6n + p) ^{141}Eu $\xrightarrow{\beta+}$ ^{141g}Sm (rule 15). Apart from the transitions following the ß-decay of ^{141g}Sm, we could assign two

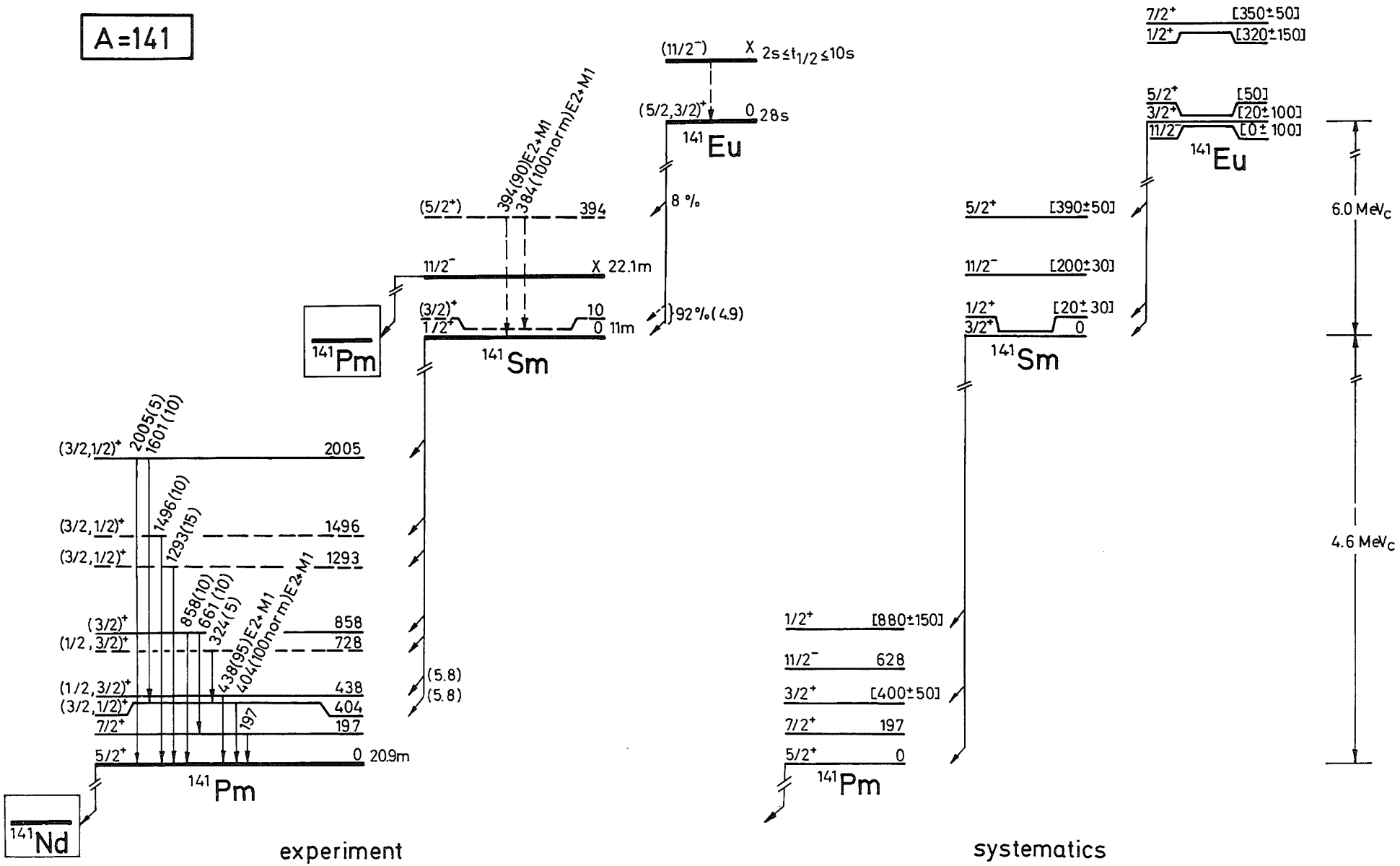

Fig. 17: The decay chain A = 141

γ-rays to the ß-decay of ^{141}Eu. The next member of this mass chain, ^{141}Gd, would be of considerable interest, e.g. for the systematics of the isotonic chain with N = 77. However, approaching the line $\sigma_n = \sigma_p$ (fig. 1) the production of this nucleus is very difficult; until now it has not yet been found.

^{141g}Sm

The half-life of ^{141g}Sm was published first by Arlt et al.[35] to be 9.0 ± 0.5 min. The authors assigned two γ-transitions at 404.0 ± 0.5 and 438.2 ± 0.5 keV to this decay. Eppley et al. announced in ref.[34] a pending publication of the groundstate decay of ^{141}Sm. In ref.34) the authors reported mainly on the high-spin decay of ^{141}Sm, but some additional information about the low-spin decay is also mentioned. For the half-life of ^{141g}Sm 11.3 ± 0.3 min was obtained. In the spectra shown in ref.34) several transitions are marked as belonging to the groundstate decay; some of these transitions meet energy sum relations. The approximate position of the levels and some information about the spin assignments could be extracted from fig. 12 of ref.34), where the level positions of different Pm - isotopes are compared. These levels and the corresponding transitions are given in fig. 17.

In a recent work, Ekström et al.[36] measured I = 1/2 for the ground-state spin of ^{141}Sm and I = 5/2 for ^{141}Pm. This explains an analysis of the 511 keV annihilation radiation, where we found after subtraction of all contributions of neighboring activities identified in our spectra that no strong $ß^+$-component remained due to a direct decay into the groundstate of ^{141}Pm. From level systematics a very low-lying $1/2^+$-state is expected in ^{141}Sm.

From our measurements we assigned γ-rays at 404, 438, 1292 and 1601 keV to the decay of ^{141g}Sm. The strong transitions at 404 and 438 keV were found not to be in coincidence. Conversion data show that the multipolarity of both transitions is E2 + M1. Since these are the strongest transitions, we introduced two levels for them.

^{141}Eu

Based on the excitation function and the energy distance $E_\gamma - E_K$, two γ-rays at 394 and 384 keV were assigned to the decay of ^{141}Eu. In the spectra of fig. 18 the decrease of these transitions can be compared with those of 9.5 s ^{139m}Sm and of 1.2 min ^{142m}Eu. The decay clearly showed two components: a long-lived one of 28 ± 6 s and a shorter one of 4^{+6}_{-2} s.

From the increase of the γ-ray intensities following the ß-decay of ^{141g}Sm, one concludes that this radiosiotope was produced primarily via the 28 s ß-decay of ^{141}Eu. Using the intensities of the γ-transitions in ^{141}Pm one finds that the two transitions at 384 and 394 keV each occur in about 4 % of the decays of ^{141}Eu. The groundstate of ^{141}Eu must decay by allowed ß-decay to the $1/2^+$ groundstate or to very low-lying $1/2^+$ or $3/2^+$ levels in ^{141}Sm, since no further strong γ-transitions were observed and no level with $I \geq 5/2$ is expected below the ß-decaying $11/2^-$ isomer in ^{141}Sm. This restricts the groundstate spin of ^{141}Eu to $(1/2, 3/2, 5/2)^+$. However, a low-lying $1/2^+$ level is not expected in ^{141}Eu from level systematics. In the decay scheme of fig. 17 we tentatively arranged the transitions at 384 and 394 keV in such a way that they reproduce the predicted $5/2^+$ and $3/2^+$ level in ^{141}Sm.

The short-lived (4 s) parent of the 28 s activity is possibly due to the expected high-spin isomer of ^{141}Eu (Yrast rule 14). An assignment to ^{141}Gd seems unlikely, since the production cross-section of this nucleus is rather small when compared to ^{141}Eu. A low lying $11/2^-$ isomeric state in ^{141}Eu is supported by level systematics. It can decay by an E3-transition which is in agreement with the observed half-life of several seconds. An M4-transition can be excluded according to rule 11, since for an energy of less than 100 keV such a transition would have to be enhanced by more than a factor 10^5. Above 100 keV no transition of higher multipolarity (E3, M4) belonging to ^{141}Eu was observed in the spectra of conversion electrons.

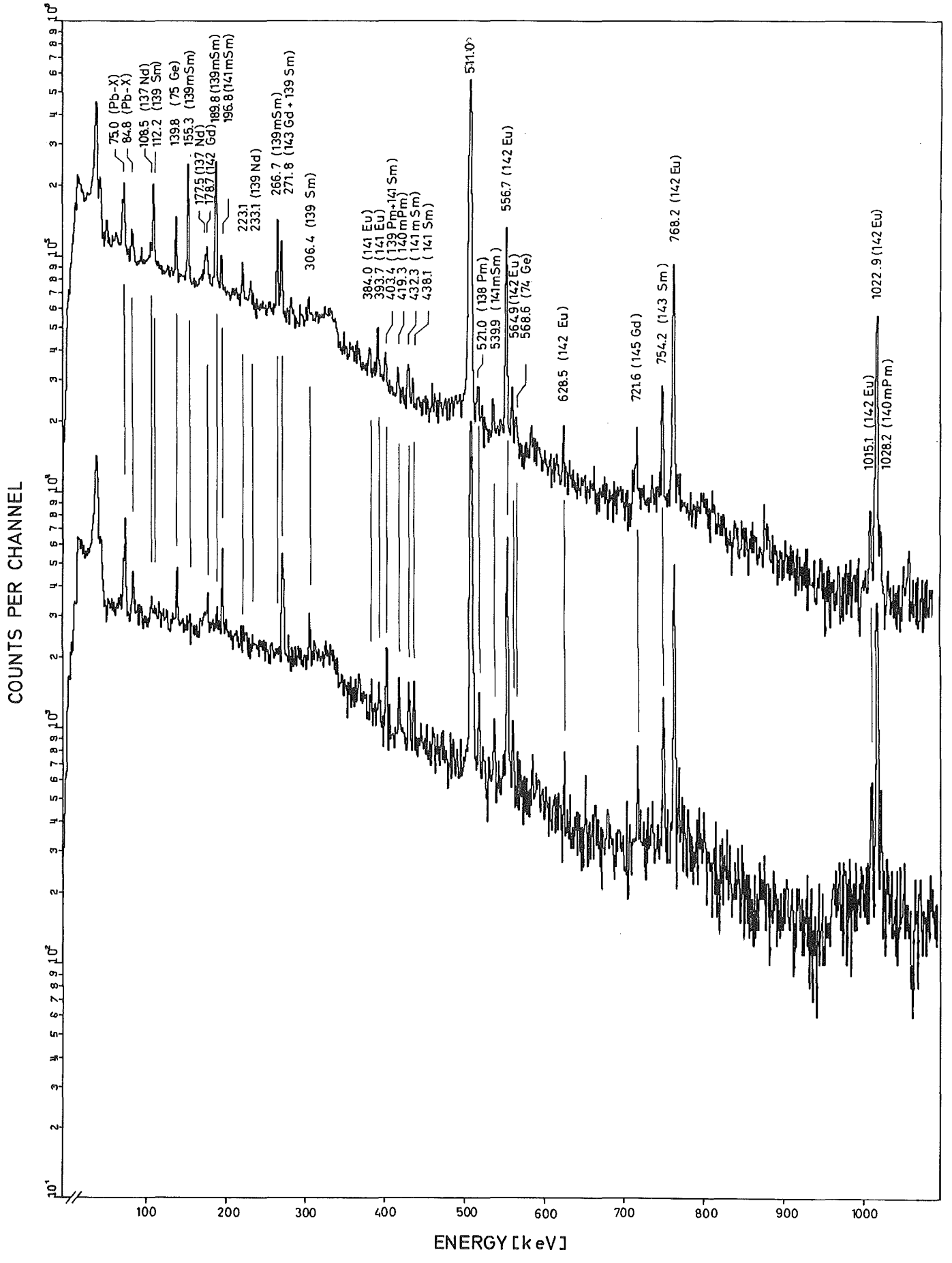

Fig. 18: γ-ray spectra obtained 1o s (upper part) and 4o s after the irradiation of ^{144}Sm with 1o4 MeV α-particles.

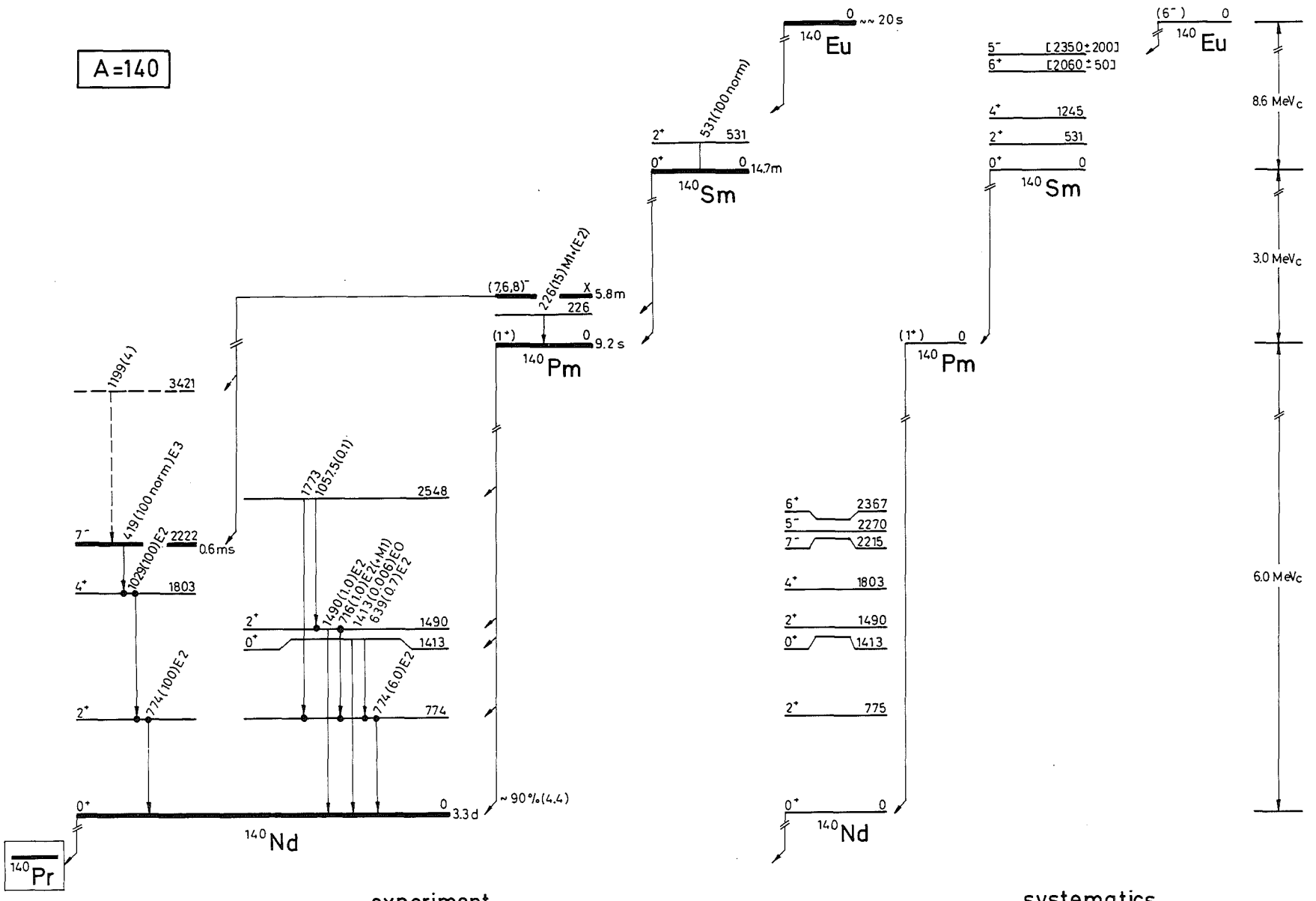

Fig. 19 a: The decay chain A = 140

5. The decay chain A = 140

In the mass chain A = 140 the new isotope ^{140}Eu was just observable, despite its low production rate at E_α = 104 MeV. Data supplemental to refs.35,37,38) are presented for ^{140}Sm and $^{140m+g}$Pm. The low-spin state ^{140g}Pm (s. fig. 19) was produced via ß-decay of ^{140}Sm (rule 15), in order to populate among others excited 0^+ states in the even-even daughter nucleus ^{140}Nd. For the investigation of 0^+ levels, which are of special theoretical interest, the newly developed conversion electron spectrometer[7,8] is very suitable, because it has a high resolving power in a broad energy range and allows the detection of E0 transtions even at energies as high as 2 MeV.

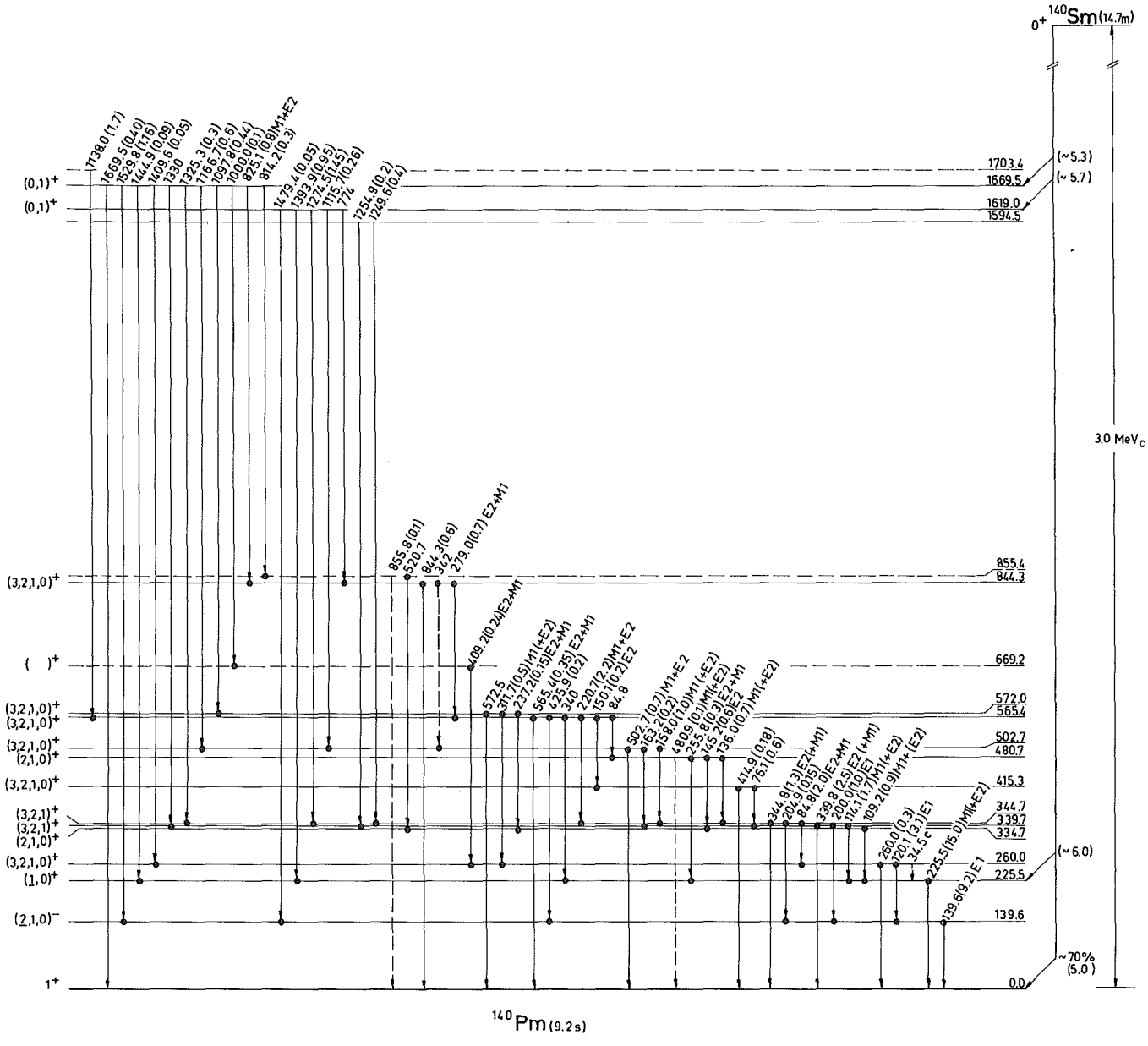

Fig. 19 b: The decay scheme of ^{140}Sm

^{140}Pm

The decays of the high-spin isomer and of the 1^+ groundstate of ^{140}Pm were described by Arl't et al.[35], who observed a 9.2 s component of the 774 keV transition in ^{140}Nd which they assigned to the decay of low-spin ^{140}Pm. We produced this 1^+ state via the reaction ^{142}Nd (α,6n) ^{140}Sm $\xrightarrow{\beta+}$ ^{140}Pm. The half-life of 14.7 min of ^{140}Sm made mass separations possible.

The level at 1414 keV

In the spectra of conversion electrons (cf. fig. 20) we observed an E0 transition of 1413.5 keV which is related to an 0^+ state already quoted by Sakai[38] from unpublished data. This 0^+ level of ^{140}Nd was not observed in the reaction ^{142}Nd(p,t)^{140}Nd (ref.39). In addition we observed the corresponding $0_2^+ \rightarrow 2_1^+$ transition of 639 keV which was assigned on the basis of the energy sum relation, the observed γγ-coincidences and the multpolarity. The experimental branching ratio $W(E0, 0_2^+ \rightarrow 0_1^+)/W(E2, 0_2^+ \rightarrow 2_1^+) = (1.0 \pm 0.2) \cdot 10^{-2}$ was compared to the predictions of different theoretical models. The vibrator model[40] resulted in a value of $1.7 \cdot 10^{-3}$ for this branching ratio; on the other hand, we obtained within the Gneuss-Greiner model[41] a branching ratio of $1.06 \cdot 10^{-2}$ which is in excellent agreement with the experimental value.

The level at 1490 keV

The existence of this level (ref.38) is confirmed by (p,t)-measurements[39]. The 774 and 716 keV transitions are observed in coincidence and fulfill together with the 1490 keV transition the energy sum relation: 773.5 + 716.0 $\cong$ 1489.8 keV. We assign the 1490 and 716 keV transitions to be the $2_2^+ \rightarrow 0_1^+$ and $2_2^+ \rightarrow 2_1^+$ transitions of the reported 2_2^+-level at 1490 keV, since, based on the experimental multipolarities, the I^π-value of the level can be restricted to 2^+.

We tentatively assigned a further transition of 1199 keV to the high-spin ß-decay of ^{140}Pm. Since this transition was not observed

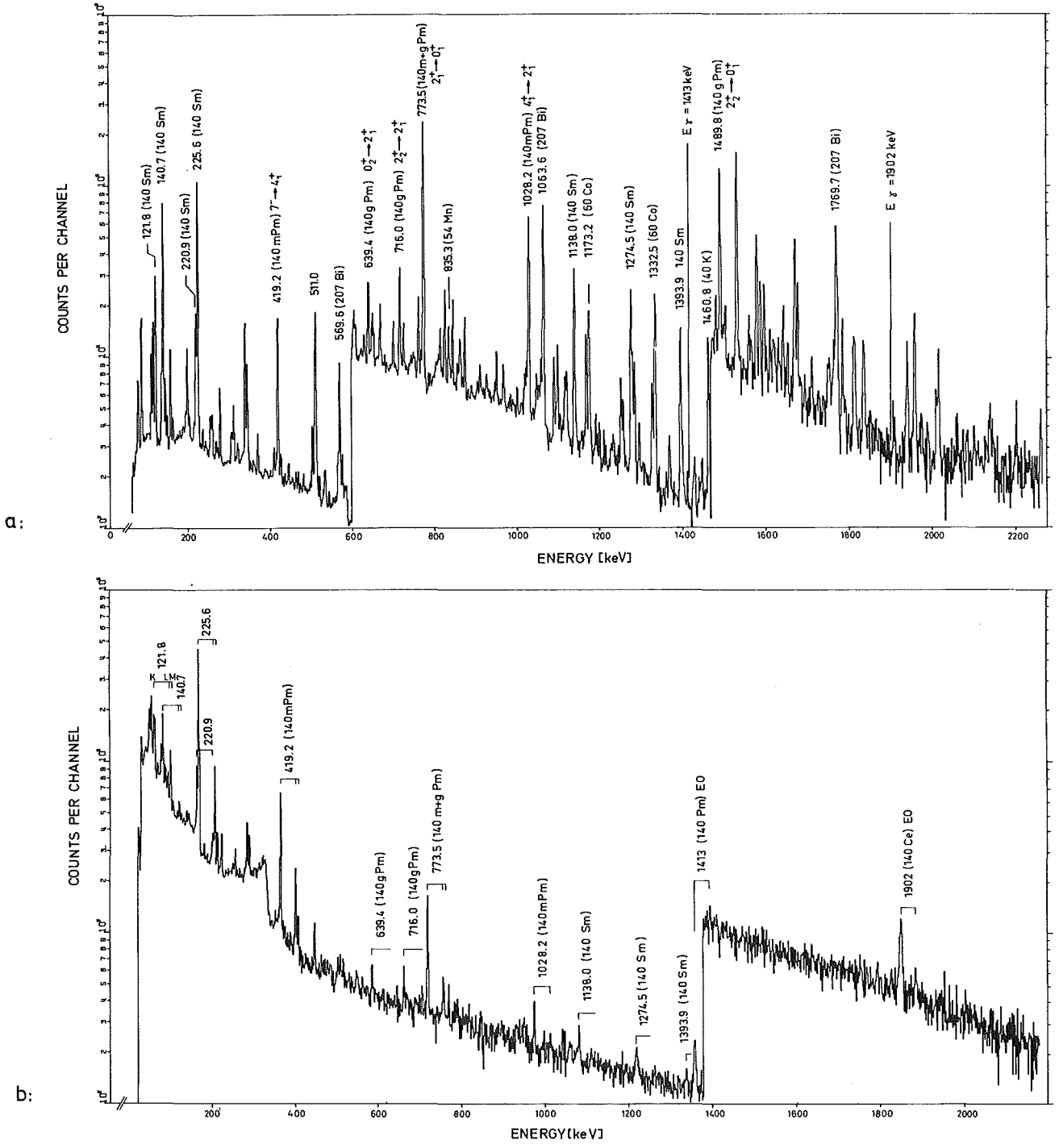

Fig. 2o: γ-ray (a) and conversion electron (b) spectrum of the mass chain A = 14o obtained from mass separated sources after the irradiation of ^{142}Nd with 9o MeV α-particles. The γ-ray spectrum has been measured with the anti - compton spectrometer.

in coincidence with the three transitions of 419, 774 and 1028 keV, it has to be placed on top of the 7^- isomeric level, and not directly above the groundstate, because such a low lying high-spin level should have been observed during in-beam studies of ^{140}Nd.

^{140}Sm

Bleyl et al.[37] assigned transitions of 137 ± 5 and 228 ± 5 keV to the 14.7 min decay of ^{140}Sm. We studied the decay of ^{140}Sm with mass separated sources after irradiating ^{142}Nd with 90 MeV α-particles. From a comparison of γ-ray and conversion electron spectra (s. fig. 20) we obtained the Z-assignment (rule 4) and conversion coefficients for the transitions. After γγ-coincidence measurements we could construct the partial decay scheme shown in fig. 19b. The placement of the levels results from many coincidence and energy sum relations. The spin assignments are based on the assignment $I^\pi = 1^+$ for the ^{140}Pm groundstate (ref. 38) and on log ft-values.

^{140}Eu

We identified the ß-decay of ^{140}Eu by the occurence of the known $2^+ \rightarrow 0^+$ transition of 531 keV in ^{140}Sm which is a strong transition in in-beam measurements[27]. The half-life of 20^{+15}_{-10} s is given with large error bars, because the production by ^{144}Sm(α,7n+p)^{140}Eu proceeds with a small cross-section. Thus, the 531 keV transition appears only very weakly during the first 10 s after the irradiation of ^{144}Sm with 104 MeV α-particles.

Branching of ß-rays

In the A = 140 decay chain only a rough estimate of log ft-values was possible, which, however, allowed a classification according to rule 9. In order to obtain the amount of ß-rays feeding the 1^+ groundstate of ^{140}Pm and the 0^+ groundstate of ^{140}Nd, we used (i) an analysis of the 14.7 min component of the annihilation radiation (which was in accordance with the results of ref. 37) and (ii) a comparison of the itensities of the 531 and 226 keV

transitions in alternating in- and off-beam measurements. We found that the 226 keV transition occurs in 15±3 % of the decays of ^{140}Sm. Since the 14.7 min decay of ^{140}Sm and the 9.2 s ground-state decay of ^{140}Pm soon reach a radioactive balance, we could determine the intensities of the γ-rays following the ^{140}Pm decay relative to the 226 keV transition of the ^{140}Sm decay. Because the 226 keV transition occurs in 15 % of the decay of ^{140}Sm, also the intensities of the transitions of the ^{140}Pm decay could be normalized to the total number of decays. From the intensity, feeding the excited levels of ^{140}Nd, one obtains that about 90 % of the ^{140}Pm decays directly populate the groundstate of ^{140}Nd.

6. The decay chain A = 139

This mass chain exhibits special features with respect to the $11/2^-$ isomers which are of theoretical interest. When comparing the isomeric decay of the neighboring nuclei ^{139}Sm and ^{139}Pm (s. fig. 21), one finds for the $11/2^- \rightarrow 5/2^+$ E3 transitions approximately the same energy (190 and 189 keV respectively). However, the half-lives of these isomeric decays of 9.5 s and 0.5 s, respectively, differ by a factor of 20. This strong retardation for ^{139m}Sm ought to be explained e.g. either by an anomalous configuration of the $5/2^+$-level (e.g. a strong admixture of a one-phonon excitation[42]), or by different deformations of the $11/2^-$-levels. Such deformations will be discussed in a subsequent publication (part II).

^{139}Pm

In 1967 and 1968 Bleyl et al.[43,37] found in the annihilation radiation from activated ^{142}Nd targets a 4.0 ± 0.2 min component, which they assigned to the reaction ^{142}Nd(d,5n)^{139}Pm. We identified γ-rays at 403 (30), 367 (8) and 467 keV (8) as belonging to this radioisotope and found for its half-life 4.1 ± 0.3 min. Spectra of conversion electrons showed that all three transitions have the multipolarity E2 + M1.

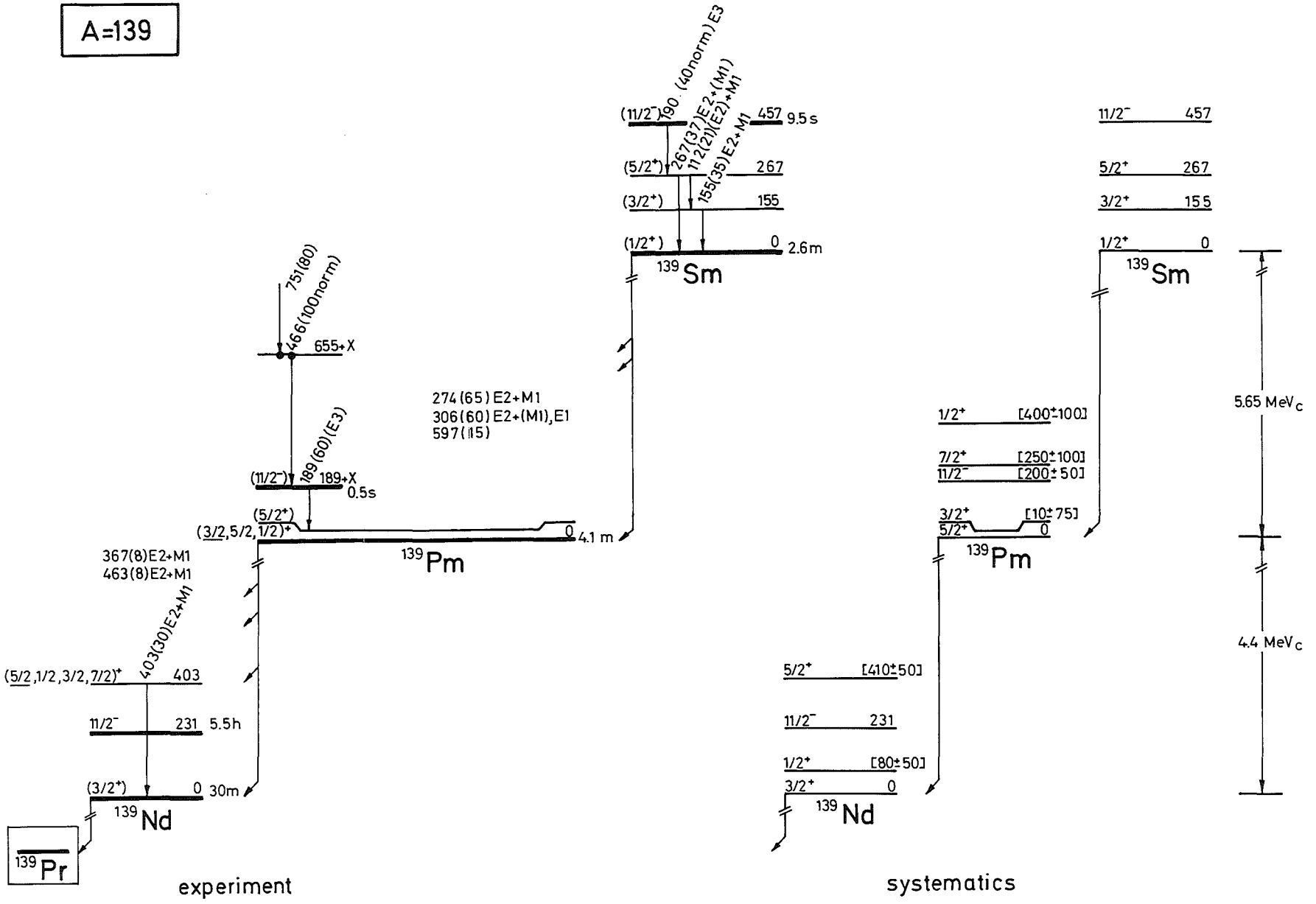

Fig. 21: The decay chain A = 139

The level at 403 keV

The transition of 403 keV is the strongest and should correspond to a level at that energy. The measured multipolarity and the $3/2^+$ groundstate of ^{139}Nd (s. ref. 47) restrict I^π to $(1/2...7/2)^+$. Of these, the level systematics favours $5/2^+$.

The groundstate of ^{139}Pm

As discussed below, the production of the 4 min groundstate of ^{139}Pm via the reaction ^{141}Pr(α,6n) proceeds almost completely through a transition of 466 keV feeding the $11/2^-$ state (rule 14), which decays only via γ-transitions. We observed the 403 keV transition in 30 $\pm$ 10 % of the 466 keV transition. Taking the other γ-rays and possibly non-observed transitions into account, a direct ß-feed into the ^{139}Nd groundstate in-between 40 and 70 % is suggested. This allowed ß-decay restricts the groundstate spin of ^{139}Pm to $(5/2, 3/2, 1/2)^+$. The level systematics almost exclude $I = 1/2^+$, but suggest close lying levels of $3/2^+$ and $5/2^+$.

The 0.5 s isomer of ^{139}Pm

From the excitation function we could assign a 189 keV transition to ^{139}Pm. It is the only observed transition in ^{139}Pm which decays with a half-life of about 0.5 s and must originate from an isomeric level. Its multipolarity can be confined to M3 or E3, if unreasonable enhancement or hindrance factors (e.g. 10^5 for M2) are excluded. In-beam studies[61] revealed two strong coincident transitions at 466 (100) and 751 keV (80) besides the one at 189 keV (60), while no further transitions of comparable γ-ray intensity were observed. From the theoretical total conversion coefficients of the 189 keV transition (E3: 1.2; M3: 6.6) and its γ-intensity the total (γ+e)-intensity depopulating the 0.5 s isomer can be calculated for the two multipolarities to be $\sim$130 (E3) or $\sim$460(M3). Since a missing intensity of 360 can be excluded, the

189 keV transition should have the multipolarity E3. The E3 multipolarity restricts I^{π} of the isomer to $(11/2,9/2)^-$. Of these, the $11/2^-$ is favoured by systematics.

^{139g}Sm

We assigned γ-rays at 274 (65), 306 (60) and 597 (15) keV to the groundstate decay of ^{139}Sm on the basis of excitation functions and the $E_\gamma - E_K$ distance of the conversion electrons. The three γ-rays decay with a half-life of 2.6 ± 0.2 min and show growth from feeding by the $11/2^-$ isomer. The decay scheme of this $11/2^-$ isomer at 457.4 keV has been published earlier in ref. 42. From this isomeric decay we estimated the number of produced ^{139}Sm nuclei and the decay strengths of the 274 and 306 keV transitions. ^{139g}Sm is primarily produced via the isomeric decay, as can be seen from the almost complete growth of the transitions and from the experimental isomeric ratio: $\sigma(11/2^-)/\sigma(5/2^+) = 18 \pm 5$. This ratio was obtained by comparing the prompt and the delayed component of the 111.8 keV transition (cf. fig. 21), where the delayed component results from the isomeric decay. Therefore, we obtained from intensities and decay rates of the 190 keV E3-transition and the 306 keV transition that the 274 and 306 keV transitions occur in 65 ± 10 % and the 597 keV transition in 15 ± 5 % of the decays of ^{139g}Sm.

7. The decay of ^{138}Pm

^{138}Pm decays with a half-life of 3.5 ± 0.3 min into many excited levels of the even-even nucleus ^{138}Nd (s. fig. 22). The identification of these levels is of considerable interest in order to test in how far the Gneuß-Greiner model[41] can reproduce them. Additonal levels in ^{138}Nd, which have been identified in in-beam experiments, are given in a separate level scheme in fig. 22. Our results from an (α,xn)-reaction are in agreement with data from an (^{16}O,xn)-experiment (ref. 45)as well as with (p,xn)-data (ref.46). While in the HI-reaction preferentially high spin states were observed, the (p,xn)-reaction led to a stronger population of lower-spin levels. These in-beam results will be discussed together with the theore-

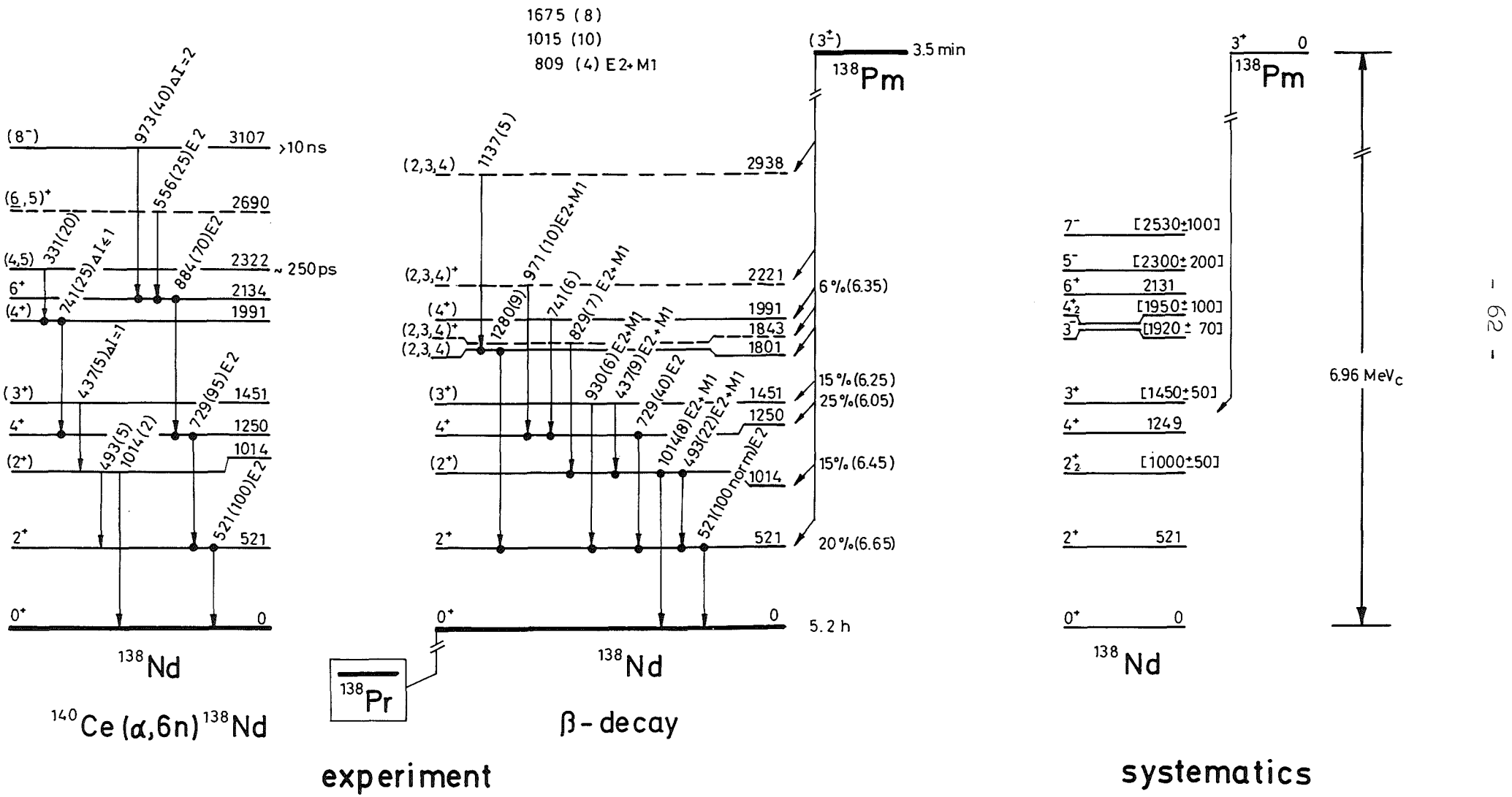

Fig. 22: The decay scheme of ^{138}Pm

tical interpretation of the nucleus ^{138}Nd in a separate publication in the near future.

In fig. 22, tentatively assigned levels, which are suggested only by one coincidence relation, are given by a dashed line.

The level at 521 keV

The position of this level resulted from the coincidence relations and the large intensity of the 520.8 keV transition. Since the level decays by an E2 transition into the 0^+ groundstate it has the spin 2^+.

The level at 1250 keV

The level decays with an E2 transition into the 2_1^+ level, and consequently has $I^\pi = (4, 3, 2, 1, 0)^+$. Since no crossover transition into the groundstate could be found and since the γ-ray of 729 keV is observed with high intensity during in-beam measurements, the spin value $I^\pi = 4^+$ - in agreement with level systematics - is most probable.

The level at 1014 keV

The assignment of this level results from the observed coincidence and the crossover transition. Since the 1014 keV γ-ray has the multipolarity E2 or M1, the level has $I^\pi = (1, 2)^+$. According to level systematics, a spin of 2^+ is favoured.

The level at 1451 keV

Since the 930 keV transition has the multipolarity M1 or E2, the spin of this level can be confined to $(4, 3, 2, 1, 0)^+$. Because we do not observe a direct transition to the groundstate and because the depopulation of the level is observed in in-beam experiments, we can conclude that the spins $(2, 1, 0)^+$ are less probable. From systematics one expects a 3^+ level at this energy.

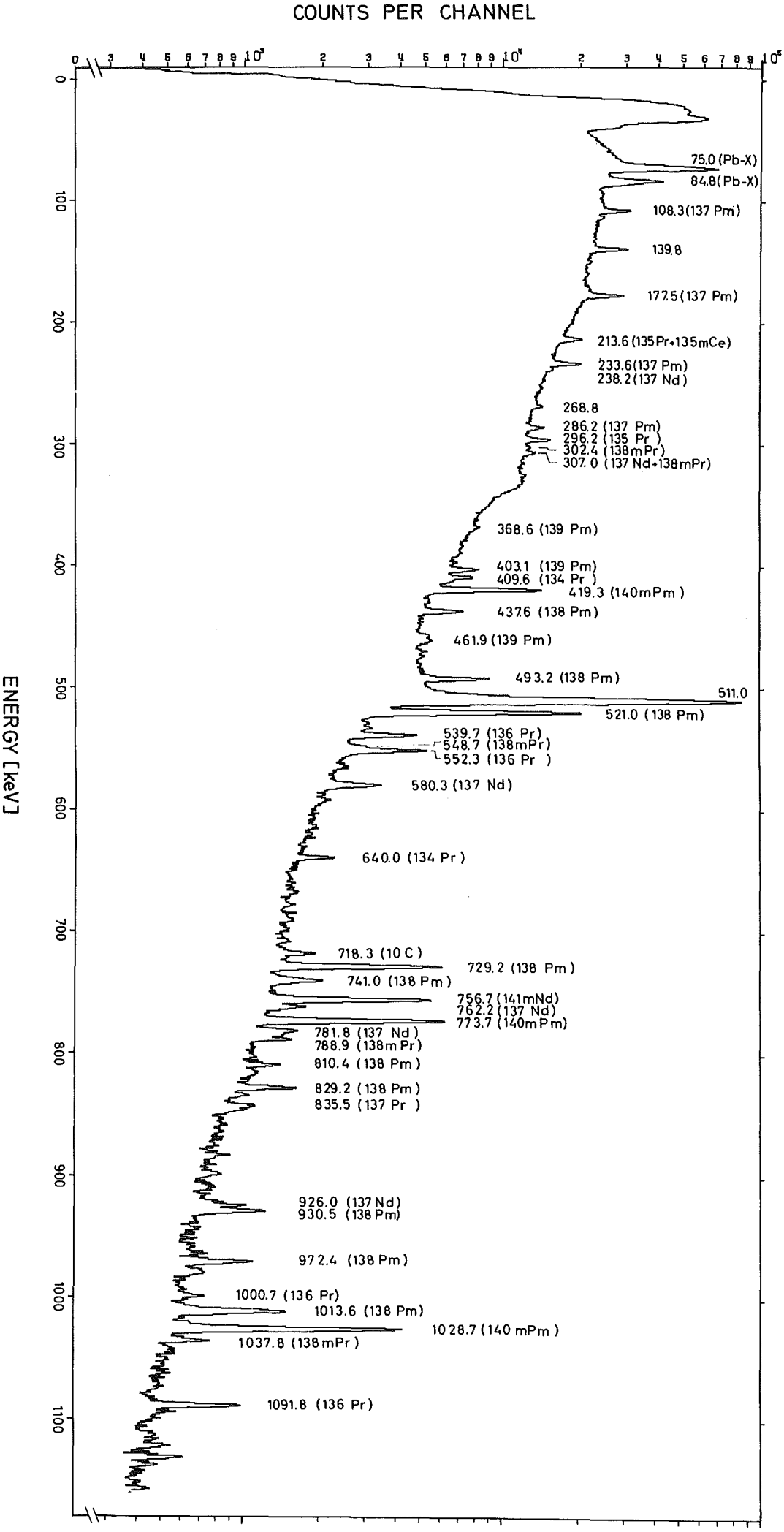

Fig. 23: γ-ray spectrum obtained 2 min after the irradiation of ^{141}Pr with 104 MeV α-particles.

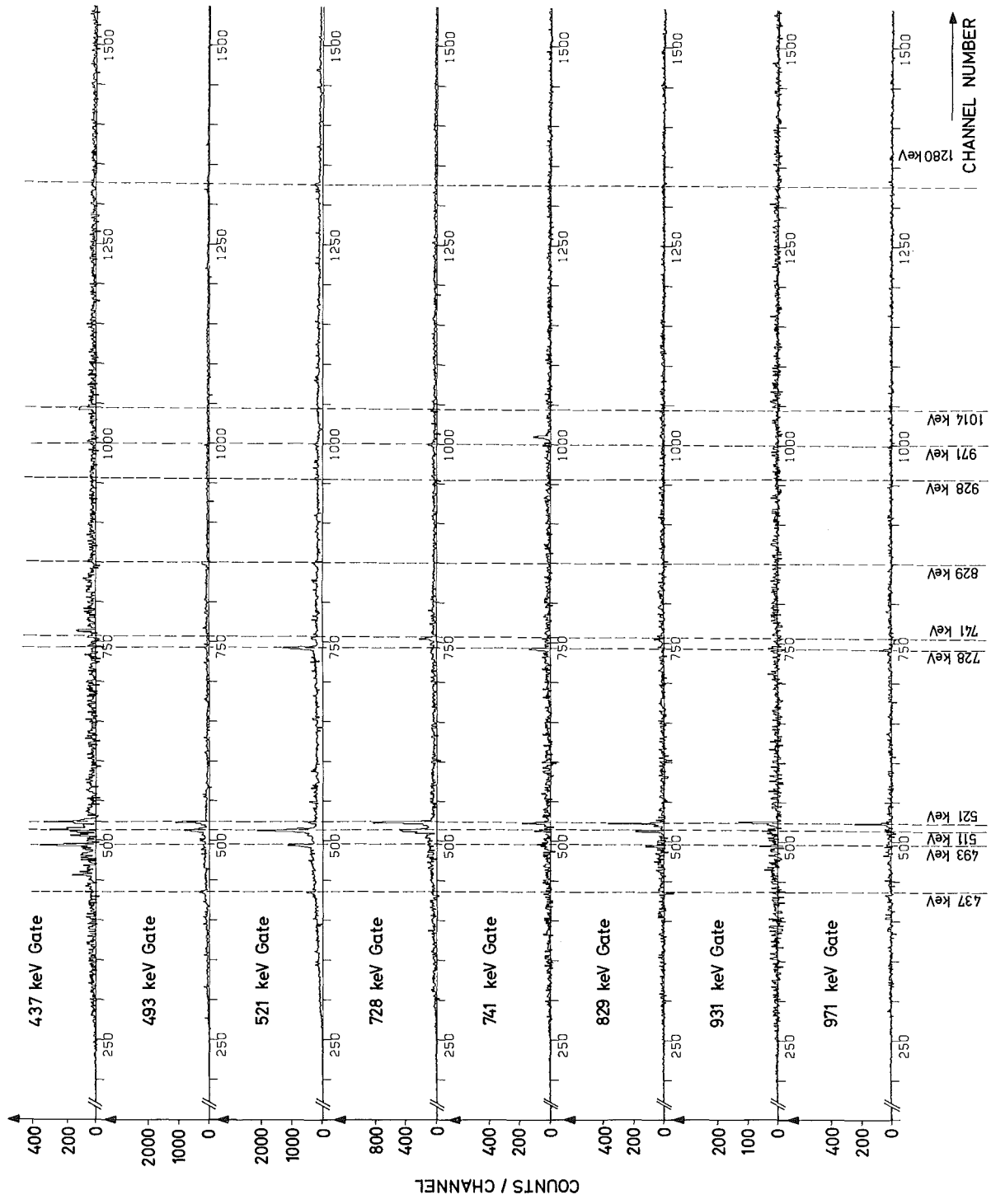

Fig. 24: Coincidence spectra for transitions in ^{138}Nd with gates at E_γ = 437, 493, 521, 728, 741, 829, 931 and 971 keV.

The level at 1991 keV

Since the 741 keV transition is observed in coincidence with E_γ = 332 keV in in-beam measurements, its multipolarity can be restricted to E1, E2, M1 or M2 (rule 12). A pure $\Delta I = 2$ transition can be ruled out from in-beam angular distribution measurements. Thus, the spin of the 1991 keV level is confined to 3, 4 or 5. The strong population of the level in in-beam experiments favours I = 4, 5. The groundstate spin of 3^+ of ^{138}Pm and the observed ß-feed into the 1991 keV level with a log ft - value of 6.35 favours an assignment of $I^\pi = 4^+$, which agrees with predictions from level systematics.

The levels at 1801, 1843, 2220 and 2938 keV

Since it is shown below that the groundstate of ^{138}Pm probably has the I^π value of 3^+, all these levels, which are observed to be populated in the ß-decay, probably have a spin-value of 2, 3 or 4. The log ft-values between 6 and 7 only admit allowed or non-unique first forbidden ß-decay.

The groundstate of ^{138}Pm

The ß-decay of ^{138}Pm feeds levels in ^{138}Nd, which are most probably the 2^+ and 4^+ state of the quasirotational groundstate band. Since the log ft-values for these ß-decays lie around 6.5, the groundstate of ^{138}Pm has most likely $I^\pi = 3^+$. According to the coupling rules one expects in ^{138}Pm a low lying 3^+ level with the configuration $\left[\pi(d_{5/2}) \times \nu(s_{1/2})\right]_{3^+}$.

8. The decay chain A = 137

Of this mass chain (cf. fig. 25) the ß-decay of ^{137}Nd has been studied in detail (ref. 47) and will be published separately in the near future. Since meanwhile a decay scheme of ^{137}Nd has been published by Buttsev et al.[48] which disagrees with our results, we will present here besides the level scheme our experimental evidence with respect to the most important discrepancies.

Our present knowledge of the parent nucleus ^{137}Pm is far less detailed. The investigation of its ß-decay will become interesting, since probably many levels of high spin and negative parity are populated in ^{137}Nd. The levels have lately been described successfully for other nuclei in a Nilsson model with a strong Coriolis interaction (s. ref. 43).

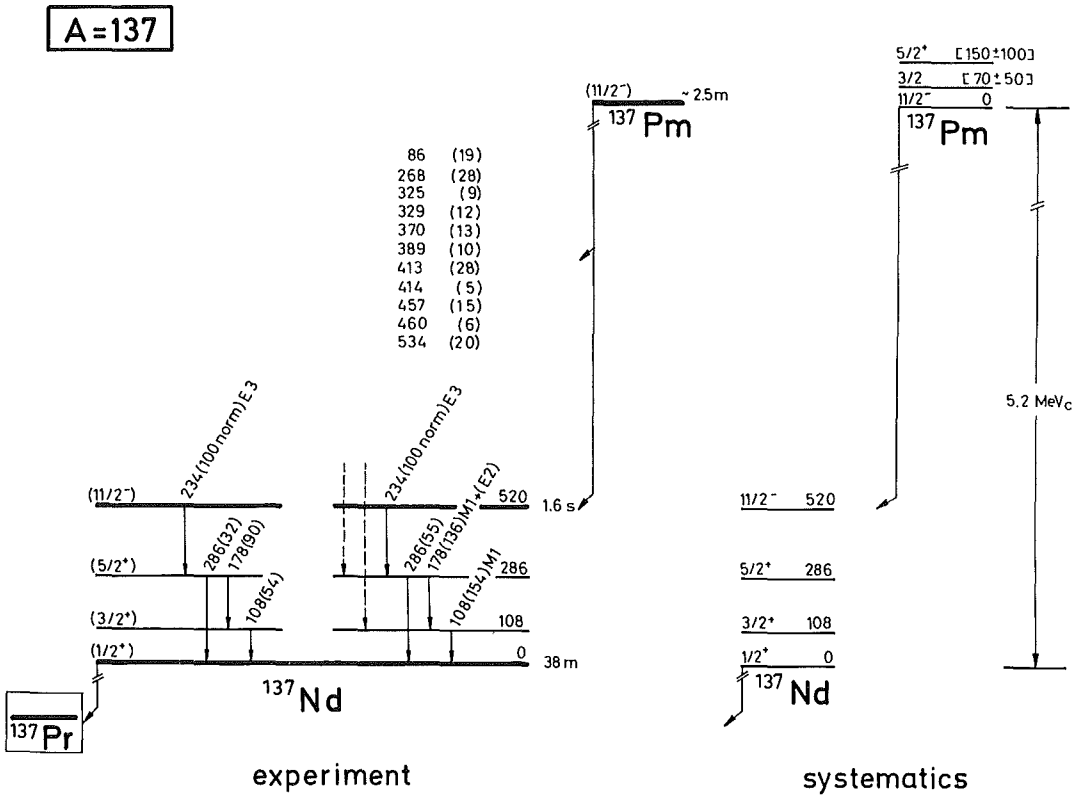

Fig. 25 : The decay chain A = 137

^{137}Pm

The decay of the 1.6 s isomer of ^{137}Nd was studied by Droste et al.[50]. Our activations by ^{140}Ce(α,7n) ^{137m}Nd yielded similar results on the cascade $11/2^- \rightarrow 5/2^+ \rightarrow 3/2^+ \rightarrow 1/2^+$ with a $5/2^+ \rightarrow 1/2^+$ crossover transition, which cascade is typical for the N = 77 isotones. However, after α-activation of ^{141}Pr we observed this cascade with a much longer half-life of 2.5 ± 0.3 min. Because of the reaction mechanism and due to rule 18, double isomerism in ^{137}Nd is improbable and we assign this 2.5 min ß-decay to ^{137}Pm.

The γ-ray intensities following the ß-decay are quite different from the intensities in the isomeric decay. Almost half the population of the $5/2^+$ and $3/2^+$ level in ß-decay does not result from the decay of the $11/2^-$ isomer. We could assign many further transitons to the 2.4 min ß-decay of ^{137}Pm (see fig. 25) by performing a mass separation after irradiating ^{141}Pr with 104 MeV α-particles. A γ-ray spectrum of these measurements is shown in fig. 26. We have to perform γγ-coincidence measurements before the newly assigned γ-transitions can be placed in the decay scheme.

The strong population of the $11/2^-$ isomer in this decay points to a spin $I \geq 7/2$ for the 2.5 min level of ^{137}Pm. From level systematics a low lying $11/2^-$ level in ^{137}Pm is expected which may even be the groundstate. This level should be populated strongly (Yrast rule 14) and can feed the $11/2^-$ level of ^{137}Nd as well as additional high-spin states which decay to the $5/2^+$ and $3/2^+$ levels by not yet placed transitions.

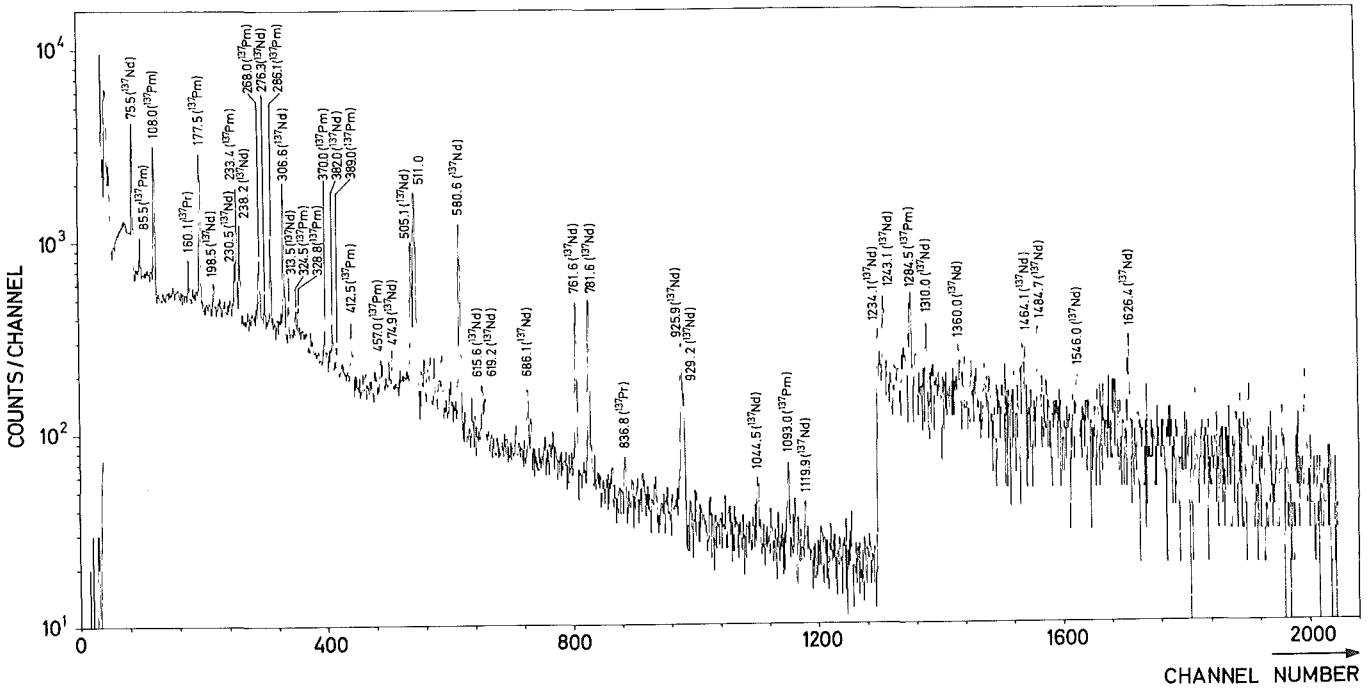

Fig. 26 γ-ray spectrum of the mass chain A = 137 obtained from mass separated sources after the irradiation of ^{141}Pr with 104 MeV α-particles.

Isomers in ^{137}Nd

In addition to the well-known 1.6 s isomer of ^{137}Nd[50,42] Buttsev et al.[48] reported on a second isomer which they deduced from a relatively strong X-ray component belonging to Nd and decreasing with a half-life of 20 min. In order to produce this radioisotope we irradiated ^{140}Ce as well as ^{141}Pr with 104 MeV α-particles, and having performed mass separations on A = 137, we measured the X-ray spectra. No component belonging to Nd was found 20 min after the irradiation (s. fig. 27). Since in our experiments preferentially high-spin states are populated, we can exclude from our data the existence of a second high-spin isomer in ^{137}Nd.

Since for nuclides in the neighborhood of ^{137}Nd no 20 min activity is known, this component observed in ref.[48] perhaps belongs to the low-spin decay of ^{137}Pm. From level systematics a very low lying $3/2^+$ level is expected which could decay to the assumed $11/2^-$-groundstate only via a M4 transition of low energy and should, therefore, preferentially undergo ß-decay. This level would be populated in the present experiments only to a very small amount and, therefore, would be not observable in our X-ray spectra.

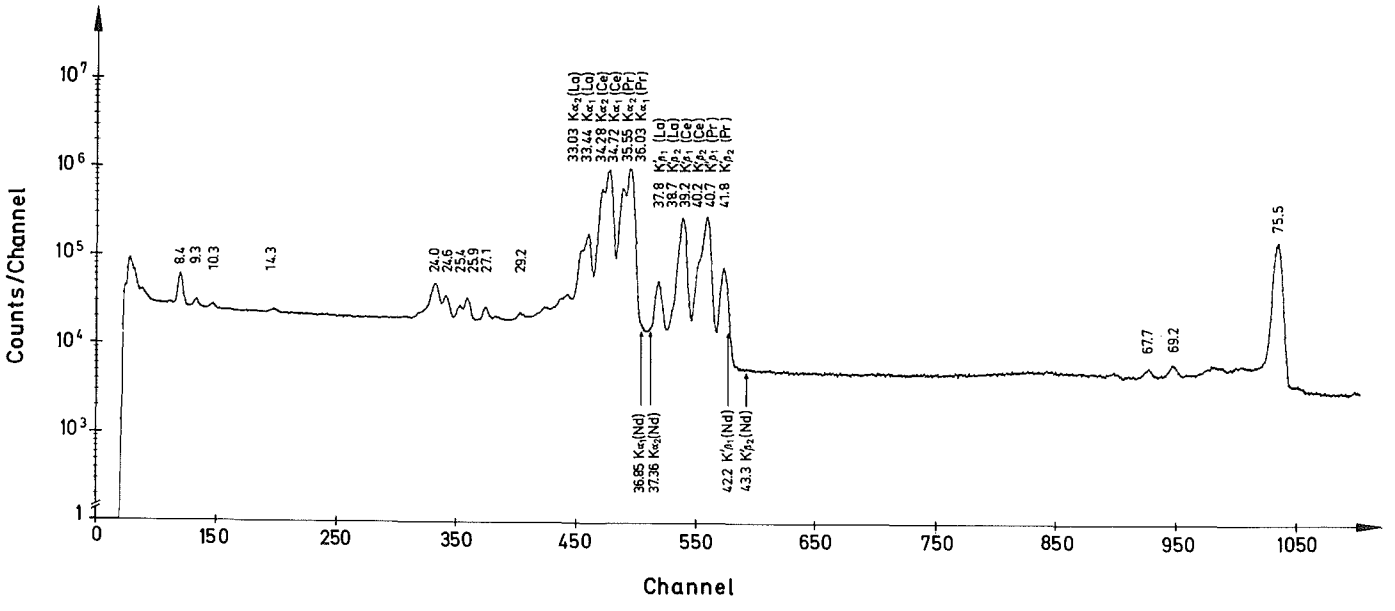

Fig. 27: X-ray spectrum obtained from a mass separated source after the irradiation of ^{140}Ce with 104 MeV α-particles.

^{137}Nd

The decay scheme of ^{137}Nd shown in fig. 28 has been discussed in detail in ref. 47 . The decay scheme obtained by Buttsev et al.[48] differs - in addition to some weakly populated levels which were not identified in our data - essentially with respect to the assignment of the two strong transitions of 75 and 306 keV . Furthermore, a different spin assignment for the level at 75 keV results. In ref. 48 from γγ-coincidences and from conversion electron measurements with extremely high resolution the 75 keV line was deduced to have two components separated by ∿ 0.2 keV with an intensity ratio of 3:1. The stronger of these components was assigned to depopulate the level at 75 keV. Its total intensity should be equal to the populating γ-intensity and, therefore, no ß-feed into this level should occur. Thus, a spin of 7/2 was assigned to the 75 keV level in ref. 48.

In contrast to these results, we did not observe the 75 keV line to be in coincidence with another γ-transition of approximately the same energy. In fig. 29a, the coincidence spectrum with the gate set on E_γ = 75.5 keV is shown and an enlarged part of this spectrum is given in fig. 29b together with the coincidence spectrum for E_γ = 306 keV . This latter one demonstrates the strength of the 75 keV-transition being in coincidence with E_γ = 306 keV. In all these coincidence spectra, the averaged background, taken from gates on both sides of the peak, has been subtracted. Taking the double statistical error as an upper limit, we can exclude a γ-intensity larger than 4 % of the total 75 keV γ-intensity to be in coincidence with E_γ = 75 keV. In addition, we tried to resolve the two possible components of the 75 keV lines by means of a large orange typ magnetic ß-spectrometer.[¥] In fig. 30a the spectrum of the K-conversion electrons of the 75 keV transition with E_e = 33.2 keV is shown. Due to the resolution of the spectrograph of 0.5 % (= 290 eV at 33.2 keV), it was impossible to separate two components with a distance of 200 eV as quoted in ref.48 .

¥ We gratefully acknowledge the assistance of M.Schwall, Inst.f. Experimentelle Kernphysik des Kernforschungszentrums Karlsruhe, who performed these measurements.

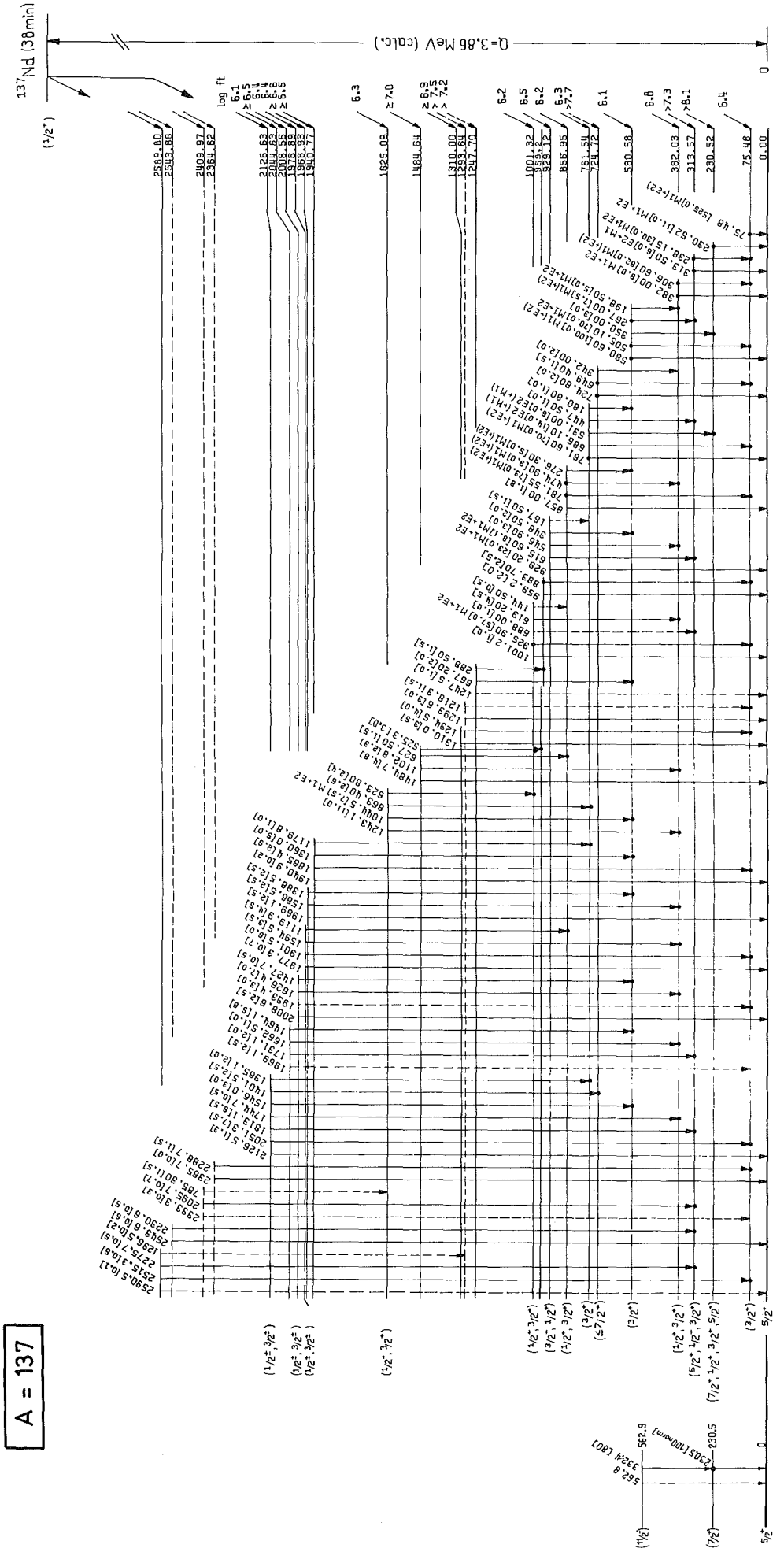

Fig. 28: The decay scheme of ^{137}Nd (right-hand side) and the decay of the $11/2^-$-isomer of ^{137}Pr (left-hand side).

a:

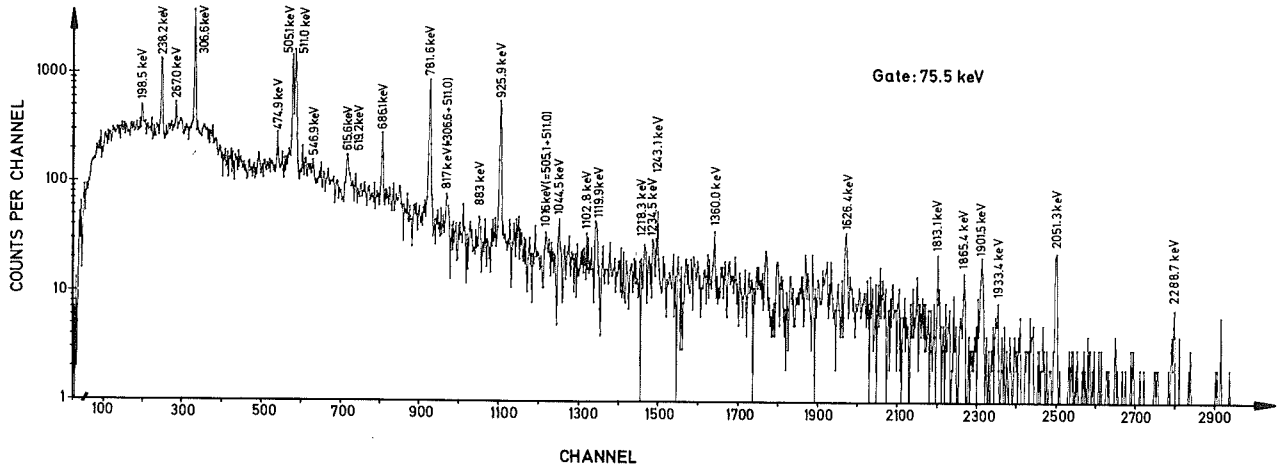

b:

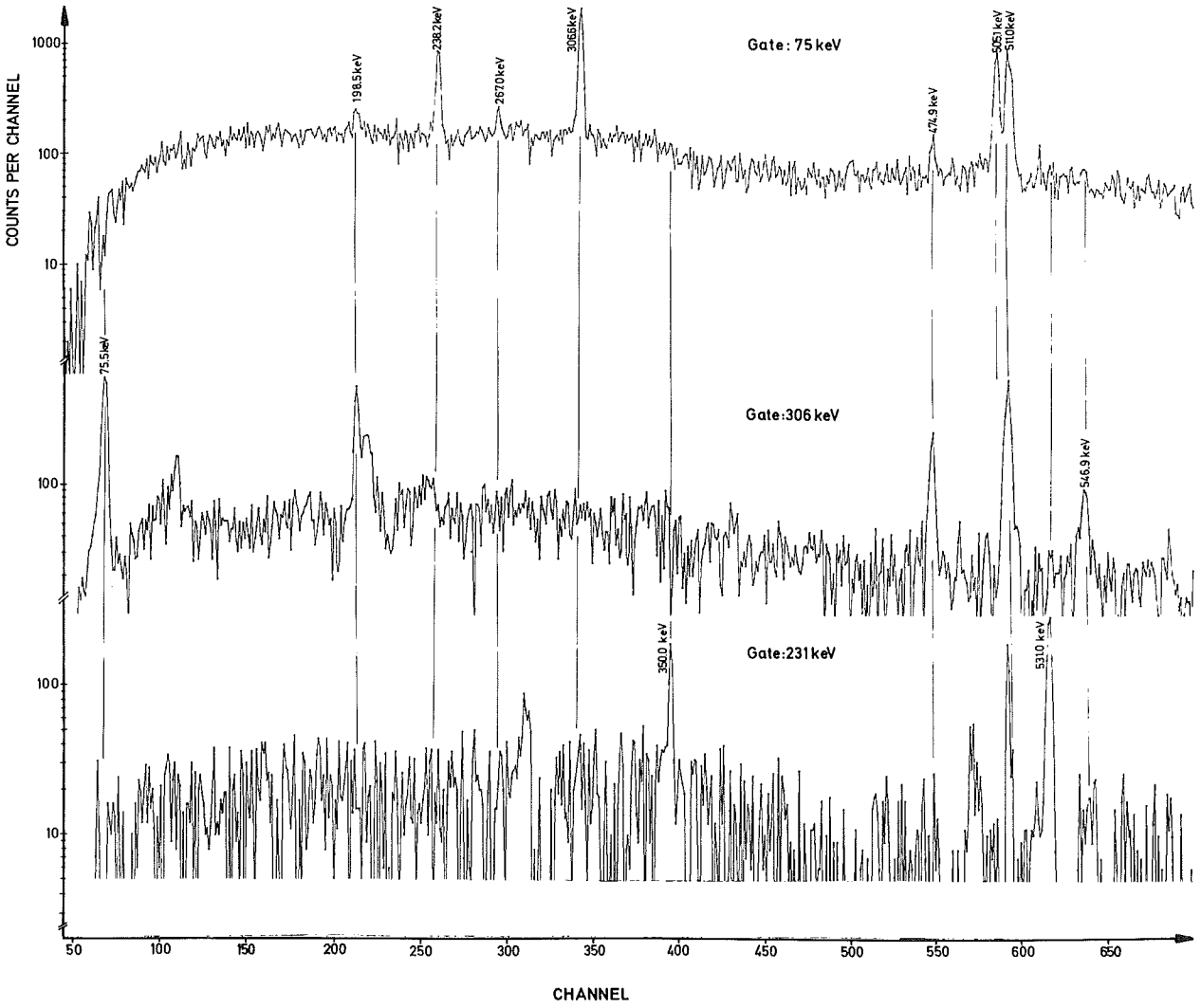

Fig. 29: Coincidence spectra for transitions following the ß-decay $^{137}Nd \rightarrow {}^{137}Pr$.

a) Gate at 75 keV (small scale)

b) Gates at 75, 306 and 231 keV

On the other hand, when fixing the energy distance of a possible second component to 200 eV, we obtained a lower limit for the relative intensity of the weaker component of about 6 %. In fig.30 the measured K-conversion line of the 75.5 keV transition in ^{137}Pr together with lines of ThC" are shown. These lines of ThC" were used for energy and peak form calibration. We also tried to fit a second peak into the high energetic tail of the 33.2 keV peak of fig. 30a with an automatic search routine. After starting the fitting routine with a second peak in a distance of 200 eV we finally obtained a further weak line at 33.75 keV (s. fig.30a). Such high energetic tails of peaks probably are due to an inferior adjustment of the spectrometer.

Thus, neither from coincidence nor from conversion electron spectra, our measurements give any hint to a second transition at 75 keV with a relative intensity larger than 6 %. In thise case, one concludes from balance considerations that there exists a strong ß-feed into the level at 75 keV. This leads to a spin assignement of $I^{\pi} = 3/2^{+}$ for the 75 level as given in the decay scheme of fig. 28.

We assume the level at 231 keV to be the $7/2^{+}$ state expected from level systematics. This is confirmed by observing the 231 keV γ - ray strongly during in-beam studies[61], where Yrast levels are populated preferentially. The 231 keV transition was not observed in coincidence with $E_{\gamma} = 75$ keV during off-beam as well as in-beam measurements. Fig. 29 shows, that the only strong coincidence of the 231 keV transition observed off-beam is with $E_{\gamma} = 531$ keV, leading to a cascade which depopulates the well established 761 keV level. The in-beam $\gamma\gamma$-coincidences show a strong cascade 231-332 keV, which we tentatively assign to the transitions $11/2^{-} \rightarrow 7/2^{+} \rightarrow 5/2^{+}$ due to level systematics and to the Yrast rule (rule 14). This is confirmed by the fact, that other strong in-beam transitions were not observed in coincidence with $E\gamma = 231$ keV. Thus, the cascade 231-332 keV should depopulate a level with a half-life large compared to the coincidence resolving time of $2\tau = 30$ ns.

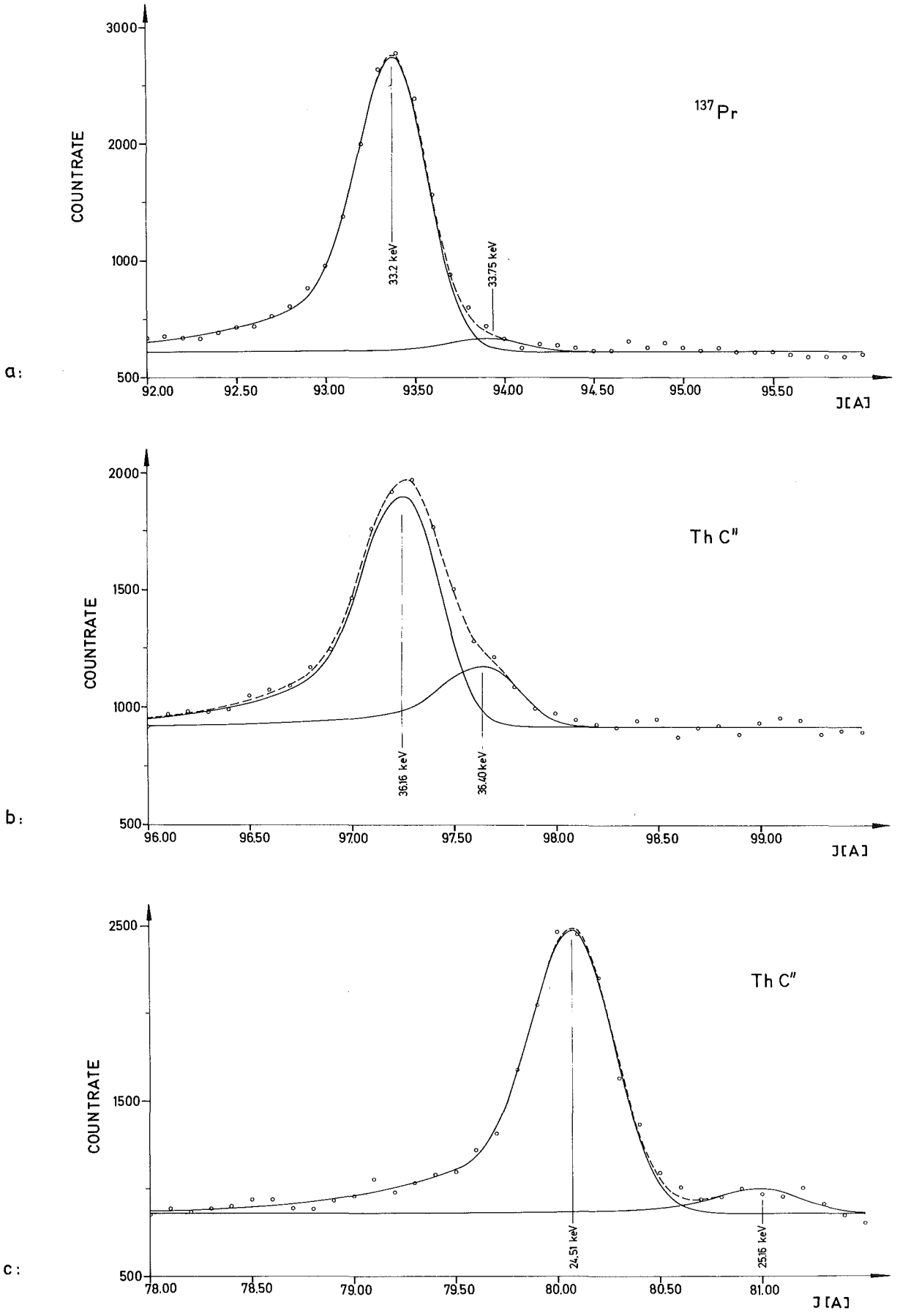

Fig. 3o a: K-conversion line (E_e = 33.2 keV) of the 75.5 keV transition in ^{137}Pr obtained with a high resolution ß-spectrometer.

b: The 36.16 and 36.4 keV lines from ^{208}Tl (Th C")

c: The 24.51 and 25.16 keV lines from ^{208}Tl (Th C")

9. The decay of ^{135}Nd

Within the 135 mass chain, we investigated especially the decay $^{135}Nd \rightarrow ^{135}Pr$ (cf. fig. 31). This decay was first reported by Brosi et al.[51], who assigned two γ-transitions at 205 and 442 keV to a 12 min-decay of ^{135}Nd. In contrast, Abdurazakov et al.[52] determined the half-life of the ß-decay to be 6 ± 1 min.These authors produced ^{135}Nd via a spallation reaction of Gd, using 600 MeV protons. Perhaps this half-life corresponds to the low-spin isomer of ^{135}Nd(cf. fig. 31). The groundstate spins of ^{135}Nd (I = 9/2) and ^{135}Pr (I = 3/2) were determined by Ekström et al.[53] by means of atomic beam resonance measurements. Recently, Conlon[54] reported a partial decay scheme which is in agreement with our results.

^{135}Nd

We produced ^{135}Nd via the reaction $^{138}Ce(\alpha,7n)\ ^{135}Nd$. Due to the relatively long half-life of ~12 min,mass separated sources could be obtained. Fig. 32 shows examples for a γ-ray spectrum and a conversion electron spectrum obtained with the anticompton - spectrometer 20 min after the irradiation. The transitions were assigned to ^{135}Nd by means of their half-life as well as by the energy difference $E_\gamma - E_K$.Up to now, coincidence measurements were not performed with sufficient statistics to place all assigned transitions in the level scheme shown in fig. 31.

The groundstate of ^{135}Pr

The groundstate spin of ^{135}Pr was measured by Ekström et al.[53] to be 3/2. Since from level systematics a low lying $3/2^+$ level is expected, we assigned positive parity to the groundstate.

The level at 41 keV

In the spectrum of conversion electrons (fig. 32b) a strong L-line corresponding to E_γ = 41.5 keV is seen. Together with the γ-inten-

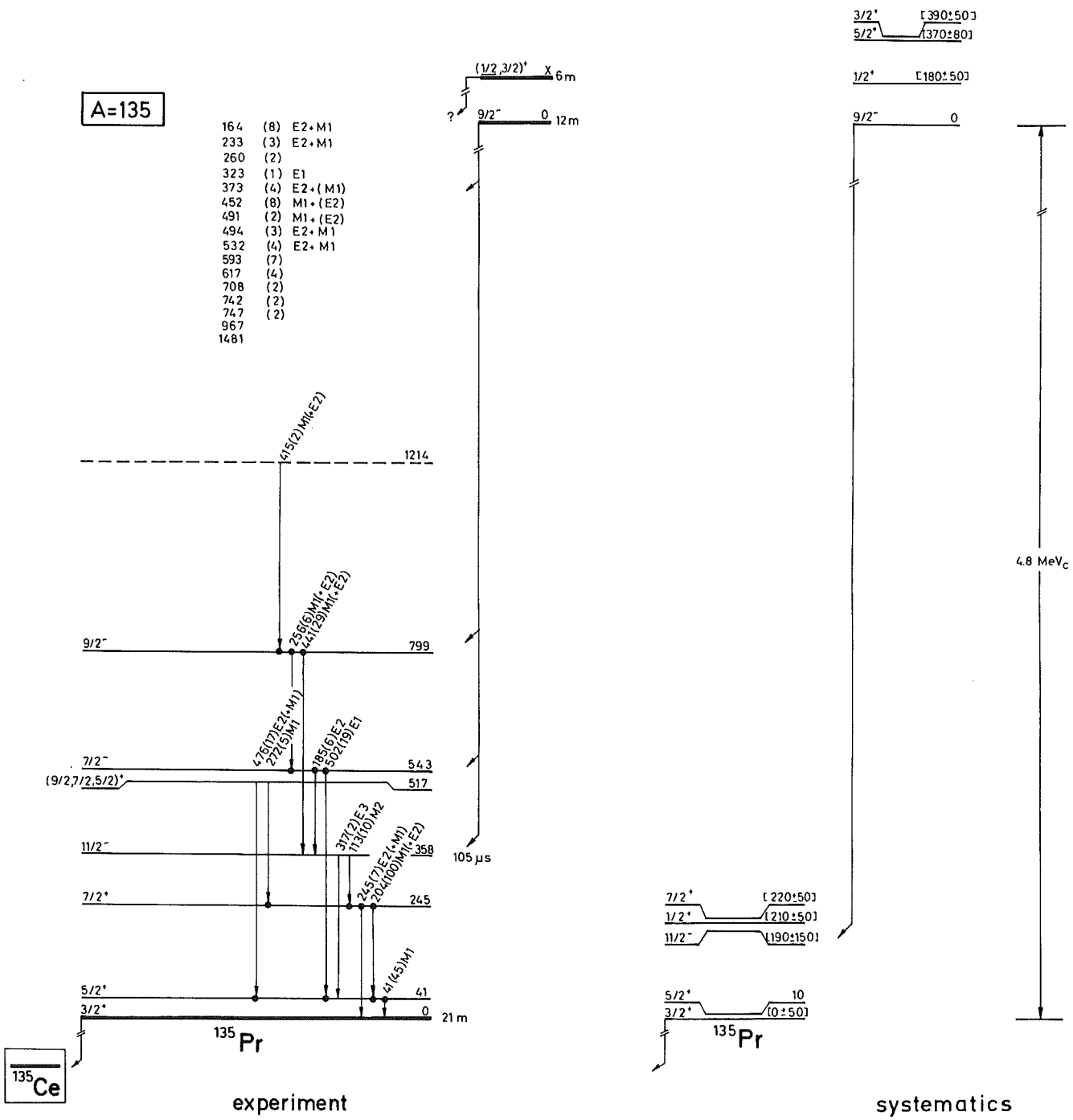

Fig. 31: The decay scheme of ^{135}Nd

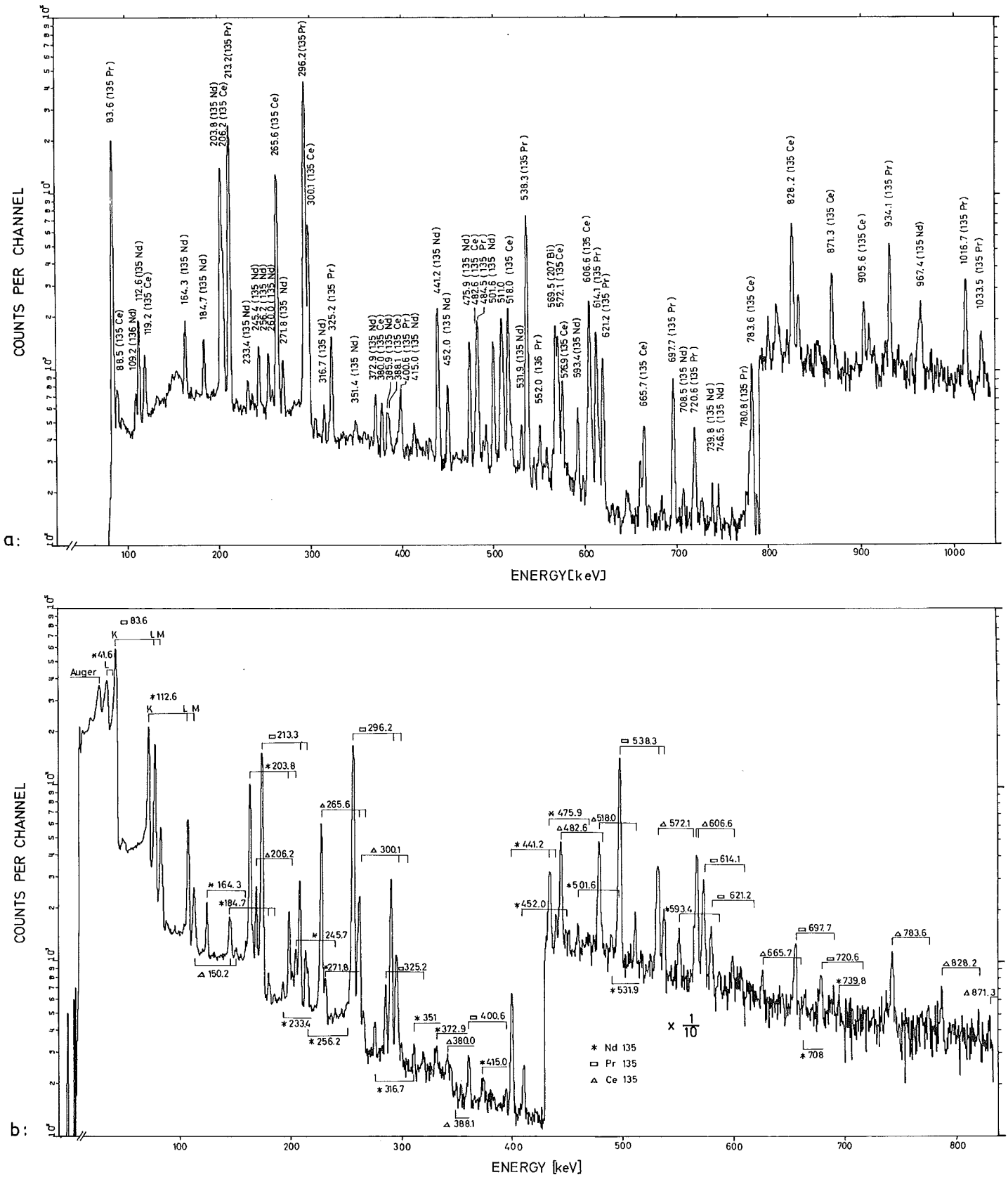

Fig. 32: γ-(ray) (a) and conversion electron (b) spectrum of the mass chain A = 135 obtained from mass separated sources 2o min after the irradiation of ^{138}Ce with 9o MeV α-particles. The gamma-ray spectrum has been measured with the anti-compton spectrometer.

sity we obtained a total L-conversion coefficient $\alpha_L = 2.0 \pm 1.3$ which points to a rather pure M1 transition. Since the total intensity of this transition is the strongest observed intensity of all transitions assigned to ^{135}Nd, we adopt a level at 41 keV with $I^\pi = (5/2, 3/2, 1/2)^+$. This placement is confirmed by the coincidence measurements.

The level at 245 keV

The strong coincident transitions at 204 and 41 keV and the corresponding crossover transition at 245 keV indicate a level at 245 keV This level has positive parity, since the 245 keV transition, feeding the $3/2^+$ groundstate, has the multipolarity E2 or M1. Based on this multipolarity, the highest possible spin is $7/2^+$; this assignment is most probable, because the level is strongly fed during in-beam measurements. In addition, a $7/2^+$ level at about this energy is expected from level systematics. The strong M1 component of the 204 keV transition feeding the level at 41 keV suggests a positive parity and therefore confirmes $I^\pi = 5/2^+$ for this level. The ordering of the 41 and 204 keV transitions is based on the relative intensities and is supported by level systematics.

The level at 358 keV

Since the M2 transition of 112.6 keV was observed in coincidence with the 204 keV transition, we adopted a level at 358 keV. Taking conversion into account, one obtains for the 112.6 keV transition a total intensity of 90 ± 10 % of the 204 keV intensity in in-beam measurements as well as in the radioactive decay. The level at 358 keV should be an isomeric state, since the Weißkopf-estimate for the highly converted M2 transition of 112.6 keV is 10 µs. This is confirmed by in-beam $\gamma\gamma$-coincidence measurements, where many strong γ-transitions [61] (e.g. 373 keV) are not observed in coincidence with $E_\gamma = 204$ keV, though they should be placed on top of this transition in the level scheme. Spin and parity of the level at 358 keV are most probably $11/2^-$, because an E3 crossover transition of 317 keV into the $5/2^+$-level is observed. Since no further strong transitions to lower lying levels were observed, spins less

than 11/2 are improbable according to rule 13. Furthermore, the level is strongly populated in in-beam experiments (Yrast rule 14), and Conlon[54] observed a decrease of the 204 and 112 keV transitions with a half-life of 105 ± 10 µs.

The level at 517 keV

The placement of the level is obtained from an energy sum relation and the fact that the two transitions of 467 and 272 keV are observed in coincidence with a high energetic transition of 1481 keV , which feeds the level at 517 keV.

The levels at 543 and 799 keV

Both levels could be fixed by energy sum relations and several coincidences. The multipolarities of the transitions at 185 and 501 keV and correspondingly at 256 and 441 keV lead to unique assignments of the I^{π}-values. A $7/2^-$ and a $9/2^-$ level have been predicted from theoretical calculations[25] in the experimentally observed energy range.

We thank B. Feurer, who performed the mass separations, Dipl.-Phys. M. Schwall (I E K P, Kernforschungszentrum Karlsruhe) for the measurements with the magnetic spectrometer, and the cyclotron staff for their good cooperation.
The Bundesministerium für wissenschaftliche Forschung has supported this work.

References

1) Sheline, R.K., Sikkeland, T. and Chanda, R.N.: Phys. Rev. Lett. 7 (1961) 446

2) Clarkson, J.E., Diamond, R.M., Stephens, F.S. and Perlman, I.: Nucl. Phys. A 93 (1967) 272

3) Conlon, T.W. and Elwijn, A.J.: Nucl. Phys. A 142 (197o) 359

4) Smith, G.L. and Draper, J.E.: Phys. Rev. C1 (197o) 1548

5) Stephens, F.S., Leigh, J.R. and Diamond, R.M.: Nucl. Phys. A 17o (1971) 321

6) Wilhelm, A.: Arbeitsbericht Nr. 42, Kernforschungszentrum Karlsruhe Zyklotron - Laboratorium (unpublished)

7) van Klinken, J. and Wisshak, K.: Nucl. Inst. Meth. 98 (1972) 1

8) Wisshak, K.: Jahresbericht des II. Physikalischen Instituts, Heidelberg (Germany) (1971) p. 42 (unpublished)

9) Haase, V.: KFK - Report No. 73o (1968)

1o) Garvey, G.T., Gerace, W.J., Jaffe, R.L., Talmi, J. and Kelson, J.: Rev. Mod. Phys. 41 (1969) S1

11) Lederer, C.M., Hollander, J.M. and Perlman, I.: Table of Isotopes, 6 Ed., J. Wiley & Sons, 1967

12) Zweifel, P.F.: Phys. Rev. 1o7 (1957) 329

13) Horen, D.J. (Ed.): Nuclear Data sheets (197o)

14) Shera, E.B., Ikeda, A. and Sheline, R.K.: Phys. Lett. 4o B (1972) 349

15) Davidson, J. in: Wu, C.S. and Moszkowski, S.A.: Beta Decay, J. Wiley & Sons, New York (1965) p. 1o4

16) Grover, J.R. and Gilat, J.: Phys. Rev. 157 (1967) 814

17) Peker, L.K. in: Proc. Winter School for Nuclear Theory and High Energy Physics (1969) p. 163-2o9; UCRL - trans - 1399 (unpublished)

18) Gallagher, C. J. and Moszkowski, S.A.: Phys. Rev. 111 (1958) 1282

19) Carlé, P. and Kerek, A.: AFI Am. Report, Stockholm (197o) 3.1.9 (unpublished)

2o) Arl't, R., Baier, G., Musiol, G., Peker, L.K., Pfrepper, G. and Shtrusnij, K.: Jzv. Akad. Nauk. SSSR, Ser. Fiz. 34 (197o) 4o9

21) Geiger J.S. and Graham R.L.: Arkiv Fysik 36(1966)191

22) Firestone, R.S.: Ann. Report, Michigan State University (USA) 1971 (unpublished)

23) Hesse, K.: Z. Physik 226 (1969) 328

24) Neubert, W., Alexander, K.F., Rotter, H. Chojnacki, S., Droste, C., Lewitowicz, J. and Morek, T.: Nucl. Phys. A 131 (1969) 225

25) Habs, D.: Thesis, Univ. Heidelberg, 1973 (unpublished)

26) Keller, K.A. and Münzel, H.: Radiochim. Acta 9 (1968) 176

27) Habs, D., Klewe-Nebenius, H., Löhken, R., Göring, S., van Klinken, J., Rebel, H. and Schatz, G.: Z. Physik 25o (1972) 179

28) Goncharov, K.S., Klyucharev, A.P., Pis'Minetskii, S.A., Rakivmenko, Y.N., Remaev, V.V., Romanii, I.A. and Skakun, E.A.: Sov. Journ. of Nucl. Phys. 14 (1972) 1

29) Remaev, V.V., Korda, Y.S., Klyucharev, A.P. and Smirnova, A.M.: Sov. Phys. JETP 16 (1963) 1162

3o) Edwards, V.R.W., Ganguly, N.K., Montgue, D.G., Ramavataram, K., Zucker, A. and Plummer, D.J.: Proc. Int. Conf. Montreal, Canada (1969) p. 277 (unpublished)

31) Julian, G.M. and Fessler, T.E.: NASA TN D-7o4o (1971) 22

32) Ludziejewski, J., Koldewijn, P. and Arnold, H.: Nucl. Phys. A 184 (1972) 473

33) Alexander, K.F.: Roc. Int. Conf. on Nuclear Structure Dubna (USSR) (1968) p. 15

34) Eppley, R.E., Todd, R.R., Warner, R.A., McHarris, W.C. and Kelly, W.H.: Phys. Rev. C5 (1972) 1o84

35) Arl't, R., Baier, G., Musiol, G., Peker, L.K., Pfrepper, G. and Sktrusnij, K.: Jzv. Akad. Nauk. SSSR, Ser. Fiz. 34 (197o) 754

36) Ekström, C., Ingelman, S., Olsmats, M. and Wannberg, B.: Physica Scripta 6 (1972) 181

37) Bleyl, H.J., Münzel, H. and Pfennig, G.: Radiochim. Acta 1o

(1968) 1o6

38) Sakai, M.: INS-J-127, Tokyo (1971) (unpublished)

39) Ball, J.B., Auble, R.L., Rapaport, J. and Fulmer, B.C.: Phys. Lett. 3o B (1969) 533

4o) Reiner, A.S.: Nucl. Phys. 27 (1961) 115

41) Gneuss, G. and Greiner, W.: Nucl. Phys. A 171 (1971) 449

42) van Klinken, J., Göring, S., Habs, D., von Hartrott, M., Klewe-Nebenius, H., Löhken, R., Rebel, H. and Schatz, G.: Z. Physik 246 (1971) 369

43) Bleyl, H.J., Münzel, H. and Pfennig, G.: Radiochim. Acta 8 (1967) 2oo

44) Beerj, D.B., Kelly, W.H. and McHarris, W.C.: Phys. Rev. 188 (1969) 1875

45) Dehnhardt, W.: Thesis, Univ. Heidelberg, 197o (unpublished)

46) Sakai, M.: INS-J-13o, Tokyo (1971) (unpublished)

47) Klewe-Nebenius, H.: Thesis, Univ. Heidelberg, 1973 (unpublished)

48) Buttsev, V.S., Vylov, T., Gromov, K.Y., Kalinnikov, V.G., Gromova, I.I., Morozov, V.A., Muminov, T.M., Fuya, K. and Khalikulov, A.B.: JINR-P6-68o4 (1972) (unpublished)

49) Stephens, F.S., Diamond, R.M., Leigh, J.R., Kammuri, T. and Nakai, K.: Phys. Rev. Lett. 29 (1972) 438

5o) Droste, Ch., Neubert, W., Lewitowicz, J., Chojnacki, S., Morek, T., Wilhelmi, Z. and Alexander, K.F.: Nucl. Phys. A 152 (197o) 579

51) Brosi, A.R. and Ketelle, B.H.: ORNL-43o6 P7 (1968)(unpublished)

52) Abdurazakov, A.A., Arl't, R., Babadzhanov, R., Baier, G., Morozov, V.A., Musiol, G., Tyrroff, K. and Shtrusnij, H.: Jzv. Akad. Nauk. SSSR., Ser. Fiz. 34 (197o) 769

53) Ekström, C., Ingelman, S., Olsmats, M. and Wannberg, B.: Nucl. Phys. A 196 (1972) 178

54) Conlon, T.W.: AERE-R7287, Harwell (1973)

55) Elliot, J.C. and Young, F.C.: Nucl. Sci. Eng. 5 (1959) 55

56) Jansen, G., Morinaga, H. and Signorini, C.: Nucl. Phys. A 128 (1969) 24

57) Malan, H., Münzel, H. and Pfennig, G.: Radiochim. Acta 5, (1966) 24

58) Hager, R.S. and Seltzer, E.C.: Nuclear Data A4 (1968) 1

59) Funke, L., Fromm, W.D. and Keller, H.J.: Proc. Int. Conf. Munich, (1973) p. 93

60) Arnold, H., Koldevijn, P., Kownacki, J., Nedziejewki, J., Ryde, H. and Sujkowki, Z.: Proc. Int. Conf. Munich, (1973) p. 95

61) Habs, D., Nowicki, G., Klewe-Nebenius, H., Wisshak, K., Buschmann, J., Rebel, H. and Schatz, G.: Proc. Int. Conf. Munich, (1973) p. 183

Appendix

In this appendix, we have compiled the data which were used in the present work for identification and assignments of transitions and levels of the new radionuclides. In addition, all transition energies and intensities as well as conversion data with the respective errors are compiled.

Table 1: Time standards for half-life determinations

Nucleus	γ-ray |keV|	$T_{1/2}$	Reference
^{28}Al	1778	2.305±0.006 min	55)
^{145m}Gd	721	1.42 ±0.12 min	56)
^{140m}Pm	419	5.80 ±0.05 min	43)
^{139m}Sm	155	9.5 ±1.0 s	42)
^{143}Eu	1108	2.61 ±0.03 min	57)

Tab. 2: γ-ray energies and intensities and conversion data for all transitions assigned in the present investigation

Gd-142 (1.5 ± 0.3) min

E_γ |keV|	I_γ	α_K	K/L	Multipolarity
179.0 ± 0.6	7 ± 3	< 0.4		E1, E2 + M1
(526)	100 norm	(Gd-142 prompt)		

Gd-143 (1.9 ± 0.3) min

E_γ |keV|	I_γ	α_K	K/L	Multipolarity
117.8 ± 0.5	10 ± 3	4.2 ± 1.5	3.2 ± 1.0	M2
271.7 ± 0.5	100 norm	(9.8 ± 2.0) * E-2	6.7 ± 1.5	M1 (+E2)
389.4 ± 0.5	4.0 ± 1.0			
588.2 ± 0.5	15 ± 3			
668.2 ± 0.5	15 ± 3	(7.5 ± 2.5) * E-2		E1, M1 + E2
785.6 ± 0.5	4 ± 1			
798.8 ± 0.5	15 ± 3	< 5 * E-3		E1, M1 + E2
824.8 ± 0.5	10 ± 3	< 4 * E-3		E1, M1 + E2
916.4 ± 0.5	5 ± 1	< 4 * E-3		E1, M1 + E2
1819.4 ± 1.0	5 ± 2			

Table 2: cont'd

Gd-144 (4.4 ± 0.3) min

E_γ |keV|	I_γ	α_k	K/L	Multipolarity
270.5 ± 0.5	0.8 ± 0.2	(1.3 ± 0.3)* E-2		M1 + E2
273.8 ± 0.5	1.1 ± 0.3	(1.3 ± 0.3)* E-2		M1 + E2
333.2 ± 0.5	12.0 norm	(7.4 ± 1.5)* E-3	8.3 ± 2.0	M1
347.0 ± 0.5	4.0 ± 0.4	(1.4 ± 0.6)* E-3		E1
622.0 ± 0.5	2.1 ± 0.4			
629.8 ± 0.5	3.8 ± 0.4			
641.9 ± 0.5	2.0 ± 0.4			
867.7 ± 0.5	2.2 ± 0.4			
(741)	(100 ± 40)	(Gd-144 prompt)		

Eu-140 (20 ± 15) sec

E_γ |keV|	I_γ	α_K	K/L	Multipolarity
531.0 ± 0.5	100			

Eu-141 (28 ± 6) sec

E_γ |keV|	I_γ	α_K	K/L	Multipolarity
384.1 ± 0.5	4.0 ± 1.0	(3.1 ± 1.0) * E-2		M1 + E2
393.8 ± 0.5	3.5 ± 1.0	(4.2 ± 1.5) * E-2		M1 + E2
(438)	43 norm	(Sm-141)		

Eu-142 (<30) sec

E_γ |keV|	I_γ	α_K	K/L	Multipolarity
628.5 ± 0.5	7 ± 3	(5.0 ± 2.5) * E-2		E2 + (M1)
768.2 ± 0.5				
(526)	100 norm	(Gd-142 prompt)		

Eu-142m_1 (1.20 ± 0.15) min

E_γ |keV|	I_γ	α_K	K/L	Multipolarity
556.8 ± 0.4	94 ± 5	(3.0 ± 1.0) * E-3		E1
563.9 ± 0.5	6 ± 2	(1.2 ± 0.6) * E-2		E2 + (M1)
768.2 ± 0.4	100 norm	(4.0 ± 1.0) * E-3		E2
1015.7 ± 0.5	6 ± 2			
1022.9 ± 0.4	94 ± 5	3.0 ± 1.0 * E-3		

Table 2:cont'd

(7 ± 3) sec activity (probably $^{142m2}Eu$)

E_γ |keV|	I_γ	α_K	K/L	Multipolarity
179.0 ± 0.6	100 norm	< 0.4		E1, E2 + M2

Sm-139m (9.5 ± 1.0) sec

E_γ |keV|	I_γ	α_K	K/L	Multipolarity
111.8 ± 0.3	59 ± 7	(9.4 ± 3) * E-1	7.5 ± 3.0	E2 + M1
155.3 ± 0.3	85 ± 9	3.6 ± 1.0 * E-1	5 ± 2.5	E2 + M1
190.1 ± 0.3	100 norm	7.0 ± 1.5 * E-1	0.9 ± 0.2	E3
267.3 ± 0.5	92 ± 10	6.0 ± 2.0 * E-2		E2(+ M1)

Sm-139 (2.6 ± 0.3) min

E_γ |keV|	I_γ	α_K	K/L	Multipolarity
273.4 ± 0.5	65 ± 15	(5.0 ± 2.0) * E-2		E2 + M1
306.3 ± 0.5	60 ± 15	(3.0 ± 1.2) * E-2		E2(+ M1), E1
597 ± 1	15 ± 5			
(190)	(40 norm)	Sm-139m		

Table 2 : cont'd

Sm-140 (14.7 ± 1.0) min

E_γ [keV]	I_γ	α_K	K/L	Multipolarity
76.1 ± 0.7	0.6 ± 0.2			
84.8 ± 0.7	2.0 ± 0.2		α_L: (6.2 ± 2.5)*E-1	E2 + M1
109.2 ± 0.5	0.9 ± 0.1	(8.7 ± 2.6)*E-1	6.8 ± 2.4	M1
114.1 ± 0.5	1.7 ± 0.1	(8.1 ± 2.4)*E-1	7.2 ± 2.0	M1
120.1 ± 0.5	3.1 ± 0.2	(2.2 ± 0.7)*E-1		E1
136.0 ± 0.5	0.7 ± 0.1	(5.5 ± 1.6)*E-1	8.6 ± 3.0	M1
139.6 ± 0.5	9.2 ± 0.5	(9.8 ± 2.9)*E-2	7.6 ± 1.5	E1
145.2 ± 0.5	0.6 ± 0.1	(3.2 ± 0.8)*E-1		E2
150.1 ± 0.5	0.20 ± 0.05	(3.2 ± 0.8)*E-1		E2
158.0 ± 0.5	1.0 ± 0.1	(3.6 ± 0.9)*E-1	6.4 ± 1.6	M1
163.2 ± 0.5	0.19 ± 0.05			
200.0 ± 0.5	1.0 ± 0.1	(5.4 ± 1.4)*E-2		E1
204.9 ± 0.5	0.15 ± 0.04			
220.7 ± 0.5	2.2 ± 0.2	(1.5 ± 0.3)*E-1	5.7 ± 1.0	E2 + M1
225.5 ± 0.5	15.0 norm	(1.4 ± 0.3)*E-1	8.8 ± 1.3	M1
237.2 ± 0.5	0.15 ± 0.02	(1.2 ± 0.4)*E-1		E2 + M1
255.8 ± 0.5	0.32 ± 0.03	(9.5 ± 1.9)*E-2		E2 + M1
260.0 ± 0.5	0.32 ± 0.03			
279.0 ± 0.5	0.68 ± 0.05	(6.9 ± 1.0)*E-2	8.7 ± 3.5	E2 + M1
306.7 ± 0.5	0.21 ± 0.02	(4.3 ± 0.9)*E-2		E2 +(M1)
311.7 ± 0.5	0.47 ± 0.04	(5.5 ± 0.8)*E-2		M1 +(E2)
339.8 ± 0.5	2.5 ± 0.2	(2.8 ± 0.4)*E-2	8.6 ± 2.0	E2 +(M1)
344.8 ± 0.5	1.3 ± 0.1	(3.0 ± 0.5)*E-2		E2 +(M1)
369.9 ± 0.5	0.29 ± 0.03	(2.3 ± 0.7)*E-2		E2 +(M1)

Sm - 140 cont'd

E_γ |keV|	I_γ	α_K	K/L	Multipolarity
409.2 ± 0.5	0.24 ± 0.02	(2.5 ± 0.8)*E-2		M1 +(E2)
425.9 ± 0.5	0.23 ± 0.02			
444.7 ± 0.5	0.16 ± 0.02			
467.9 ± 0.5	0.12 ± 0.01	(1.2 ± 0.6)*E-2		E2 + M1
480.9 ± 0.5	0.13 ± 0.01	(1.2 ± 0.5)*E-2		E2 + M1
502.7 ± 0.5	0.7 ± 0.1	(1.3 ± 0.5)*E-2		M1 + E2
533.9 ± 0.5	0.34 ± 0.03	(8.5 ± 2.5)*E-3		E2 +(M1)
565.5 ± 0.5	0.29 ± 0.03	(9.0 ± 1.8)*E-3		E2 + M1
604.1 ± 0.5	0.28 ± 0.03			
608.4 ± 0.5	0.19 ± 0.02			
668.0 ± 0.5	0.36 ± 0.03	(3.7 ± 1.1)*E-3		E2
700.7 ± 0.5	0.26 ± 0.03	(7.6 ± 1.9)*E-3		M1 +(E2)
725.5 ± 0.5	0.26 ± 0.03	(6.9 ± 1.7)*E-3		M1 +(E2)
761.2 ± 0.5	0.62 ± 0.05	(4.0 ± 0.8)*E-3		E2 +(M1)
805.1 ± 0.5	0.07 ± 0.01			
825.1 ± 0.5	0.77 ± 0.07	(3.9 ± 0.8)*E-3		E2 + M1
862.1 ± 0.5	0.30 ± 0.03			
873.8 ± 0.5	0.49 ± 0.05			
904.3 ± 0.5	0.06 ± 0.01			
999.8 ± 0.5	0.10 ± 0.01			
1022.6 ± 0.7	0.28 ± 0.03			
1057.8 ± 0.7	0.31 ± 0.03			
1097.8 ± 0.7	0.44 ± 0.05			
1115.7 ± 0.7	0.26 ± 0.03			
1138.0 ± 0.7	1.7 ± 0.2			

Table 2: cont'd

Sm - 140 cont'd

E_γ |keV|	I_γ	α_K	K/L	Multipolarity
1166.8 ± 0.7	0.62 ± 0.06			
1188.9 ± 0.7	0.13 ± 0.01			
1249.6 ± 0.7	0.37 ± 0.04			
1254.9 ± 0.7	0.22 ± 0.02			
1283.3 ± 0.7	0.45 ± 0.05			
1325.4 ± 0.7	0.31 ± 0.03			
1393.9 ± 0.7	0.95 ± 0.09			
1409.6 ± 0.7	0.05 ± 0.01			
1444.9 ± 0.7	0.09 ± 0.01			
1479.4 ± 0.7	0.05 ± 0.03			
1529.8 ± 0.7	1.2 ± 0.1			
1577.4 ± 0.7	0.39 ± 0.04			
1669.5 ± 0.7	0.40 ± 0.04			
(531)	(100 ± 20)	(Sm-140 prompt)		

Sm-141g (11.0 ± 1.0) min

E_γ |keV|	I_γ	α_K	K/L	Multipolarity
403.9 ± 0.5	48.0 ± 15.0	(1.8 ± 0.3)*E-2		E2 + M1
438.2 ± 0.5	43.0 ± 15.0	(1.2 ± 0.3)*E-2		E2 +(M1)
(511)	100 norm			
1292.3 ± 0.5	9.0 ± 1.0			
1601.0 ± 0.5	7.0 ± 1.0			

Table 2: cont'd

Pm-137 (2.4 ± 0.4) min

E_γ |keV|	I_γ	α_K	K/L	Multipolarity
85.5 ± 0.5	19 ± 4			
108.2 ± 0.5	154 ± 10	1.0 ± 0.3	6.3 ± 1.2	M1
177.5 ± 0.5	136 ± 10	(2.5 ± 0.5)*E-1	7.0 ± 2.0	M1 + (E2)
233.5 ± 0.5	100 norm	(3.1 ± 0.6)*E-1	1.5 ± 0.2	E3
268.0 ± 0.5	28 ± 5			
285.5 ± 0.5	55 ± 6	(4.8 ± 1.0)*E-2		E2 + (M1)
324.5 ± 0.5	9 ± 3			
328.5 ± 0.5	12 ± 4			
370.0 ± 0.5	13 ± 4			
389.0 ± 0.5	10 ± 3			
412.5 ± 0.5	28 ± 5			
414.0 ± 0.5	5 ± 1			
457.0 ± 0.5	15 ± 4			
460.0 ± 0.5	6 ± 1			
534.0 ± 0.5	20 ± 4			

Table 2: cont'd

Pm-138 (3.5 ± 0.3) min

E_γ |keV|	I_γ	α_K	K/L	Multipolarity
437.0 ± 1.0	9 ± 3	(1.5 ± 0.3) * E-2		E2 + M1
493.0 ± 1.0	22 ± 3	(1.1 ± 0.3) * E-2	4.0 ± 1.5	E2 + M1
521.0 ± 1.0	100 norm	(9.0 ± 2.0) * E-3		E2
729.0 ± 1.0	39 ± 5	(4.0 ± 1.0) * E-3	5.5 ± 2.0	E2
741.0 ± 1.0	6 ± 2			
809.0 ± 1.0	4 ± 1.5	(5.5 ± 2.0) * E-3		E2 + M1
829.0 ± 1.0	7 ± 1	(4.1 ± 1.5) * E-3		E2 + M1
931.0 ± 1.0	6 ± 2	(3.1 ± 1.0) * E-3		E2 + M1
971.0 ± 1.0	10 ± 2	(1.8 ± 0.6) * E-3		E2 + M1
1014.0 ± 1.0	8 ± 4	(1.8 ± 0.6) * E-3		E2 + M1
1015.0 ± 1.0	10 ± 4			
1137.0 ± 1.0	5 ± 2			
1280.0 ± 1.0	9 ± 4			
1675.0 ± 1.0	8 ± 4			

Pm-139m ($0.5 \pm^{0.2}_{0.4}$) s

E_γ |keV|	I_γ	α_K	K/L	Multipolarity
188.5 ± 0.5	60 ± 10			(E3)
(466)	100 norm	(Pm-139 prompt)		

Pm-139g (4.1 ± 0.3) min

E_γ |keV|	I_γ	α_K	K/L	Multipolarity
403 ± 1	30 ± 5	(1.8 ± 0.4) * E-2		E2 + M1
367 ± 1	8 ± 2	(3.2 ± 1.2) * E-2		E2 + M1
463 ± 1	8 ± 2	(2.5 ± 1.2) * E-2		E2 + M1
(466)	100 norm	(Pm-139 prompt)		

Pm-140 (9.2 ± 0.5) s

E_γ |keV|	I_γ	α_K	K/L	Multipolarity
639.4 ± 0.5	0.7 ± 0.1	(5.4 ± 1.3)*E-3		E2
716.0 ± 0.5	1.0 ± 0.1	(3.9 ± 0.6)*E-3		E2
773.5 ± 0.5	5.9 ± 1.0	(2.7 ± 0.5)*E-3	6.3 ± 1.0	E2
1412.9 ± 0.5	< 0.02	> 4.0 *E-1	4.6 ± 1.4	E0
1489.8 ± 0.5	1.0 ± 0.1	(5 ± 4)*E-4		E1, E2
1057.7 ± 0.5	0.1 ± 0.05			
1773.2 ± 0.7	< 0.05			

Table 2 cont'd

Pm-140m (5.8 ± 0.3) min

E_γ |keV|	I_γ	α_K	K/L	Multipolarity
419.2 ± 0.5	107 ± 10	(3.6 ± 0.5)*E-2	3.9 ± 0.6	E3
773.5 ± 0.5	100 norm	(2.7 ± 0.5)*E-3	6.3 ± 1.0	E2
1028.1 ± 0.5	93 ± 10	(1.5 ± 0.4)*E-3		E2
1197.6 ± 0.5	3.7 ± 0.6			

Pm-142m (2.39 ± 0.1) ms

E_γ |keV|	I_γ	α_K	K/L	Multipolarity
208.9 ± 0.5	100 norm	(0.4)		
241.1 ± 0.5	20 ± 10			
433.5 ± 0.5	85 ± 5	(0.03)		E2 + M1

Nd-135 (12.0 ± 1.0) min

E_γ |keV|	I_γ	α_K	K/L	Multipolarity
41.5 ± 0.5	45 ± 10		α_L: 2.0 ± 1.0	M1 + E2
112.6 ± 0.3	9.7 ± 0.6	6.3 ± 1.4		M1
233.3 ± 0.5	2.6 ± 0.3	(1.0 ± 0.2)*E-1		E2 +(M1)
245.4 ± 0.3	6.9 ± 0.5	(6.4 ± 1.3)*E-2	7.22 ± 3.8	E2 +(M1)
256.1 ± 0.3	5.7 ± 0.6	(9.0 ± 1.6)*E-2		M1 + E2
260.0 ± 0.5	1.7 ± 0.5			
271.9 ± 0.3	5.4 ± 0.4	(9.3 ± 1.5)*E-2	6.93 ± 2.9	M1 + E2
316.8 ± 0.3	2.2 ± 0.2	(7.0 ± 1.3)*E-2	2.05 ± 0.7	E3
322.6 ± 1.0	1.2 ± 0.4	(1.5 ± 0.4)*E-2		E1
372.9 ± 0.3	4.3 ± 0.4	(2.1 ± 0.5)*E-2		M1 +(E2)
386.0 ± 0.5	2.8 ± 0.5			
415.2 ± 0.3	2.1 ± 0.3	(2.3 ± 0.8)*E-2		M1
441.3 ± 0.3	28.6 ± 2.9	(1.7 ± 0.3)*E-2		M1 +(E2)
452.0 ± 0.3	8.1 ± 0.8	(1.5 ± 0.3)*E-2		M1
475.9 ± 0.3	17.0 ± 1.7	(8.7 ± 2.1)*E-3		E2
490.5 ± 0.5	1.7 ± 0.3	(1.4 ± 0.5)*E-2		E2 + M1
493.5 ± 0.5	3.0 ± 0.4	(9.0 ± 3.1)*E-3		E2 +(M1)
501.6 ± 0.3	19.1 ± 1.5	(2.3 ± 0.8)*E-3		E1
531.9 ± 0.3	3.6 ± 0.5	(8.0 ± 3.4)*E-3		M1
593.4 ± 0.3	7.1 ± 0.8	(1.2 ± 0.2)*E-2		M1
616.6 ± 0.5	3.6 ± 0.8			
708.4 ± 0.5	1.6 ± 0.3	(1.2 ± 0.6)*E-2		M1, E3
739.7 ± 0.5	1.6 ± 0.3			
746.5 ± 0.5	1.9 ± 0.3			

Table 2: cont'd

Nd-137 (38.0 ± 1.0) min

E_γ |keV|	I_γ	α_K	K/L	Multipolarity
75.5 ± 0.1	133 ± 15	α_L:(36 ± 9) * E-2	L/M:4.7±0.5	M1 +(E2)
110.8 ± 0.3	< 2			
144.4 ± 0.5	< 0.5			
167.5 ± 0.5	< 1.5			
180.8 ± 0.5	1.0 ± 0.2			
198.5 ± 0.1	5.0 ± 0.5	(15 ± 3) *E-2	2.8 ± 0.9	M1 + E2
230.5 ± 0.1	10.0 ± 1.0	(10 ± 2) *E-2	5.9 ± 1.8	M1 + E2
238.2 ± 0.1	27.5 ± 2.0	(8.3 ± 1.6)*E-2	6.4 ± 1.3	M1 + E2
267.0 ± 0.1	7.5 ± 1.0	(8.5 ± 1.7)*E-2	5.4 ± 2.2	M1 +(E2)
276.3 ± 0.1	5.0 ± 0.8	(8.9 ± 1.8)*E-2	3.6 ± 1.5	M1 +(E2)
288.5 ± 0.3	< 1.5			
306.6 ± 0.15	78.0 ± 4.0	(5.3 ± 0.8)*E-2	6.8 ± 1.0	M1 +(E2)
313.5 ± 0.15	6.0 ± 1.0	(3.4 ± 1.0)*E-2		M1 + E2
342.0 ± 0.5	< 2.0			
348.5 ± 0.25	< 2.0	(7.6 ± 3.0)*E-2	5.5 ± 2.8	
350.0 ± 0.5	3.0 ± 1.0			
360.8 ± 0.3	< 1.0			
382.0 ± 0.15	8.0 ± 1.0	(2.3 ± 0.5)*E-2	7.8 ± 3.9	M1 + E2
447.5 ± 0.5	< 1			
474.9 ± 0.15	9.0 ± 1.5	(1.6 ± 0.2)*E-2	8.4 ± 3.3	M1 +(E2)
505.1 ± 0.3	70 ± 10	(1.3 ± 0.4)*E-2	6.8 ± 1.0	M1 + E2
525.3 ± 0.15	3.0 ± 0.5	(1.8 ± 0.5)*E-2		M1 +(E2)
531.0 ± 0.15	6.0 ± 1.0	(0.7 ± 0.3)*E-2		E2 +(M1)
540.7 ± 0.5	< 2.0			

Table 2:cont'd

Nd-137 cont'd

E_γ |keV|	I_γ	α_K	K/L	Multipolarity
546.9 ± 0.15	3.0 ± 1.0	(2.0 ± 1.0)*E-2		
580.6 ± 0.1	100 norm	(1.0 ± 0.2)*E-2		M1 +(E2)
598.6 ± 0.5	< 1.5			
615.6 ± 0.1	8.1 ± 0.8	(0.9 ± 0.5)*E-2		M1 + E2
619.2 ± 0.1	4.5 ± 0.5	(1.2 ± 0.6)*E-2		M1 + E2
623.8 ± 0.5	2.4 ± 0.5	(0.9 ± 0.5)*E-2		M1 + E2
627.5 ± 0.5	< 1.4			
649.4 ± 0.3	< 1.5	(1.1 ± 0.6)*E-2		M1 + E2
667.2 ± 0.5	< 2.0			
686.1 ± 0.1	14.0 ± 2.0	(0.4 ± 0.1)*E-2		E2 +(M1)
688.0 ± 0.5	< 1.0			
724.8 ± 0.3	< 2.0			
761.6 ± 0.2	70.0 ± 10.0	(0.48±0.07)*E-2	7.5 ± 1.1	M1 +(E2)
781.6 ± 0.1	73.0 ± 8.0	(0.46±0.07)*E-2	6.7 ± 1.0	M1 +(E2)
785.3 ± 0.3	< 1.5			
814.4 ± 0.2	< 2.0			
857.0 ± 0.2	< 1.8			
863.4 ± 0.4	< 2.6			
883.7 ± 0.2	< 2.5			
925.9 ± 0.15	57.0 ± 0.15	(0.28±0.04)*E-2	9.5 ± 2.4	M1 + E2
929.2 ± 0.15	23.0 ± 3.0	(0.30±0.05)*E-2		
959.2 ± 0.5	< 0.5			
1001.2 ± 0.5	< 2.0			
1044.5 ± 0.15	7.5 ± 0.8	(0.22±0.04)*E-2		M1 + E2
1102.8 ± 1.0	2.3 ± 0.5			

Nd-137 cont'd

E_γ |keV|	I_γ
1119.9 ± 0.2	4.5 ± 1.0
1179.8 ± 0.5	< 1.0
1218.3 ± 0.3	< 1.5
1234.5 ± 0.2	4.0 ± 0.6
1243.1 ± 0.2	11.0 ± 1.0
1247.5 ± 0.5	< 1.0
1293.6 ± 0.2	3.0 ± 0.5
1296.5 ± 0.5	< 0.2
1310.0 ± 0.4	3.5 ± 0.5
1360.0 ± 0.2	5.0 ± 1.0
1365.1 ± 0.2	< 2.0
1388.5 ± 0.2	< 2.5
1401.5 ± 0.15	2.5 ± 0.5
1427.1 ± 0.3	< 0.5
1464.1 ± 0.2	5.8 ± 1.0
1484.6 ± 0.2	4.8 ± 0.8
1546.0 ± 0.2	3.0 ± 0.6
1586.5 ± 0.2	2.5 ± 0.5
1594.5 ± 0.2	3.5 ± 0.5
1608.0 ± 1.0	< 0.8
1626.4 ± 0.2	7.0 ± 0.5
1662.5 ± 0.3	< 1.0
1731.1 ± 0.3	< 2.0
1744.6 ± 0.5	< 0.5
1769.5 ± 0.3	< 1.5
1791.3 ± 0.5	< 0.5
1813.1 ± 0.2	6.5 ± 0.8
1865.3 ± 0.2	2.8 ± 0.5
1893.5 ± 0.5	< 2.0
1901.5 ± 0.1	6.0 ± 0.5
1933.5 ± 0.3	3.0 ± 0.5
1940.8 ± 0.5	< 0.2
1969.0 ± 0.2	2.5 ± 0.5
1977.3 ± 0.5	< 0.7
2000.2 ± 0.5	< 0.5

E_γ |keV|	I_γ
2008.6 ± 0.2	2.5 ± 0.5
2051.3 ± 0.2	7.5 ± 0.5
2095.7 ± 0.5	< 0.7
2126.5 ± 0.3	< 1.3
2144.6 ± 0.2	< 0.5
2230.6 ± 0.5	< 0.5
2275.7 ± 1.0	< 0.5
2288.7 ± 0.3	< 1.5
2333.3 ± 1.0	< 0.3
2365.6 ± 0.5	< 0.1
2515.3 ± 0.5	< 0.7
2543.5 ± 0.5	< 0.6
2570.5 ± 0.5	< 0.3
2590.5 ± 1.0	< 0.1
2639.5 ± 1.0	< 0.3
2753.8 ± 1.0	< 0.1
2801.0 ± 1.0	< 0.1
2831.0 ± 1.0	< 0.1

Table 2: cont'd

Pr-135 (21 ± 1) min

E_γ |keV|	I_γ	α_K	K/L	Multipolarity
83.6 ± 0.5	80 ± 17	(2.9 ± 0.9)*E-0	12 ± 4	M1
213.2 ± 0.3	100 norm	(1.4 ± 0.2)*E-1	7.9 ± 1.1	M1
296.2 ± 0.3	222 ± 13	(4.5 ± 0.5)*E-2	7.1 ± 1.0	M1 +(E2)
325.1 ± 0.3	5.8 ± 0.9	(3.6 ± 0.7)*E-2	5.6 ± 1.4	E2 + M1
400.7 ± 0.5	3.0 ± 0.3	(2.2 ± 0.4)*E-2		M1 +(E2)
484.5 ± 0.3	13.3 ± 1.7	(1.4 ± 0.3)*E-2		M1 +(E2)
538.3 ± 0.3	64 ± 5	(1.2 ± 0.2)*E-2		M1
613.9 ± 0.3	15.0 ± 1.4	(8.9 ± 1.6)*E-3	7.1 ± 2.5	M1
620.9 ± 0.3	10.2 ± 0.9	(5.2 ± 1.0)*E-3		E2
697.7 ± 0.3	8.6 ± 1.1	(6.4 ± 1.4)*E-3		M1
720.7 ± 0.3	4.1 ± 0.6	(7.0 ± 2.5)*E-3		M1 or E3
780.6 ± 1.0	3.0 ± 0.7	(3.7 ± 2.1)*E-3		E2 + M1
934.2 ± 0.3	6.1 ± 0.7	(2.7 ± 1.4)*E-3		E2 + M1

Table 3: Production ratios for different Yrast-levels (estimated values from both in-beam and off-beam data). The values were taken at about the maximum of the excitation function and are assumed to be correct to within 30 %.

Nucleus	High-spin level	Low-spin level	$\frac{\sigma(\text{high-spin})}{\sigma(\text{low -spin})}$
^{142}Gd	4^+	2^+	4
^{144}Gd	5^-	2^+	4
^{139}Sm	$11/2^-$	$3/2^+$	> 18
^{140}Sm	4^+	2^+	20
^{141}Sm	$11/2^-$	$1/2^+$	> 30
^{142}Sm	5^-	2^+	5.5
^{143}Sm	$11/2^-$	$1/2^+$	13
^{139}Pm	$15/2^-$	$11/2^-$	2.5
^{137}Nd	$11/2^-$	$5/2^+$	5
^{138}Nd	4^+	2^+	10
^{139}Nd	$11/2^-$	$3/2^+$	> 14
^{140}Nd	4^+	2^+	> 20
^{141}Nd	$11/2^-$	$3/2^+$	9
^{135}Pr	$15/2^-$	$7/2^+$	6
^{137}Pr	$15/2^-$	$7/2^+$	4
^{132}Ce	4^+	2^+	2.5
^{134}Ce	4^+	2^+	3.5
^{136}Ce	4^+	2^+	> 30
^{137}Ce	$19/2^-$	$15/2^-$	2.5
^{138}Ce	4^+	2^+	18

Table 4: Calculated Q-values in MeV (from Garvey et al.[10])

Z \ A	135	136	137	138	139	140	141	142	143	144	145
$_{64}Gd$						5.40	7.18	4.63	6.24	3.85	5.16
$_{63}Eu$				9.38	6.69	8.47	5.92	7.54	5.15	6.45	
$_{62}Sm$			6.42	3.73	5.51	2.96	4.58	2.18	3.49		
$_{61}Pm$		7.83	5.15	6.93	4.38	6.00	3.60	4.91			
$_{60}Nd$	4.76	2.08	3.86	1.31	2.92	0.53	1.84				
$_{59}Pr$	3.50	5.29	2.73	4.35	1.96	3.26					

Fig. A1 - A4: Experimental excitation functions obtained in in-beam experiments. The smooth curves represent theoretical calculations as described in ref. 47.

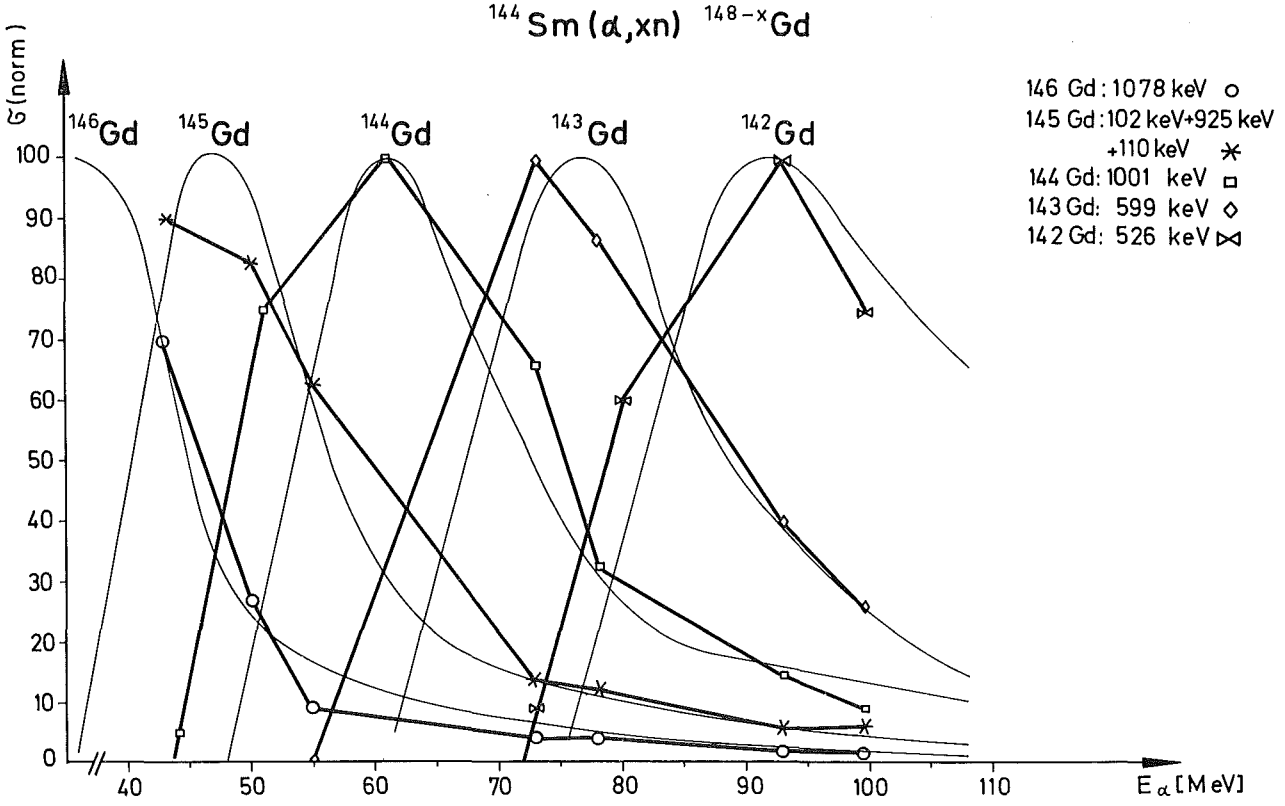

Fig. A1:

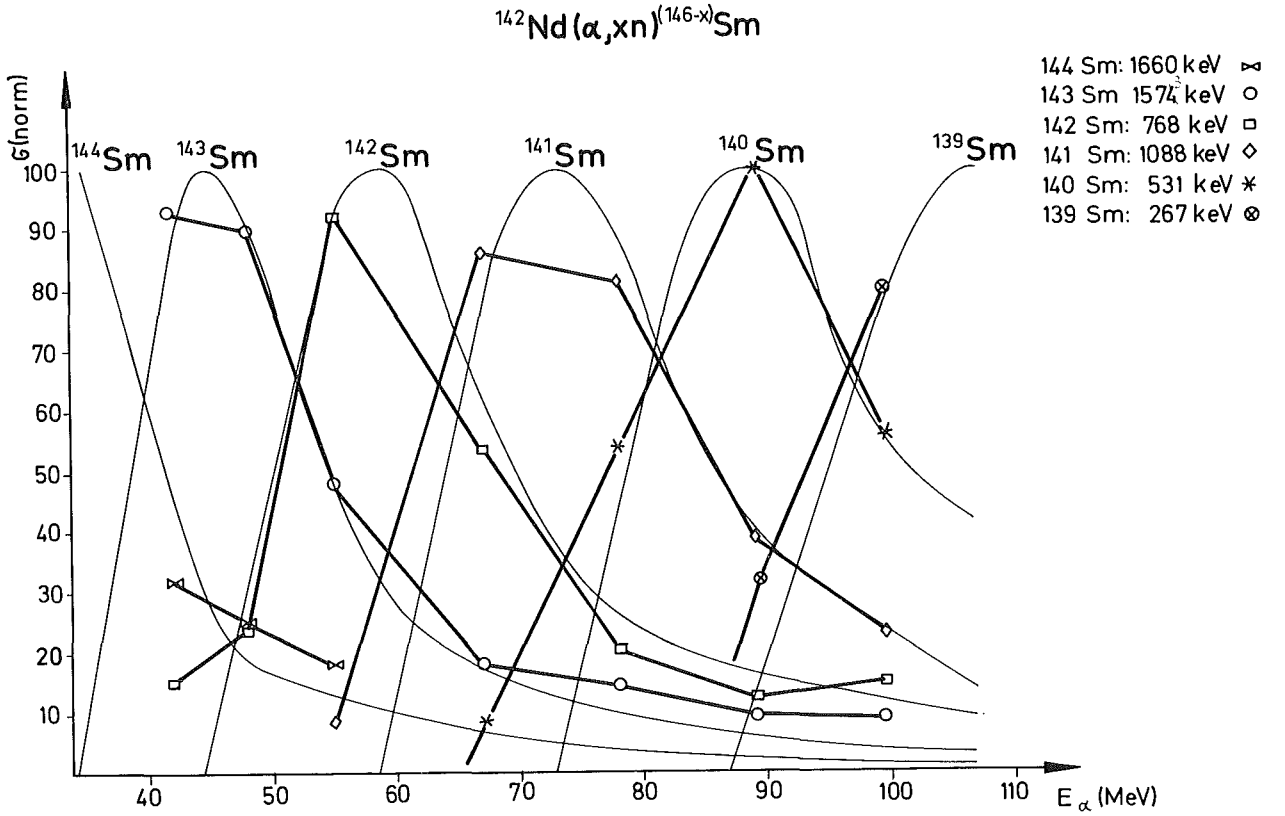

Fig. A2:

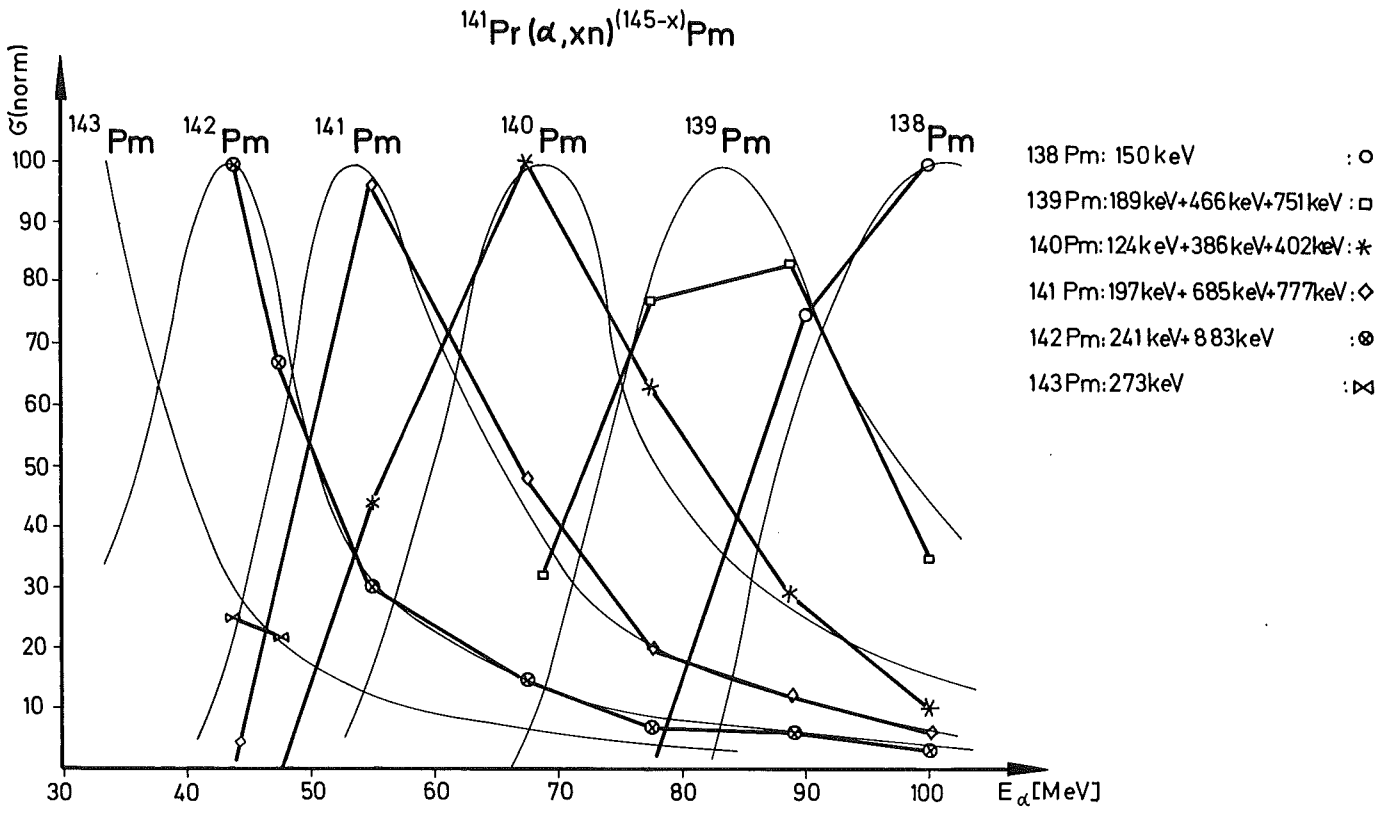
141Pr (α,xn)(145-x)Pm
σ(norm)
143 Pm
142 Pm
141 Pm
140 Pm
139 Pm
138 Pm
138 Pm: 150 keV : ○
139 Pm: 189 keV + 466 keV + 751 keV : □
140 Pm: 124 keV + 386 keV + 402 keV : ✳
141 Pm: 197 keV + 685 keV + 777 keV : ◇
142 Pm: 241 keV + 883 keV : ⊗
143 Pm: 273 keV : ⋈
Eα [MeV]

Fig. A3:

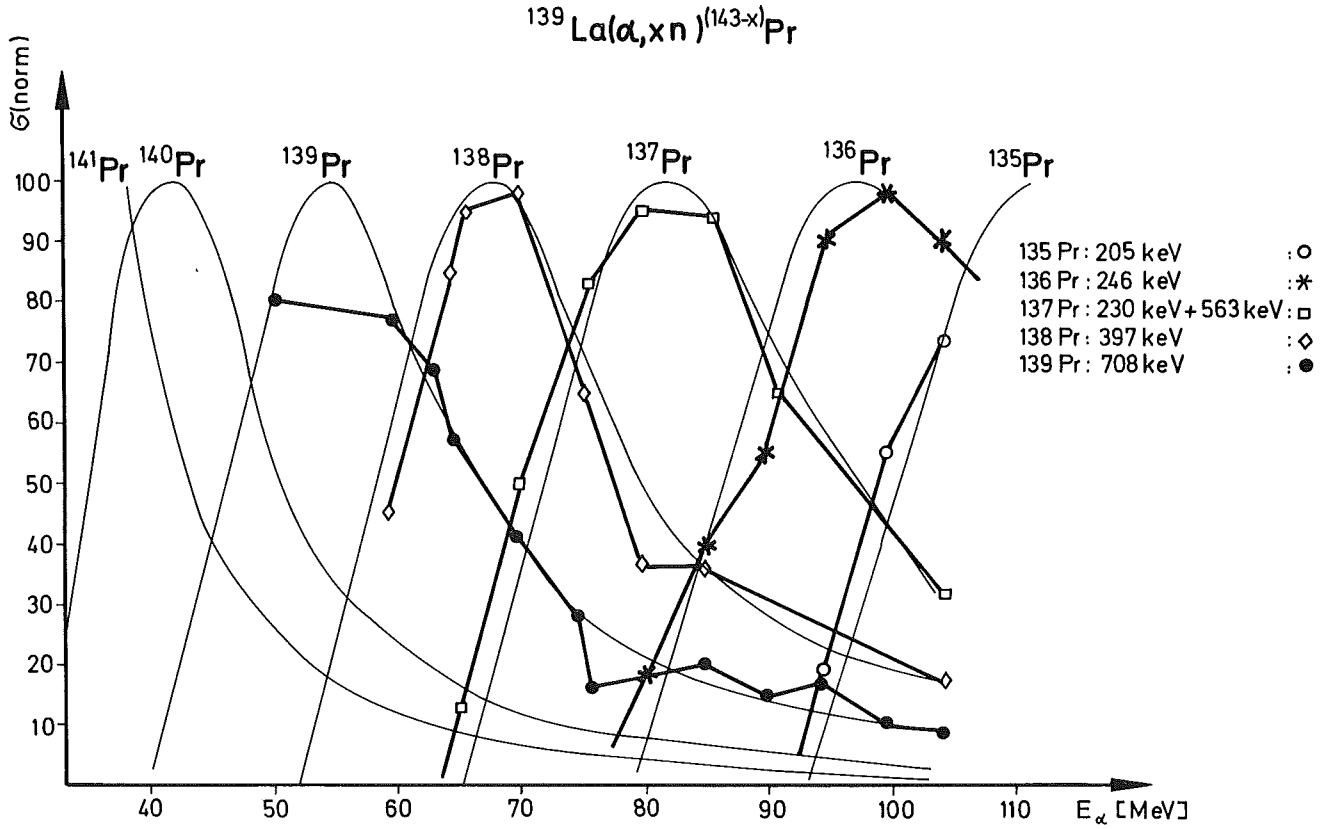
139La(α,xn)(143-x)Pr
σ(norm)
141Pr
140Pr
139Pr
138Pr
137Pr
136Pr
135Pr
135 Pr: 205 keV : ○
136 Pr: 246 keV : ✳
137 Pr: 230 keV + 563 keV : □
138 Pr: 397 keV : ◇
139 Pr: 708 keV : ●
Eα [MeV]

Fig. A4:

Fig. A5 - A8: Theoretical conversion coefficients and K/L - ratios obtained from an interpolation of the tables of Hager and Seltzer [58].

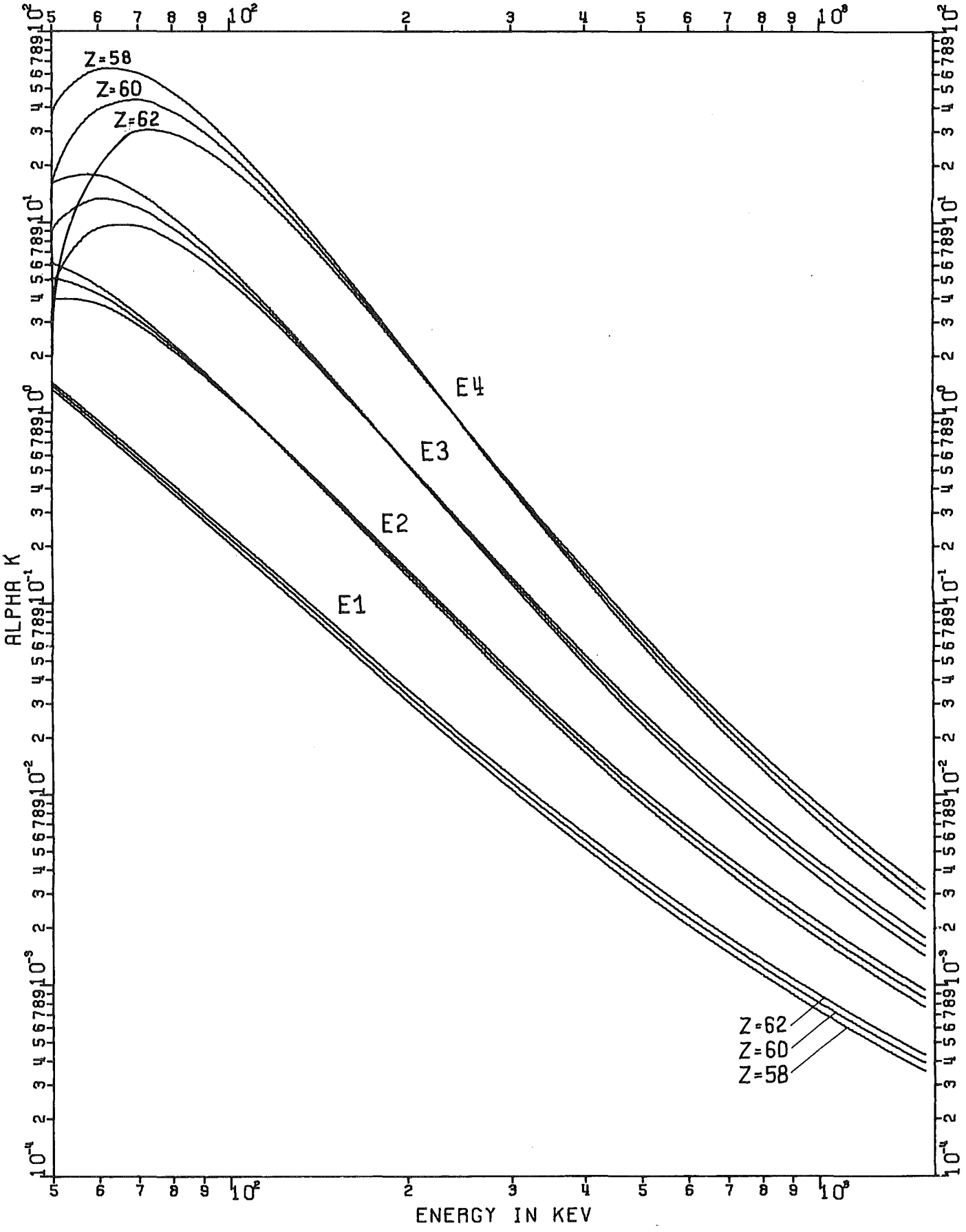

Fig. A5:

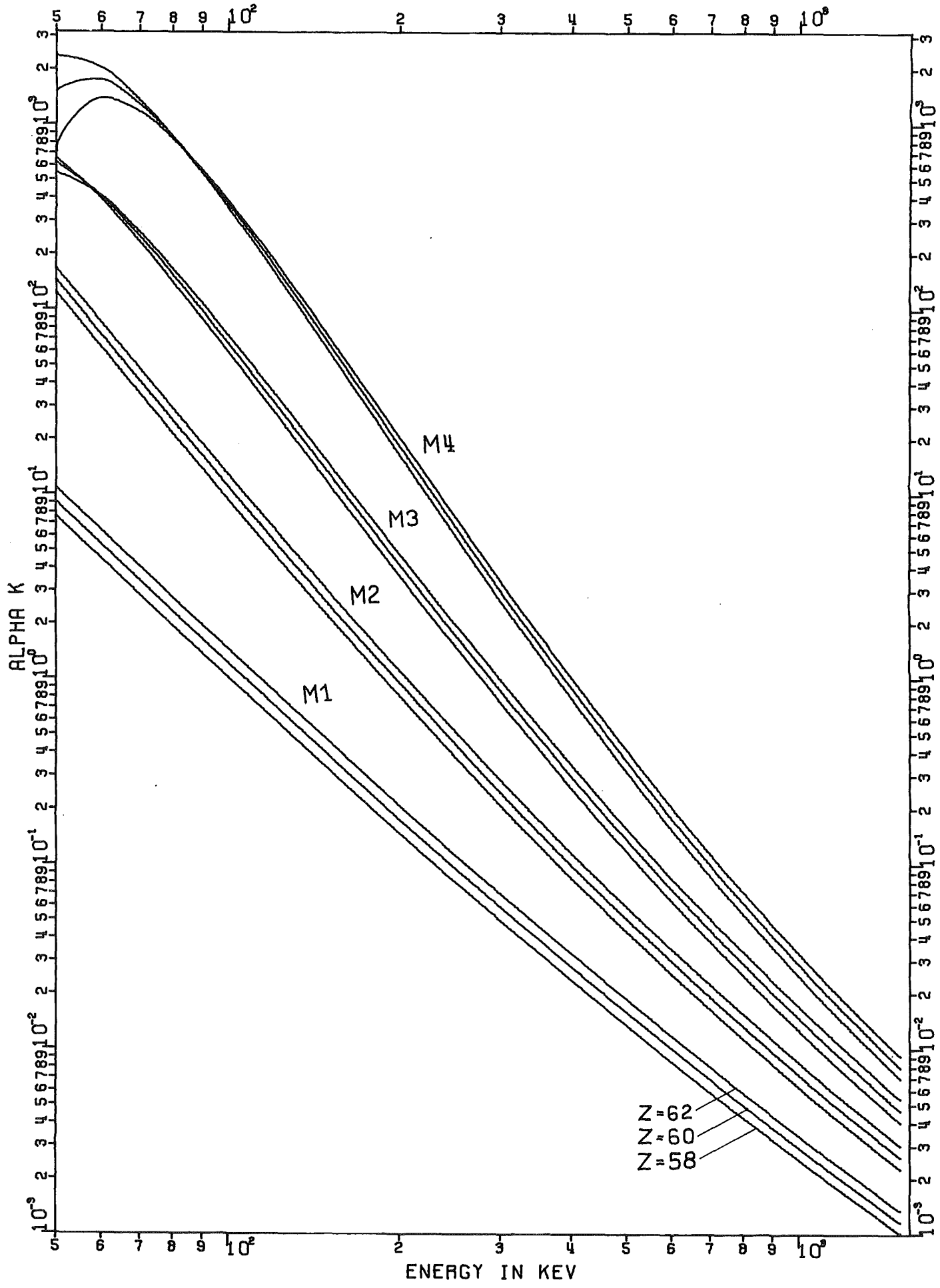

Fig. A6:

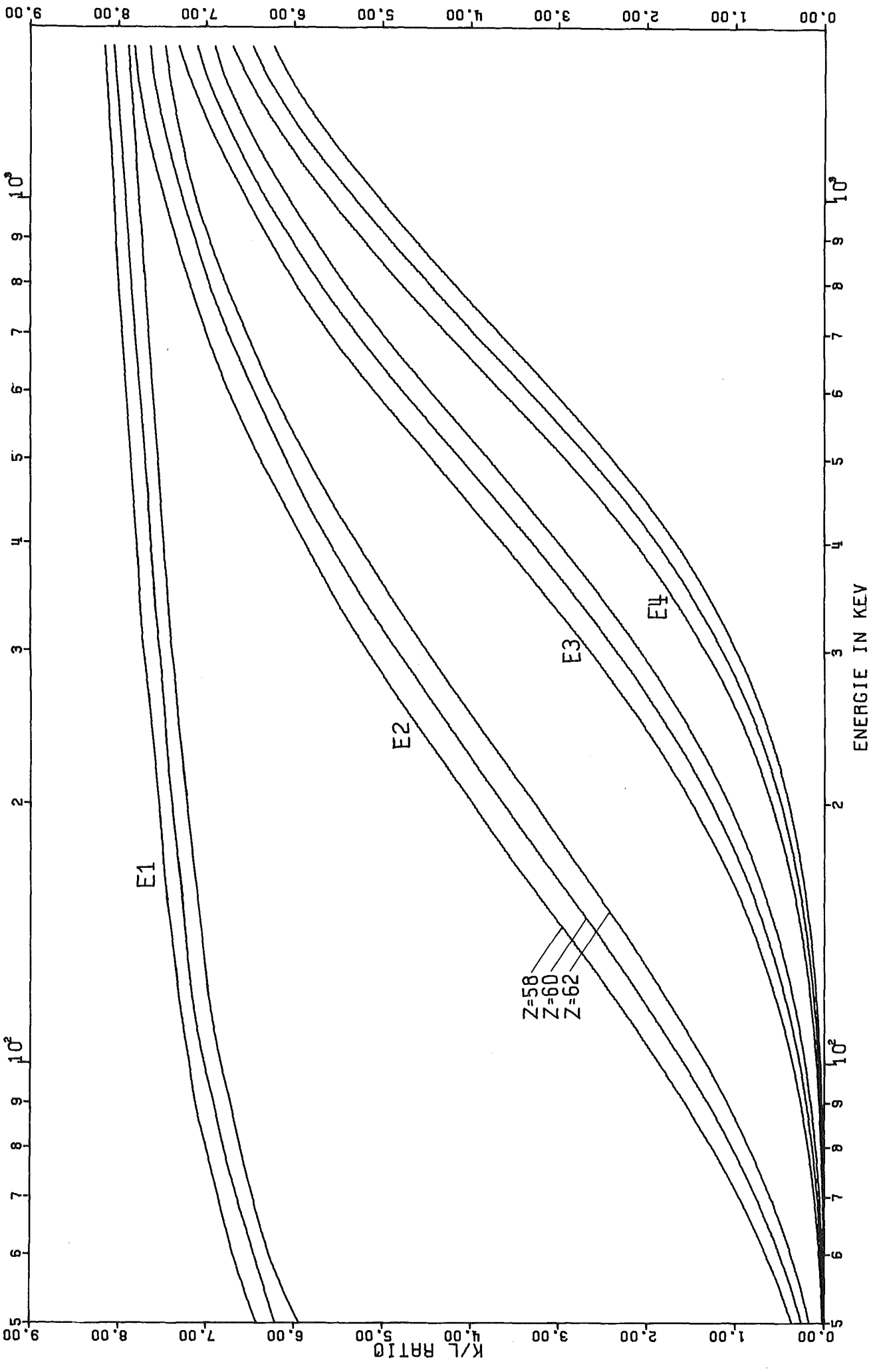

Fig. A7:

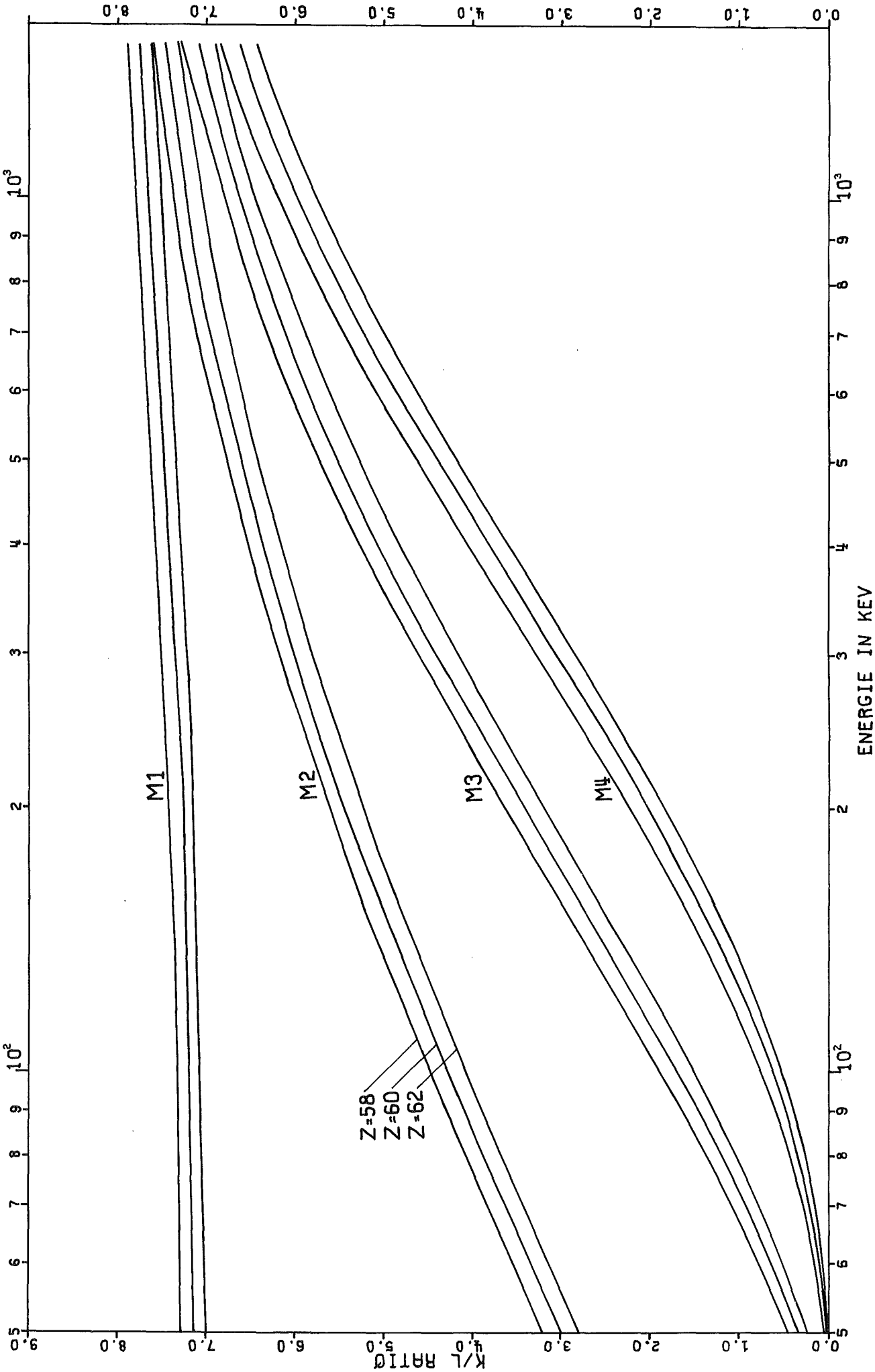

Fig. A8: